TLR-4 agonism induces CD25^{+} MHCII^{high} dendritic cells in association with tolerogenic antigen recognition

By

Alexander Bastian

(Under the direction of Mark D. Mannie, Ph.D.)

December 2022

Department of Microbiology and Immunology at East Carolina University Brody School of Medicine

Autoimmune disease is a result of the breakdown in immunological self-tolerance leading to destruction of self-tissues mediated by the aberrant immune attack. In Multiple Sclerosis (MS), CD4^{+} T cells mediate destruction of myelin in the central nervous system (CNS) leading to debilitating symptoms in afflicted individuals. MS is the leading cause of non-injury disability in young adults, impacting nearly 1 million people in the United States alone. As is the case for many autoimmune diseases, there is no cure for MS, highlighting the urgent need for new therapeutic platforms. A therapeutic approach to reestablish self-tolerance is likely to be more effective and have less side effects than current treatments, highlighting the importance for developing such an approach. At the center of this approach lies CD4^{+} FOXP3^{+} regulatory T cells (Tregs), which are a subset of T cells that suppress the immune system and play an integral role in controlling autoimmunity. Therapies aimed at increasing Tregs, especially in a disease-targeted manner, have the potential to reestablish self-tolerance and cure autoimmunity.

All T cells, including Tregs, must recognize antigen on antigen presenting cells (APCs) to perform effector functions. Therefore, targeting an APC niche that supports the development of Tregs is an effective approach for development of autoimmune therapeutics. Dendritic cells (DCs) are a class of APCs known to support Treg development and function. In this study, we show that agonism of Toll-like receptor 4 (TLR-4) with lipopolysaccharide (LPS) or monophosphoryl Lipid A (MPLA) on DCs leads to a $CD25^{+}$ $MHCII^{high}$ DC phenotype. We show that the expression of CD25 is unique to DCs and that it binds IL-2 from the environment without detectable downstream signaling. Importantly, we show that this bound IL-2 can be utilized by responder T cells, highlighting a potential function of CD25 on DCs. We then combined TLR-4 agonism with our lab's DC-targeting tolerogenic vaccine, GMCSF-MOG, which we have previously shown leads to high levels of Tregs and amelioration of experimental autoimmune encephalomyelitis (EAE) in mice. When GMCSF-MOG is combined with MPLA, Treg levels are increased and extend out to 78 days post injection. The enhanced and extended Treg levels observed when MPLA is included in the vaccine likely play a role in accelerating the GMCSF-MOG-mediated amelioration of EAE and preventing observed EAE relapse. At the crux of DC-mediated tolerance induction is the efficiency of the antigen recognition event. Lower affinity TCR ligation supports tolerance through lower induction of costimulatory molecules (CD40L) and increased induction of inhibitory molecules (PD-1). Furthermore, inhibiting the CD40L/CD40 axis increases Treg induction. Overall, we show that TLR-4 agonism leads to $CD25^{+}$ $MHCII^{high}$ DCs and functions as a tolerogenic adjuvant when combined with the DC-targeting GMSCF-MOG vaccine through support of low-efficiency Treg-favorable antigen recognition events.

TLR-4 agonism induces CD25^{+} MHCII^{high} dendritic cells in association with tolerogenic antigen recognition

A Dissertation Presented to

The Faculty of the Department of Microbiology and Immunology

Brody School of Medicine at East Carolina University

In Partial Fulfillment of the Requirements of the Degree of

Doctor of Philosophy in Microbiology and Immunology

By

Alexander Bastian

December 2022

TLR-4 agonism induces CD25^{+} MHCII^{high} dendritic cells in association with tolerogenic antigen recognition

By

Alexander G. Bastian

APPROVED BY:

DIRECTOR OF DISSERTATION: _____
Mark D. Mannie, Ph.D.

COMMITTEE MEMBER: _____
Jamie C. Dewitt Ph.D.

COMMITTEE MEMBER: _____
Brandon L. Garcia, Ph.D.

COMMITTEE MEMBER: _____
Akshaya K. Meher, Ph.D.

COMMITTEE MEMBER: _____
R. Martin Roop, II, Ph.D.

COMMITTEE MEMBER: _____
James P. Coleman, Ph.D.

CHAIR OF THE DEPARTMENT OF MICROBIOLOGY AND IMMUNOLOGY: _____
Everett C. Pesci, Ph.D.

DEAN OF THE GRADUATE SCHOOL: _____
Kathleen T. Cox, Ph.D.

ACKNOWLEDGEMENTS

First and foremost, I would like to acknowledge my family for always being there for me. I want to thank my mom and dad for always supporting me in every aspect of my life, since the day I was born. I can't believe how lucky I am to have such wonderful and supportive parents. I also want to thank my sister Eleana and brother-in-law Gary for their support via virtual game nights.

I want to thank my committee members Drs. R. Martin Roop, Brandon Garcia, Jamie DeWitt, Akshaya Meher and James Coleman. I am very grateful for all the support, understanding, and flexibility each of them has shown during my time here and especially during the dissertation writing process. Most importantly, I would like to express my gratitude to Dr. Mannie for accepting me into the lab years ago and allowing me to be remain largely independent as I progressed despite the many setbacks. My experience in this lab fortified my passion for immunology and prepared me for future success.

I would like to acknowledge all the previous and current members of the Mannie Lab for providing me with support, technical skills, reagents, and mindless chatter when it was needed. The lab was chaotic at times, but it was a great environment for me to come into my own as a researcher and scientist. I need to especially acknowledge Dr. Daniel Wilkinson, Dr. Cody Moorman and Hoda Jabbour for performing experiments that are shown in this dissertation.

Importantly, I would like to thank my friends that have helped provide me with a sense of stability throughout this entire graduate school process. I want to particularly thank Cody Moorman, Deko Devins and the entire Devins family, Ashley Knudson, Ryan Garrigues, and Alex Arteaga for providing me with the necessary reprieves via phone calls and vacations; our respective friendships mean everything to me. Additionally, I would like to thank Melissa

Lempicki, Dr. Kayla DeOca, and Dr. Ian Barton for their friendship within the program helping make each day easier.

Lastly, I need to thank Hoda Jabbour. Her support throughout this entire process, both professionally and personally, has been completely invaluable to me. She made this entire process, that everyone dreads so much, bearable and I can't thank her enough for all she does for me on a daily basis.

TABLE OF CONTENTS

LIST OF FIGURES

LIST OF ABBREVIATIONS

Ag	**antigen**
APC	**antigen presenting cell**
BBB	**blood brain barrier**
CD	**cluster of differentiation**
CD25	**IL-2 receptor alpha chain**
CD86	**costimulatory molecule involved with Ag presentation**
CD122	**IL-2 receptor beta chain**
CD132	**common gamma chain**
CD11c	**surface marker of mouse dendritic cells**
CFA	**complete Freund's adjuvant**
CNS	**central nervous system**
CTLA-4	**cytotoxic T lymphocyte antigen-4**
DC	**dendritic cell**
EAE	**experimental autoimmune encephalomyelitis**
F4/80	**surface marker of mouse macrophages**
FIG	**FOXP3-IRES-GFP, FOXP3 reporter**
FOXP3	**forkhead box P3**

GFP	**green fluorescent protein**
GM-CSF	**granulocyte-macrophage colony stimulating factor**
HEK	**human embryonic kidney**
IL	**interleukin**
IL-2	**interleukin-2**
IL-4	**interleukin-4**
IPEX	**immunodysregulation polyendocrinopathy enteropathy X-linked syndrome**
iTreg	**induced regulatory T cell**
IFN-β	**interferon-beta**
mAb	**monoclonal antibody**
M-CSF	**macrophage colony stimulating factor**
MFI	**mean fluorescence intensity**
MHC	**major histocompatibility complex**
MHCII-Ag	**MHCII complex with presented antigen**
MOG	**myelin oligodendrocyte glycoprotein**
MS	**multiple sclerosis**
NFM	**neurofilament medium polypeptide**

OVA	**ovalbumin**
PBMC	**peripheral blood mononuclear cells**
pSTAT5	**phosphorylated STAT5**
PRR	**pattern recognition receptor**
SD	**standard deviation**
SEM	**standard error of the mean**
SPL	**splenocytes**
STAT	**signal transducer and activator of transcriptional proteins**
T1D	**type 1 diabetes**
Tcon	**conventional FOXP3$^-$ T cell**
TCR	**T cell receptor**
TGF-β	**transforming growth factor-beta**
TNF-α	**tumor necrosis factor-alpha**
Tr1	**FOXP3$^-$ regulatory T cell subset**
Treg	**FOXP3$^+$ regulatory T cell**
tTreg	**thymic regulatory T cell**

CHAPTER 1

INTRODUCTION

1.1 INNATE AND ADAPTIVE IMMUNITY

The immune system is commonly divided into two categories, innate and adaptive. The innate immune system is responsible for quick recognition and destruction of invading foreign pathogens. Innate functions rely on evolutionary memory of pathogens. Receptors recognize patterns found on multiple pathogens, to provide a general protection against common pathogens (1). Cells that make up the innate immune system include dendritic cells (DCs), macrophages, neutrophils, among others (2). Neutrophils arrive first to the site of infection and use pattern recognition receptors (PRRs) to sense molecular markers such as bacterial lipids, viral RNA, and many other common antigens. Neutrophils then send out chemokines to attract other immune cells to the site of infection. Once pathogens are sensed by innate immune cells, they are engulfed, a process known as phagocytosis. Actin mobilization leads to membrane protrusions that surround the pathogen, leading to internalization. Macrophages, DCs and neutrophils are expert phagocytes (3). This internalized pathogen is shuttled along in a gradually maturing phagosome before the phagosome fuses with a lysosome. This phagolysosomal fusion leads to acidification of the compartment, as well as the introduction of several acid labile enzymes, usually enough to kill the pathogen (4, 5). The next step in an effective immune response is engaging the adaptive immune system. The bridge between the innate and adaptive immune response occurs through antigen presentation. The phagolysosome containing digested peptides

fuses with endosomes containing major histocompatibility complexes (MHC). These peptides from exogenous pathogens are loaded into MHCII complexes and put on the cell surface of professional antigen presenting cells (APCs) such as DCs, macrophages, and B cells. This presented antigen is then recognized by responder T cells which drive the adaptive immune response. This adaptive component of immunity is targeted, specific in nature, long-lasting, and generally considered to be performed by B cells and T cells (1). The specificity is achieved through the B cell receptor (BCR) and T cell receptor (TCR) which are randomly generated through recombination events leading to an estimated ~10^{12} different T and B cell clones with unique peptide-binding abilities in the body (6). This broad range of receptors allows the immune system to recognize the specific antigens involved in an infection so that the immune response can be highly targeted to attack only the antigens that are part of the infection. When T cells see their cognate antigen, they become activated and can bind to the antigen being presented by B cells (which also recognized the pathogen through BCR engagement). T cells can then activate B cells to produce antibodies specific for the pathogen, accelerating the clearance of the pathogen. These activated T and B cells can become memory cells, which provide long-lasting memory to the specific antigens they encountered, accelerating the immune response when that pathogen is encountered in the future.

1.2 IMMUNE HOMEOSTASIS

The immune system must balance effective immune responses against foreign entities while avoiding attacking self-tissues. This delicate and finely-tuned balance of desired immune activation and immune suppression is driven by myriad cellular players and chemical factors and

is known as immune homeostasis (7). The ability to effectively respond to foreign antigens is crucial for an effective immune defense. T and B cells are required for antigen-specific adaptive immune responses to invading pathogens (8-12). Antigen specificity is determined by the TCR or BCR, respectively, which are generated from random gene rearrangement. The random rearrangement of TCR and BCR generates a myriad of unique receptors that can recognize a multitude of antigens and respond to any number of potentially harmful pathogens (13). TCR and BCR are also generated that can recognize self-antigens and cause loss of self-tolerance. Therefore, the immune system must purge or suppress these autoreactive lymphocytes in order to maintain self-tolerance, and the failure to do so results in the development of autoimmunity (14). At its core, autoimmunity is a destructive immune response targeted at self-antigens. This can lead to a wide range of clinical symptoms and pathologies, resulting in over 100 different known autoimmune diseases. Most autoimmune diseases are classified according to what organs and/or tissues the immune response is mounted against, such as Multiple Sclerosis (MS) against the central nervous system (CNS), Type 1 diabetes (T1D) against the pancreas, and Graves' Disease against the thymus (15-22). Multiple self-antigens in the target tissue usually trigger the autoimmune attack, and the antigen to which tolerance was initially lost often remains unknown. Thankfully, there are many mechanisms at play to prevent the development of autoimmunity.

Central tolerance is the main mechanism preventing the development of autoimmune disease. It is a mechanism by which autoreactive T cells and B cells are eliminated from the developing lymphocyte pool as the initial selection of the T and B cell repertoire is a fundamental mechanism for preventing the development of autoimmunity. Autoreactive B cells are purged during development in the bone marrow based on self-reactivity. B cells with BCRs that strongly bind to self-proteins are negatively selected and undergo apoptosis (23-25). Similar

to B cells, self-reactive T cell clones are also purged from the repertoire. During T cell development in the thymus, newly generated TCRs are tested against self-antigens presented on MHCI and MHCII. MHCI and MHCII are presented on various cells, including thymic epithelial cells (TECs) (26). TECs express AIRE, a transcription factor that controls the expression of tissue-specific gene products that are not canonically expressed in the thymus, generating a comprehensive and systemic pool of self-antigens with which T cells are selected (27). In the thymus, T cells with TCRs that strongly recognize self-antigen are eliminated through apoptosis, a process known as negative T cell selection (28). This mechanism eliminates the T cells at highest risk to engender autoimmunity. T cells with TCRs that do not interact with MHC molecules undergo death by neglect due to a lack of activation signals. T cells with TCRs that weakly recognize self-antigen are positively selected and compose the eventual peripheral T cell repertoire. Finally, T cells with TCRs that recognize self-antigen with an intermediate-affinity differentiate into regulatory T cells (Tregs), the main suppressor cell subset (29).

Negative thymic selection, however, is incomplete and autoreactive T cells are found in the peripheral T cell repertoire (30). Therefore, any T cells with autoreactive potential must be curtailed in the periphery. Tregs prevent the activation of these possibly self-reacting T cell clones, a process known as peripheral tolerance.

1.3 REGULATORY T CELLS

Tregs are essential for the prevention of autoimmunity and are characterized by the expression of the master transcription factor, FOXP3. Humans and mice that lack Tregs as a result of mutation in FOXP3 develop a fatal autoimmune disease known as

immunodysregulation polyendocrinopathy enteropathy X-linked (IPEX) and Scurfy, respectively (31, 32). Furthermore, experimental deletion of Tregs can exacerbate or induce autoimmune diseases in animals (33). There are two main subsets of Tregs: thymically-derived Tregs (tTregs) which differentiate in the thymus and peripherally-induced Tregs (pTregs) that are generated from naive T cells in the periphery. Naïve T cells can differentiate into pTregs during antigen recognition in the presence of Treg-favorable molecules such as TGF-β, IL-2, and retinoic acid (RA) as well as through dominant low-efficiency antigen recognition (34). The differences between the subsets of Tregs are widely referenced but ultimately remain unclear (35-37). Tregs exist in higher proportions in anatomical compartments such as the mucosa, gut, lungs, skin, and liver as Treg induction is favored in order to maintain tolerance to harmless extended self-antigens such as food, allergens, and the commensal microbiota (38-42). However, Tregs display high plasticity and have been reported to lose their immunosuppressive capacity in inflammatory environments (43). Tregs are maintained by pools of self-antigen/MHCII and low levels of IL-2 which directly support FOXP3 expression and Treg effector function (44).

In addition to FOXP3, Tregs are commonly characterized by elevated expression of CD25 (IL-2 receptor α-chain) (45-48). Higher CD25 expression is associated with more stable and suppressive Tregs (49, 50). Tregs are activated by their cognate self-antigen and exert many effector functions in order to suppress immunogenic responses in the local microenvironment. Tregs enact several mechanisms, both direct and indirect, to achieve suppressive functions (51). One indirect mechanism Tregs employ is production of immunosuppressive and immunoregulatory molecules. Production of suppressive cytokines lead to an anti-inflammatory response (52). Of these cytokines produced by Tregs, TGF-β exerts a multitude of actions in innate and adaptive immunity. First, TGF-β is a strong inducer of Tregs and influences the

induction of naïve $CD4^+$ T cells into new Tregs, enriching the Treg pool in a localized environment (53). TGF-β can also suppress activation of several subsets of conventional T cells (Tcons). TGF-β also promotes differentiation of naïve T cells into Th17 cells which work with Tregs to maintain immune homeostasis in the gut where high levels of foreign antigens such as food and bacteria reside (54-59). Another regulatory cytokine expressed by Tregs is IL-35. This cytokine is secreted exclusively by regulatory subsets of cells, especially Tregs, and is an inhibitor of T cell proliferation. Tregs without IL-35 are less suppressive, highlighting the role of IL-35 in Treg-mediated suppression (60-62). Another regulatory cytokine produced by Tregs is IL-10. IL-10 dampens the expression of various pro-inflammatory cytokines such as interferon-γ (IFN- γ) and tumor necrosis factor-α (TNF- α) (63, 64). IL-10 also upregulates CD25 expression on many cells (65, 66).

In addition to regulatory cytokine secretion, the elevated expression of CD25 is one of the main indirect suppressive mechanisms utilized by Tregs. Activated Tregs express much higher CD25 on their surface compared to Tcons. This increase in CD25 can lead to sequestration of IL-2 from the environment which allows Tregs to have preferential access to IL-2, a necessary survival and proliferative factor for many T cells (67, 68). This overexpression of CD25 allows Tregs, despite only comprising about 5-10% of the $CD4^+$ T cell pool, to control access to IL-2 and maintain tolerance in quiescent environments. Resource sequestration by Tregs is not limited to IL-2. Tregs are known to sequester and consume other necessary survival factors such as glucose. Elevated expression of glucose receptors allows Tregs to outcompete nearby Tcons for glucose, leading to Tcon senescence (69).

Tregs are also capable of various contact-dependent mechanisms of suppression, both directly on Tcons as well as indirectly by impacting APCs. Tregs have several mechanisms to downregulate APCs in the environment, thereby limiting the potential of these APCs to activate other nearby T cells to help maintain immune tolerance in the microenvironment. One way that Tregs achieve this type of inhibitory activity is by constitutively expressing the coinhibitory molecule CTLA-4 on the cell surface upon TCR activation (70). The indispensable role for CTLA-4 in maintaining tolerance was elucidated through experimentation identifying that CTLA-4 deficiency in mice led to spontaneous autoimmunity which was later ameliorated by adoptive transfer of Tregs (71). The mechanism of suppression by CTLA-4 involves binding to and blocking Tcon access to the costimulatory molecules CD80 and CD86 on the surface of APCs, which are necessary for activation of T cells. In the presence of CTLA-4, the CD28-CD80/CD86 axis is disrupted, preventing T cells from accessing the necessary costimulation. Additionally, downregulation of CD80 and CD86 on APCs induced by Tregs was shown to be dependent on CTLA-4 (72). Similarly, Tregs can inhibit access of nearby Tcons to MHCII/Ag complexes through expression of LAG-3 on the surface of Tregs. LAG-3 is a CD4-like molecule capable of binding MHCII independently of antigen that inhibits MHCII access by other T cells (73). Antibodies against LAG-3 inhibited the regulatory roles of Tregs thus functionally implicating LAG-3 in Treg function. LAG-3 binds and sequesters MHCII to inhibit antigen presentation to other T cells. Through this blockade of costimulatory molecules and MHC complexes, Tregs indirectly inhibit T cell stimulation via the modulation of the APC. Additionally, Tregs can sequester both MHCII and CD80/86 from the surface of APCs via endocytosis or trogocytosis, a mechanism through which immune cells exchange membrane components (70, 74). Tregs engage with DCs presenting the cognate antigen in an interaction

quantified by a greater surface area of contact and a longer contact duration, initiated by Tregs' higher average affinity for a certain cognate self-antigen which is established during thymic selection. This interaction is antigen-dependent, allowing Tregs to decrease the antigen presentation to Tcons in an antigen-specific manner (74). Advantages in size, antigen affinity, and APC antagonism allow Tregs to dominate and physically block naïve and activated T cells from interfacing with APCs while depleting APC surface molecules needed for T cell activation.

Tregs also express ectoenzymes, CD39 and CD73, which together can convert extracellular adenosine triphosphate (ATP) to adenosine (75, 76). Adenosine binds and signals via the A2A adenosine receptor on the surface of T cells and DCs to inhibit T cell proliferation and suppress the function of DCs (77). Additionally, at certain concentrations, extracellular ATP was shown to increase T cell proliferation. Therefore, conversion of ATP to adenosine eliminates a proliferative agent (ATP) while simultaneously creating an inhibitory molecule (adenosine) (78, 79).

Tolerance to one antigen can be spread through a mechanism known as infectious tolerance. Through the Treg suppression mechanisms outlined above, Tregs form a suppressive microenvironment, spreading tolerance to adjacent T cells. Tregs that recognize their cognate antigen/MHCII on APCs are activated, inducing effector functions which reduce APC activation and suppress nearby T cells (80). Therefore, if two antigens are presented on the same APC, a Treg specific for one antigen can suppress T cells that recognize the other antigen at the surface of the APC. Not only can Tregs suppress Tcons specific for other antigens, Tregs can cause those Tcons to differentiate into Tregs through the production of TGF-β, therefore spreading the tolerance to other antigens (81). The newly generated Tregs can subsequently suppress antigen-specific immune responses and further spread tolerance to yet other antigens. Therefore, immune

responses against numerous self-antigens presented on a single APC can be suppressed by a limited number of Tregs which recognize only a few of the total self-antigens presented (80).

1.4 DEVELOPMENT AND PATHOGENSIS OF AUTOIMMUNITY

Despite systemic surveillance from Tregs, autoreactive T cells are occasionally able to escape the control of Tregs and initiate autoimmunity. There are several mechanisms through which autoimmunity develops (82). Molecular mimicry is a mechanism by which memory T cells specific for antigens from a past pathogenic exposure have cross-reactivity with a self-antigen. Upon recognition of the cross-reactive self-antigen, the T cell clone gets reactivated to mount an immune response against the self-antigen. Autoreactive T cells can then activate B cells and lead to production of autoantibodies accelerating the immune insult targeted at self-tissue (83). The best-known example of molecular mimicry is in rheumatic fever. Affliction with strep throat causes an immune response against the etiological agent *Streptococcus pyogenes*. The streptococcal M protein structurally mimics myosin in the human heart and elicits T cells specific for the M protein that can cross-react with heart tissue, eliciting an immune response targeted at the heart and leading to rheumatic carditis (84).

Another mechanism underlying autoimmunity is through bystander activation of T cells (85, 86). This mechanism involves activation of bystander T cells during strong inflammatory insult, such as during a pathogenic immune response. In this case, high levels of inflammatory mediators in the microenvironment act on all T cells in the area. This level of stimulation is accompanied by low levels of antigen recognition that normally would be below the threshold for activation in noninflamed environments but is amplified above threshold within the

inflammatory environment. Thus, an inflammatory environment can lead to T cell activation, clonal expansion, and autoimmune development by self-reactive clones (86). The role of bystander activation in autoimmunity has been shown experimentally in a model of hepatitis A infection. T cells not specific for the virus were activated by paracrine cytokines and contributed significantly to liver damage (87). As another example, activation of myelin-specific Th17 cells by high levels of paracrine IL-1β and IL-23 exacerbated experimental autoimmune encephalomyelitis (EAE), a rodent model of multiple sclerosis (MS). This bystander activation was shown to be independent of antigen-recognition of the bystander T cells. Activating T cells without TCR ligation bypasses a major regulatory checkpoint to prevent development of autoimmunity.

Another mechanism by which autoimmunity can develop is through aberrant activation of T cells. This mechanism relies on a genetic or environmental defect leading to the abnormal activation of T cells. Several examples are notable. An imbalance of leukocytes, such as elevated inflammatory cell subsets and decreased regulatory cell subsets, can lead to T cell activation. This can be due to genetic factors, environmental factors, or a combination of both. An example is seen in a lupus model, where elevated levels of a B cell subset supported aberrant activation of T follicular helper cells (Tfh) in the germinal center of lymph nodes, leading to autoantibody production. Another mechanism of aberrant activation is due to a specific MHC haplotype favoring the presentation of a particular self-antigen. The hallmark example of this is in T1D, where individuals with the allele for HLA-DR3 and HLA-DR4 are more likely to develop diabetes (88).

All these mechanisms of autoimmune initiation highlight the balance between environmental stimuli and genetic factors in the development of autoimmune disease. Numerous genome studies have identified more than 200 genetic loci associated with the susceptibility to one or more autoimmune diseases (66, 89-92). Most autoimmune diseases are associated with multiple susceptibility genes working together to produce the abnormal phenotype. Some loci show association with multiple different autoimmune diseases, indicating the loci are important for pathways maintaining general self-tolerance (93). Several genetic risk factors are directly associated with gene products involved in adaptive and innate immune responses (93, 94). In many cases, patients afflicted with a particular autoimmune disease report family members who have been diagnosed with other autoimmune diseases (95). These findings demonstrate a common underlying genetic basis for many autoimmune diseases. However, in identical twins, the cooccurrence of autoimmune disease ranges depending on the particular disease and never reaches 100%. Therefore environmental factors must also play an important role in the etiology of autoimmune diseases (96).

While autoimmune diseases vary in clinical and pathophysiologic presentation, the common mechanistic underpinning involves a breakdown in immune tolerance leading to an inflammatory immune attack targeted at self-antigens, leading to destruction of tissue. In MS, this presents as an inflammatory demyelinating disease of the CNS and is the leading cause of non-traumatic disability in young adults (97). MS presents differently from patient to patient with the most common symptoms being weakness, fatigue, pain, depression, and visual impairments along with varying levels of paralysis. The diverse presentation of symptoms correlates with timing and location of the inflammatory lesion within the brain (98). MS often begins as a relapsing-remitting disease with relapses gradually increasing in severity. After

several years, the disease often turns into a secondary progressive phase marked by continuous white and gray matter degeneration and increasing severity of physical and cognitive symptoms (99).

MS is a complex disease widely considered to be driven by $CD4^+$ T cells. Researchers believe that autoreactive T cells are activated and clonally expanded in the periphery through molecular mimicry or bystander activation and subsequently cross the blood-brain barrier (BBB). Once in the CNS, T cells are reactivated by APCs presenting their cognate myelin antigens in the brain and draining lymph nodes (100). This presentation leads to reactivation of these myelin-specific T cells, driving effector functions resulting in the recruitment of other inflammatory cells. The cell recruitment and infiltration results in the formation of inflammatory demyelinating lesions (101). EAE studies have shown that both Th1 and Th17 T cells have pathogenic roles, as EAE can be driven by adoptive transfer of myelin-reactive Th1 or Th17 T cells. Translationally, both Th17 and Th1 cells are found in lesions of MS patients and increase in the blood during the development of MS and relapses (100, 102, 103). Furthermore, skewing T cells away from disease-driving Th1 and Th17 lineages and toward a Th2 phenotype has therapeutic benefit in both EAE and MS (104, 105).

B cells have also been shown to play a complex role in MS. The pathogenic nature of B cells in MS is highlighted by the presence of B cells and autoantibodies in the CNS of MS patients. Additionally, ectopic lymphoid follicles are known to form in the CNS of MS patients and support the persistence of B cells and plasma cells (106, 107). The clinical success of anti-CD20 B cell-depleting mAbs in the treatment of MS has demonstrated an important role for B cells outside of antibody production because these treatments spare plasma cells. Conversely, B

cells including Bregs have been shown to have regulatory function through the production of anti-inflammatory cytokines IL-35 and IL-10 (108, 109). A regulatory B cell role is further highlighted by B cell knockout mice getting more severe EAE (110).

Myeloid cells such as resident microglial cells and infiltrating macrophages, monocytes, and DCs are found in MS lesions in high numbers (111). Myeloid cells are important APCs driving disease progression through activation of pathogenic Th17 and Th1 cells in the CNS and draining lymph nodes. Additionally, myeloid cells can potentiate inflammation by increasing permeability of the BBB via production of extracellular metalloproteases. This allows for an increased infiltration of immunocytes that can further drive CNS inflammation (111-113). However, myeloid cells can also relieve CNS inflammation by removing CNS debris from damaged cells, preventing inflammation often associated with cell damage. Additionally, myeloid cells can produce anti-inflammatory cytokines. For example, M2-like macrophages can express regulatory cytokines such as IL-10 and TGF-β that can help resolve ongoing neuroinflammation (114).

Propagation of the autoimmune attacks seen in MS are also due to an inhibition or dysfunction of regulatory subsets such as Tregs, Tr1 cells, and Bregs. Studies have reported that Treg numbers and suppressive ability are reduced in MS patients (102, 115). Tregs from MS patients are not as effective at controlling Tcon proliferation and express less FOXP3, indicative of a weaker regulatory capacity (116, 117). The suppressive capabilities of Bregs and Tr1 cells are also inhibited in MS patients due to reduced IL-10 production (118, 119).

Treatment of MS starts with frontline therapies that are immunomodulatory in nature and have modest efficacy. Standard frontline therapies include IFN-β which has been shown to

reduce clinical symptoms and relapses. IFN-β is thought to achieve this by reducing inflammatory cytokines and increasing anti-inflammatory cytokines as well as reducing T cell proliferation and inducing Tregs (120, 121). Second line therapies are generally immunosuppressive and are employed after symptoms progress to the point that frontline treatments are no longer successful. Second line treatments include lymphocyte depletion, most commonly with B cell depleting anti-CD20 antibodies. Additionally, fingolimod is frequently used as a second line therapy. This drug is a sphingosine analog that leads to the internalization of the sphingosine-1-phosphate receptor (S1PR1) which prevents the egress of pathogenic T cells from the lymph nodes, preventing the migration of these T cells into the CNS (122). While treatments for MS continue to evolve, the efficacy of existing treatments highlights the need for more targeted therapies.

Much of the research on MS for development of novel, targeted therapies is done using the animal model EAE. This disease model can present differently depending on the strain and species used but overall, it presents similarly to MS in that it is an inflammatory demyelinating disease driven by $CD4^+$ T cells (123-125). EAE can either be induced by injecting an emulsification of an encephalitogenic peptide with an adjuvant like complete Freund's adjuvant (CFA) to elicit active EAE, or by injection of myelin-specific T cells, known as passive EAE. EAE resembles MS immunologically and histologically but differences between the two exist. The substantial difference is that EAE is induced to a known etiological agent while MS is spontaneous and the pathogenic epitopes driving disease are unknown. These differences continue to provide hurdles for progress of MS treatments, but much of what is known about disease progression and interventions methods has come from use of the EAE model.

1.5 DENDRITIC CELLS

DCs are a crucial APC lineage vital for activation and maintenance of the T cell pool as well as playing an important role in innate immunity. DCs have many functions crucial to a healthy functioning immune system (126). First, DCs play a key role in detecting pathogens. DCs can be found at all common pathogen entry points into the body and are even known to protrude through mucosal barriers to sample antigens in the gut and lungs for preliminary protection (127, 128). DCs use innate immune receptors such as cell surface toll-like receptors (TLRs) to detect pathogens they come across. DCs also utilize intracellular receptors to detect infecting viruses or other pathogens. Engagement of innate immune receptors results in downstream signaling that changes the DC phenotype, which regulates other nearby cells to initiate the adaptive immune system, especially responder T cells. A method through which DCs communicate with surrounding cells is through secretion of cytokines and chemokines. Under different conditions, this cytokine array can vary substantially. In general, inflammatory cytokines such as IL-12, IL-1 and TNFα are expressed together apart from anti-inflammatory cytokines such as IL-10 (129). DCs are also known to secrete chemokines that recruit $CD8^+$ T cells, a crucial mechanism in proper anti-viral immune responses (130). In addition to changing cytokine profiles, a hallmark of DCs is their propensity to migrate to secondary lymphoid organs after activation. DCs upregulate chemokine receptor CCR7 which detects and follows a gradient concentration of CCL21, a chemokine secreted by the epithelial cells of draining lymph nodes (131). While the timing of this can vary, migration of DCs carrying foreign antigen occurs early in the stages of immune detection of a pathogen, as early as 8 hours post infection (132, 133).

DCs can become activated by environmental stimuli such as bacterial antigens triggering TLR signaling or by T cell engagement. Upon activation, DCs adopt a mature phenotype which involves upregulation of MHCII and costimulatory molecules on the surface. Immature DCs are known to frequently cycle MHCII to renew the antigens displayed on their surface. Upon activation, this cycling slows, and the antigens are presented continuously at high levels (134, 135).

After activation, DCs carrying antigen migrate to lymph nodes where they perform their crucial role of antigen presentation to T cells. DCs present antigen to responder $CD4^+$ and $CD8^+$ T cells on MHCII and MHCI, respectively. This leads to the activation of T cells specific for the presented antigens and subsequent clonal expansion, resulting in an immune attack targeted at the pathogen. DCs are also known for a phenomenon known as cross-presentation. Cross-presentation allows DCs to present extracellular antigens that have been internalized by the DC, which would normally be presented on MHCII molecules, on MHCI molecules for presentation to $CD8^+$ T cells. This is a unique feature of DCs that is crucial for directing antiviral and antitumor immune responses without the DCs being afflicted with viral infection or oncogenic mutations (136). Additionally, DCs are experts in tolerogenic antigen presentation, as they are crucial for maintenance of the existing Treg pool as well as differentiation of naïve T cells into the Treg lineage (137, 138).

DC can be divided into several subsets which induce diverse immune responses. Conventional or classical DCs (cDCs) are traditionally separated into cDC1 and cDC2 phenotypes. cDC1s are characterized by their cross-presentation ability and high levels of IL-12 production. cDC1 cells preferentially present antigen to Th1 cells as well as $CD8^+$ T cells,

promoting polarization of T cells to battle intracellular pathogens (139, 140). cDC1 also promote differentiation of responder and bystander $CD4^+$ T cells into the Th1 lineage by producing large amounts of IL-12. Conversely, cDC2 cells are less equipped to activate $CD8^+$ T cells and specialize in presentation to $CD4^+$ T cells, promoting differentiation into multiple helper T cell lineages including Th2, Th17, Tregs, and Th1 cells (141-143).

Langerhans cells (LCs) are a unique subset of DCs. They are skin-resident DCs that scan the environment for pathogens. Upon inflammation, LCs lose their attachment to the skin epithelium and migrate to draining lymph nodes, similarly to other DCs (141). Uniquely, LCs are not continuously renewed from bone marrow differentiation; instead, they are differentiated during embryonic development and are largely a self-renewing cell population (144). LCs are often referred to as macrophages due to their similarities to other tissue resident macrophages.

Plasmacytoid DCs (pDCs) secrete large amounts of type 1 interferons (IFN), proteins with diverse immune impacts but famous for their beneficial antimetabolic activities in combating viral infection. Unique features of these DCs are centered around IFN production. These cells play a vital role in rapid response to viral infection (141). pDCs contain high levels of innate immune receptors, such as TLR-7 and TLR-9, specializing in recognition of viral antigens (145).

Follicular DCs (FDCs) are another unique subset of DCs. They play a major role in maintaining proper structural zones and germinal centers (GC) within lymph nodes. They form a physical structure for B cells to migrate through and secrete large amounts of the chemokine CXCL13 which is responsible for B cell recruitment. In the GC, FDCs present antigen in a unique way. Classical DCs process and present antigens to T cells on MHC; however, FDCs

present antigens to B cells, so the antigens must be in their native state. To do this, FDCs utilize complement receptors 1 and 2 (CR1 and CR2, respectively) and Fc receptors to capture pathogens that have been opsonized. This native antigen is then scanned by B cells in the GC.

For years, the conventional view was that tolerance induction by DCs was achieved by DCs in an immature state. However, evidence has shown that activated DCs can exert robust tolerogenic T cell responses (146). For example, activated DCs were crucial for maintaining tolerance in a model of colitis (147, 148). Activated mature DCs that favor tolerance are known as regulatory DCs (DCregs) which mediate tolerance through decreased expression of inflammatory cytokines as well as lower levels of costimulatory surface markers. DCregs develop upon exposure to high levels of TGF-β. Neutralization of TGF-β in the gut diminishes the DCreg population and the consequent induction of Tregs (149). IL-10 and PGE_2 have also been shown to play an important role in inducing DCregs (150, 151).

Additionally, it has been occasionally reported that some DCs express CD25. $CD25^+$ DCs appear to bind IL-2 from the environment (152), but many questions remain regarding the biological function of CD25 on DCs, including whether IL-2 mediates signaling upon interaction with $CD25^+$ DCs (152-154). A previous study showed that CD25 expression on DCs was induced in response to a cocktail consisting of prostaglandin E_2 (PGE_2), tumor necrosis factor alpha (TNFα), and lipopolysaccharide (LPS), but this analysis did not assess the individual activities of PGE_2, TNFα, or LPS (151). Several previous studies noted the expression of CD25 on distinct subsets of DCs. For example, a subset of regulatory $CD25^+$ DCs expresses indoleamine 2, 3-dioxygenase (IDO), a suppressive molecule secreted by DCs that converts tryptophan into kynurenine (151, 155). In addition, CD25 is expressed on IFN-β-producing

plasmacytoid DCs (pDCs) without the need for TLR-4 agonism. CD40L stimulation also induced CD25 levels on human pDCs in the presence of IL-3 (156).

With all these subsets of DCs, it is not surprising that DCs can initiate a wide range of immune responses. DCs are implicated in immune responses ranging from highly inflammatory immunogenic attacks to robust induction of tolerance. DCs are required for proper clearance of pathogens; they are considered of major importance in the clearance of common viruses and play an indispensable role in combating bacterial infections (157, 158). Their role relies both on the initial recognition of pathogens but, more importantly, on their ability to activate antigen-specific T cells and form lasting memory. Conversely, DCs are also the main APC lineage responsible for differentiation of T cells into the Treg lineage and maintenance of the existing Treg pool through presentation of self-antigen (137). This diverse influence on the immune system is highlighted by the dual role of DCs in MS (159). DCs are implicated as APCs that can activate autoreactive T cells in the periphery and cause differentiation into pathogenic Th1 and Th17 cells in the propagation of EAE (160). Additionally, DCs in the CNS can reactivate these T cells and promote immune invasion of T cells into the CNS (161). Conversely, DCs are crucial for induction of Tregs that prevent EAE. DCs presenting the myelin peptide MOG caused an increase in the levels of Tregs and consequently reduced the induction of EAE (162). Additionally, depletion of DCs led to more severe EAE, highlighting the role of DCs in maintaining a functional Treg pool (163).

1.6 ANTIGEN RECOGNITION

The diverse immune responses induced by DCs are often controlled through DC/T cell interaction, known as an antigen recognition event. Antigen recognition incorporates many cofactors beyond TCR/MHCII-Ag interaction that are integrated to dictate cellular responses in both responder T cells and APCs. T cells and APCs express adhesion molecules to assist in the T cell docking onto the surface of the APC. This allows T cells to spend enough time near the surface to interact with cognate antigen on the surface of APCs. For example, DCs express ICAM-1 that binds to LFA-1 on T cells, assisting in stable intercellular adhesion (164). DCs control the mobility of ICAM-1 on the cell surface to form 'cluster adhesion zones' which increase antigen recognition by T cells (165). Several homophilic cell adhesion interactions also take place and have been shown to play a vital role in natural killer (NK) cell function and B cell activation (166).

In addition to adhesion molecules, costimulatory molecules play a vital role in T cell interaction. Classically known as 'signal 2' in standard antigen recognition models, CD28 on T cells interacts with CD80/CD86 on APCs, which leads to the activation of T cells. This signal licenses T cell activation in response to cognate antigen. On DCs, CD80/86 proteins are upregulated in response to T cell interaction and downstream of TLR stimulation (167). Interactions of costimulatory molecules typically do not directly lead to high levels of downstream signaling; instead, CD28/CD80 ligation enhances the interaction of all members of the immunological synapse, increasing their ability to interact and signal (168). CD28 ligation on T cells is crucial in the activation of all T cell lineages ranging from pathogenic T cells to Tregs (169, 170).

Many other cofactors that contribute to T cell and APC activation have been identified. The interaction between CD40-ligand (CD40L) on T cells and CD40 on APCs in the immunological synapse is crucial for licensing T cell responses. CD40L is upregulated on T cells after TCR recognition, and the engagement of CD40L and CD40 controls activation of both T cells and APCs. Engagement of CD40L leads to proliferative responses in T cells, and T cell expression of CD40L is required for the sustained polarization of Th1 immune responses (171, 172). The interaction between CD40 on B cells and CD40L is crucial for activation of B cells. CD40 engagement triggers B cell adhesion, proliferation, differentiation, and isotype switching (173-175). A defect in CD40 or CD40L leads to Hyper IgM syndrome, because B cells are not properly activated by T cells (176, 177). The CD40/CD40L axis is crucial for activation of APCs to assist in activation of other nearby T cells. CD40-dependent maturation of DCs is far more complex than simply the upregulation of costimulatory molecules. After CD40 engagement by CD40L, downstream CD40 signaling in DCs leads to increased expression and stabilization of the TCR/MHCII-Ag complex (178-180). Additionally, CD40 triggering in DCs leads to an extended lifespan of the DC, a major factor in driving cell-mediated immunity (181, 182). Additionally, the CD40/CD40L axis plays a crucial role in determining T cell fate. High levels of CD40L engagement favors immunogenic responses, while lower levels support Treg responses. Strong costimulation by DCs after treatment with agonistic CD40 diminished regulatory T cell expansion, and CD40-deficient DCs or blocking with anti-CD40L antibody enhanced Treg development and function *in vitro* and *in vivo* (175, 183-185).

Another important costimulatory interaction that is part of the antigen recognition event is the inducible T cell costimulatory molecule (ICOS) on APCs with its ligand (ICOSL) on T cells (186). ICOS is structurally very similar to CD28, and engagement leads to proliferation of

T cells (187, 188). This axis plays a role in determining the polarization of responder T cells. Impaired ICOSL/ICOS interaction diminished Treg and Th17 levels while strongly supporting Th1 responses (189, 190). The exact mechanisms underlying the complex impact of ICOS/ICOSL have yet to be fully uncovered. Several other molecules also engage in the immunological synapse to assist in the fine-tuned antigen recognition event.

A major component dictating the downstream impact of the antigen recognition event in the immunological synapse is the affinity of the TCR/MHC-Ag complex. As described earlier, a low affinity TCR ligation event is indicative of a self-antigen and therefore induces a more tolerant T cell response characterized by non-activation, anergy induction, or Treg differentiation of responder T cells (191, 192). When interacting with mature APCs, low affinity TCR ligation leads to anergy or lower activation potential in responder naïve CD4 T cells (192, 193). Lower affinity TCR ligation mediates decreased effector potential in responder T cells through phosphorylation of specific serine residues of downstream signaling components. These phosphorylated residues then recruit phosphatases that negatively regulate TCR signaling to impact downstream gene activation (191, 194, 195). This negative regulation leads to lower expression of T cell activation markers and less effector functionality in responder T cells (196). In addition to inducing lower activation state of Tcons, low affinity TCR recognition events favor differentiation into Tregs and support Treg function (197-199).

High affinity recognition is indicative of a foreign antigen and strong TCR ligation elicits immunogenic T cells. T cells remain in the lymph node longer following high affinity recognition to clonally expand and activate APCs before differentiating into tissue-infiltrating effector T cells (193, 196, 200). Additionally, higher levels of activation markers are expressed

on T cells following high affinity TCR ligation, allowing for more immunogenic T cell responses. These responder T cells often have higher proliferative potential and adopt a more pathogenic T cell phenotype during autoimmunity (199, 201, 202). Ultimately, affinity of TCR/MHC-Ag interaction plays a crucial role in determining T cell fate, with low affinity interactions supporting tolerogenic T cell responses and high affinity interactions encouraging immunogenic T cell responses.

1.7 VACCINES

Vaccination is the clinical induction of a desired immune response. Classic views of vaccination focus on the immunogenic responses to targeted pathogens leading to immune memory and protection from infection. The strength and duration of the immune memory depends largely on the amount of T cell engagement in response to the vaccine (203). The strongest, longest lasting immune response is induced by live attenuated vaccination. This vaccine class involves the administration of a live virus or bacteria that has been weakened so that it cannot lead to dangerous infection. Since the pathogen is alive, the immune response to the pathogen is complete and closely mimics infection by the pathogen without the danger of severe disease (204). This immune response leads to the most robust T cell and B cell engagement and memory, and live attenuated vaccination often leads to life-long memory. Live attenuated vaccines have been used to eradicate diseases, such as smallpox and polio, and continue to be effective at providing life-long immunity today in the measles, mumps, and rubella (MMR) vaccine (205).

Inactivated vaccines provide the next highest level of protection. These vaccines consist of injection of a dead pathogen, not capable of infection. This class of vaccine still engages a diverse T cell pool given it contains all pathogenic antigens but does not benefit from enhanced T cell engagement that accompanies infection. Currently used inactivated vaccines include vaccines against Hepatitis A, rabies, and influenza. Inactivated vaccines are generally not thought to provide life-long immunity but remain quite effective clinically at prevention of disease (206).

The other classes of vaccination can be grouped into a larger category known as component vaccines, which contain a particular molecular component of the pathogen. These vaccines vary significantly in the protection they provide, depending on how much T cell engagement they induce (207). Vaccines that contain a protein component or nucleic acid component that gets translated into protein, induce the highest level of protection among component vaccines. This is because protein components are presented to T cells on MHC glycoproteins and lead to T cell activation, downstream B cell activation, and associated immune memory. These include toxoid vaccines which contain an altered, harmless form of dangerous toxins produced by bacteria. Among this class is the tetanus toxoid vaccine which provides effective protection but requires a booster every ten years as only T cells and B cells specific to the toxin are activated during vaccination, leading to a relatively narrow protective T cell pool. Anti-tetanus toxoid B cells and the continued production of cross-reactive anti-toxin IgG antibodies provide ongoing immune protection against any subsequent exposure to tetanus toxin. Similarly, recombinant protein vaccines, which contain peptide fragments such as the hepatitis B and the human papilloma virus (HPV) vaccines, as well as RNA vaccines, which encode a

specific protein such as in some SARS-CoV-2 vaccines, elicit effective but shorter-lived immunity (203, 208).

The component vaccine class that elicits the lowest level of protective immunity is polysaccharide vaccines. These vaccines elicit very minimal T cell involvement, leading to weak B cell activation and poor memory (203, 207). The pneumococcal vaccine is a polysaccharide vaccine and is known to provide weak immune memory when used alone (209). To get around the lack of T cell engagement of polysaccharide vaccines, a protein component is often fused to the polysaccharide component to elicit T cell-dependent activation of polysaccharide-specific B cells which causes more robust immune memory and protection (207). This type of vaccine is known as a conjugate vaccine and has been shown to increase the immune protection to associated polysaccharide epitopes above that induced by polysaccharide vaccines (210, 211).

While vaccines are classically used to elicit targeted immunogenic responses against pathogens, several vaccines elicit tolerogenic immune responses for protection or treatment of autoimmune diseases (212). Tolerogenic vaccine strategies often focus on diminishing the autoreactive $CD4^+$ T cell response that carry out autoimmune attacks. This can be accomplished through reduction in pathogenic Th1 or Th17 subsets as well as induction of Tregs (213). The primary approach for tolerogenic vaccination is peptide-based vaccines. The most successful use of peptide-based vaccines has been in the treatment of allergic diseases. This treatment directs antigens of interest to anatomical compartments that favor tolerance such as the skin and gut (214). As previously mentioned, the skin and gut express increased levels of anti-inflammatory molecules such as IL-10 and TGF-β and have specialized APC subsets that favor Treg differentiation, making them effective compartments to target for tolerance induction (215-218).

The successful treatment of allergic diseases has enhanced the development of tolerogenic peptide-based vaccines for the treatment of MS. A substantial impediment for tolerogenic peptide-based vaccines for MS is that self-antigens driving disease appear to vary from patient to patient. Myelin basic protein (MBP), MOG, and proteolipid protein (PLP) epitopes appear involved in MS because MS patients have increased levels of antibodies and activated T cells against these myelin peptides (219, 220). However, the pathogenic epitopes that drive disease exhibit substantial inter-patient variation. This is likely explained by the fact that each MS patient inherits different sets of polymorphic MHC genes that encode MHC glycoproteins that present different arrays of self-peptides. Furthermore, epitopes driving disease may change as the disease progresses through a mechanism known as epitope spreading. The autoimmune attack might be initiated against an epitope of MOG, but as autoimmune-mediated tissue damage increases, other epitopes of MOG and additional CNS peptides also become targeted therefore spreading the autoimmune response.

Due to the dynamic and variable nature of the driving epitopes, designing antigen-specific vaccines is difficult (221, 222). It may be possible to overcome this hurdle by reinforcing immunological tolerance to multiple CNS proteins through the induction of myelin-specific Tregs which can resolve inflammation to unrelated CNS antigens through infectious tolerance (80, 223, 224). A common strategy to accomplish this is to target myelin antigens to APC subsets that favor tolerogenic responses. Our lab has worked for years on such a vaccine. The GMSCF-MOG vaccine is a fusion protein consisting of a GM-CSF domain on the N-terminus fused to a MOG35-55 antigenic domain on the C-terminus. This vaccine has been shown to be an effective prophylactic and therapeutic treatment for rodent models of EAE (225-229). The efficacy of the GMCSF-MOG therapy for EAE mechanistically lies in the induction of

MOG-specific Tregs. One subcutaneous dose of GMCSF-MOG in transgenic TCR 2D2-FIG mice leads to robust expansion of Tregs, growing from 2% to ~40% of the circulating T cell pool (230). Through the GM-CSF domain, the vaccine is believed to target MOG35-55 presentation to DCs, a Treg-favorable APC niche. The targeting nature is highlighted by the required covalent linkage of GM-CSF and MOG. The antigenic domain is also crucial as GMCSF-NFM, or GMCSF-OVA do not elicit tolerance induction (229, 230).

Vaccination, both tolerogenic and immunogenic, rely on adjuvants to enhance the immune response elicited by the vaccine. The most common adjuvants used clinically are precipitated aluminum salts, collectively known as Alum (231). Alum enhances the immune response in two ways. First, associated antigens adsorb to Alum concentrating the antigen in the targeted site and leading to higher antigen load in the microenvironment and higher immune recognition (232). Second, Alum functions as a mild irritant, enhancing recruitment of leukocytes to the site. Through these mechanisms, Alum has been shown to increase the immune response to associated antigens, measured by higher antibody titers. For this reason, Alum is included in nearly all clinically used component vaccines (232, 233). Alum has also been shown to be vital for tolerogenic vaccine activity. IFN-β-based tolerogenic vaccines rely on the presence of Alum to elicit tolerogenic activity, and Alum has been shown to adsorb self-antigen and support activation of Tregs (121, 228, 234-236).

In addition to Alum, FDA-approved adjuvant formulations containing squalene and monophosphoryl lipid A (MPLA) in oil emulsions have been used clinically as adjuvants (237). MPLA is derived from LPS, a potent stimulator of the immune system. LPS, also known as endotoxin, is the main component of gram-negative bacterial cell walls (238). LPS binds to TLR-

4 and elicits robust intracellular signaling and subsequent activation of the immune system and associated inflammation. LPS is pyrogenic and represents the main cause of bacterial sepsis, making it too dangerous to be used as an adjuvant (239, 240). MPLA is a detoxified form of LPS that maintains many functions needed for stimulation of the immune system without the dangerous pyrogenic side effects associated with LPS (240, 241). MPLA (referred to as MPL in the context of adjuvants) was used in older HPV vaccines and provides a novel approach to enhancing the immune response. Typically studied in the context of vaccination, the exact mechanisms of action of MPLA are not completely understood although MPLA has the potential to elicit more targeted immune responses than Alum in the context of viral or bacterial vaccination (240, 241).

CHAPTER 2

MATERIALS AND METHODS

2.1 Mice

C57BL/6J (000664), B6.Cg-Foxp3tm2Tch/J (FIG Foxp3-IRES-GFP 006772), C57BL/6-Tg(Tcra2D2,Tcrb2D2)1Kuch/J (2D2 MOG35-55-specific TCR transgenic 006912) mouse strains were obtained from the Jackson Laboratory (Bar Harbor, ME) and were housed and bred in the Department of Comparative Medicine at East Carolina University Brody School of Medicine. 2D2-FIG mice were obtained through cross breeding of FIG and 2D2 mice. Animal use and animal care were performed in accordance with approved Animal Use Protocols and guidelines of the East Carolina University Institutional Animal Care and Use Committee., 2D2-FIG, mice were derived through intercross breeding and routinely screened by FACS analysis of peripheral blood mononuclear cells (PBMCs) with antibodies for the 2D2 Vβ11 and Vα3.2 TCR proteins. GFP expression from FIG mice was used as a surrogate marker of FOXP3 expression. FIG mice were screened via PCR, with positive mice determined via a single 325 base pair band measured on a 1% agarose gel.

2.2 Reagents and generation and purification of recombinant proteins

Lipopolysaccharide (*Escherichia coli*, J5 (Rc Mutant)) was acquired from List Labs (Campbell, CA). Monophosphoryl Lipid A (*Salmonella minnesota*, R595) was acquired from Invivogen

(San Diego, CA). Peptides MOG35-55 and NFM13-37 were obtained from Genscript (Piscataway, NJ). Monoclonal antibody MR-1 (hamster anti-mouse CD40L IgG) was purchased from BioXcell (West Lebanon, NH). Fusion proteins GMCSF-MOG and GMCSF-NFM were comprised of the murine GM-CSF cytokine as the N-terminal domain and the relevant antigenic peptide as the C-terminal domain, with a 8-histidine tag for purification. Recombinant proteins GM-CSF and IL-2 contained the 8-histidine tag C-terminus but did not contain an antigenic peptide domain. These recombinant proteins were produced by stably-transfected human embryonic kidney (HEK) cells or from Chinese hamster ovary (CHO-S) cells. Expression supernatants were collected every 3-4 days and cells were reseeded under selection pressure by G418 (Biovision, Waltham, MA). For purification, the collected supernatants were incubated with resin of Ni-NTA Agarose beads. Expression supernatant was incubated for 1 hour with resin followed by gravity drip through a column containing a resin bed. The resin bed was then extensively washed with wash buffer (50 mM NaH2PO4, 500 mM NaCl, pH 8.0) with increasing amounts of imidazole (10-, 20-, or 60-mM imidazole, pH 8.0). Recombinant proteins were then eluted with 250 mM imidazole (pH 8.0) and were concentrated and diafiltrated in Amicon Ultra-15 centrifugal filter devices (EMD Millipore, Billerica, MA). Recombinant rat TGF-β was expressed by use of HEK cells and purified in the same method as above with use of a different buffer (150 mM NaCl, 50 mM Tris-HCl, pH 8.0) with increasing amounts of imidazole (10 mM, 20 mM, 40 mM, 60 mM imidazole). Elution was performed with the same wash buffer containing 250 mM imidazole. Protein quantity was assessed by absorbance at 280 nm, and purity was assessed by SDS-PAGE. Bioactivity of each GM-CSF domain preparation was determined by the ability to drive proliferation of bone marrow cells, and the antigenic peptide domain was assessed in proliferative assays of 2D2 T cells (MOG35-55 and NFM13-37).

Bioactivity of IL-2 was assessed by the ability to induce proliferation of SJL-PLP T cells. Bioactivity of TGF-β was assessed by the ability to induce Tregs from splenocyte cultures.

2.3 Flow cytometric analyses of lymphocytes, splenocytes, and PBMCs

Inguinal lymph nodes and spleen were dissected from mice and placed into 10 ml of HBSS. Dissected spleens were pressed through a wire mesh screen and a 70 μm cell strainer (Corning, NY) to obtain single-cell suspensions. Lymph nodes were digested with collagenase type II (100 U/ mL or 400 U/ mL) in HBSS supplemented with Mg^{2+} and Ca^{2+}. Cells were then passed through a 70 μm cell strainer. Blood was obtained via submandibular vein puncture and was added to 200 μL sodium citrate (130 mM). Cells were washed in 3 ml HBSS with 2% FBS and stained with cocktails of respective fluorochrome-conjugated antibodies for 1 hour at 4°C in the dark. For staining, 0.5-1.0 μL of each fluorochrome conjugated antibody was added to a master mix tube with 100 μL of cRPMI for each tube. After all antibodies were added, 100 μL of the mix was added to each sample tube. Just one antibody was added for each single stain control tube. For blood, erythrocytes were lysed by incubating samples for 10 min on ice with 3 ml of ammonium chloride lysis buffer (150 mM NH_4Cl, 10 mM $NaHCO_3$, 1.2 mM EDTA- pH 7.2). Lysis was repeated when necessary. For cell culture, cells were removed from culture conditions and washed once with HBSS + 2% FBS. To obtain 'count' data, 10,000 reference beads were added to samples immediately before flow cytometric analysis (AccuCount blank particles or FITC-, PE-, or APC-conjugated EasyComp fluorescent particles 3.0-3.4 μm, Spherotech, Lake Forest, IL). The use of reference beads enabled comparisons of absolute cell numbers among different samples.

For intercellular staining of FOXP3, blood was collected, and RBCs were lysed as previously described. PBMCs were fixed for 20 minutes using 2% paraformaldehyde (PFA) before addition of cRPMI to neutralize PFA. Cells were then permeabilized with a 20-minute incubation in permeabilization buffer (1x PBS + 2% FBS + 0.5% saponin + 0.1% tween-20). After permeabilization, cells were resuspended in staining buffer (1x PBS + 2% FBS + 0.1% saponin + 0.1% tween-20) along with 5 µL of each fluorochrome-conjugated antibody and then incubated for 2 hours at 4°C in the dark. Cells were extensively washed between fixing, permeabilization, and staining treatments.

For intracellular staining of pSTAT5, cells were taken out of culture and placed in tubes ($1x10^5$ cells/ tube) in 200 µL of pre-warmed media. Cells were stimulated with 1 µM GM-CSF or 100 nM IL-2 at 37°C for 40 minutes. Cells were fixed by adding 1 mL of cold 4% PFA to each tube. Cells were incubated for 40 minutes at room temperature and then were washed twice with HBSS + 2% FBS. Cells were permeabilized by resuspending cells in 100 µL ice cold methanol and incubated for 40 minutes at room temperature. Cells were washed twice with HBSS + 2% FBS before resuspending in cRPMI. 15 µL anti-pSTAT5 and 1 µL of all surface marker antibodies were added to each tube, vortexed, and stained for 1 hour at room temperature.

To stain for CD40L, cells were cultured for 4 hours at 37°C before addition of fluorescently labeled anti-CD40L antibody. Cells were cultured for an additional 2 hours at 37°C before being washed and stained. Fluorochrome-conjugated mAbs were obtained from BioLegend and included CD3-BV421, PE/Dazzle 594, PE (17A2), CD4-BV785, BV421, APC (GK1.5), CD25-BV421, PE, APC, APC/Cy7 (PC61 or 3C7), CD44-BV421 (IM7), TCR-Vβ11-PE, APC (KT11), CD86-FITC (GL-1), I-A^b- APC (AF6-120.1). CD19-BV421, PE (6D5), CD11c-BV21, BV785

(N418), CD11b- FITC, BV421 (M1-70), CD40L-PE (MR-1), CD40-PE/Cy7 (3/23), FOXP3-Alexa Fluor 488 (150D). Flow cytometry was performed on either an LSR II from Becton Dickinson (San Jose, CA) or an Aurora 5 laser from Cytek (Fremont, CA). Analysis of flow data was done on either FlowJo Software (Ashland, OR) or FCS Express from De Novo Software (Pasadena, CA).

2.4 Dendritic cell culture

GM-CSF and IL-4 were obtained by use of baculovirus expression systems in Sf9 cells. The supernatants from this culture system were sterile filtered before use. DC cultures were started with bone marrow from the tibias and femurs of C57BL/6 mice between 6-8 weeks of age. Bone marrow cells were added to untreated petri dishes in complete RPMI (cRPMI; 10% heat-inactivated fetal bovine serum, 2 mM glutamine, 100 μg/mL streptomycin, 100 U/mL penicillin, 50 μM 2-mercaptoethanol) and supplemented with 1 U/mL murine GM-CSF. Cells were cultured for 4 days before a full media change and then supplemented with 1 U/mL GM-CSF and 1 U/mL IL-4. Cells were cultured 2 more days before another media change. Cells were then supplemented with GM-CSF and IL-4 with or without 100 ng/ mL LPS. Cells were then cultured for another 24 hours before analysis. To remove cells from the dishes, cells were incubated for 10 minutes at room temperature with release buffer (1x PBS + 2.5 mM EDTA, 0.5% BSA) and then blasted off with a pipette. cRPMI was then added to the release buffer to neutralize the EDTA.

2.5 Treg culture

For initial activation, 2D2-FIG splenocytes were harvested and cultured at 2 x 10^6 cells / mL in cRPMI with 1 μM MOG35-55, and 10 nM TGF-β. Cells were cocultured for 3-4 days before a full media change. Cells were then reseeded in cRPMI with 1 nM CD25-IL2 fusion protein as described previously (242). Media was changed every 3-4 days supplemented with 1 nM CD25-IL2 until Tregs reach 90% purity as determined by flow cytometry. When Treg numbers began to decline, the line was reactivated by adding Tregs at a 10:1 ratio with irradiated DCs cultured as described above along with 1 μM MOG35-55, 10 nM TGF-β and 1 nM CD25-IL2. Cells were then removed from reactivation after 3-4 days and kept in 1 nM CD25-IL2.

2.6 Induction and assessment of EAE

CFA (Incomplete Freund's Adjuvant with 4 mg/ml heat-killed *Mycobacterium tuberculosis* H37Ra, BD Biosciences, Franklin Lakes, NJ) was mixed 1:1 with MOG35-55 in PBS. The CFA/antigen mixture was emulsified by sonication. EAE was elicited by injection of 200 μg MOG35-55 in a total volume of 100 μl emulsion via two subcutaneous injections of 50 μl across the lower back. Each mouse received separate intraperitoneal injections (200 ng) of Pertussis toxin in PBS on days 0 and 2. All immunizations were performed under isoflurane anesthesia (Abbott Laboratories, Chicago, IL). Mice were assessed daily for clinical score and body weight. The following scale was used to score the clinical signs of EAE: 0, no disease; 0.5, partial paralysis of tail without ataxia; 1.0, flaccid paralysis of tail or ataxia but not both; 2.0, flaccid paralysis of tail with ataxia or impaired righting reflex; 3.0, partial hind limb paralysis marked by inability to walk upright but with ambulatory rhythm in both legs; 3.5, same as 3.0 but with full paralysis of one leg; 4.0, full hindlimb paralysis; 5.0, total hindlimb paralysis with forelimb

involvement or moribund. A score of 5.0 was a humane endpoint for euthanasia. When mice were at or above a score of 2.0, they received subcutaneous injections of saline and manual bladder expression twice daily. Mice that did not exhibit EAE had a score of zero, and these scores were included in the group average. Mice that exhibited humane endpoints as assessed by body weight loss, body score, or clinical score of 5.0 were subjected to humane euthanasia and were omitted from scoring thereafter.

2.7 Preparation of vaccines

MPLA is dissolved in dimethyl sulfoxide (DMSO). For control purposes, all vaccines given when at least one group was administered MPLA contained equal amounts of DMSO. "MPLA + GMCSF-MOG" vaccines contained 80 μL of 1 mg/ mL MPLA in DMSO + 2 nmoles GMCSF-MOG in 20 μL of PBS for a total volume of 100 μL/ mouse. In the same experiment, "saline" mice received 80 μL DMSO and 20 μL PBS, and "GMCSF-MOG alone" mice received 80 μL DMSO + 2 nmoles GMCSF-MOG in 20 μL PBS. All solutions were combined and mixed to give one homogeneous vaccine.

2.8 Statistical Analysis

To determine statistical significance, comparisons among three groups or more were analyzed via use of ANOVA with the Holm-Sidak multiple comparisons test unless otherwise noted. Comparisons between two groups were analyzed by Student's *t*-test. A p-value <0.05 was considered significant. For experiments that obtained the same measurement over several timepoints, a repeated measures ANOVA was used unless otherwise stated. Error bars represent standard deviation (SD) of the group unless otherwise noted in the figure legends.

CHAPTER 3

TLR-4 AGONISM LEADS TO INCREASED EXPRESSION OF FUNCTIONAL CD25 ON DENDRITIC CELLS COUPLED TO EXPRESSION OF MHCII AND CD86

3.1 ABSTRACT

CD25 is variably expressed on DCs, but functional consequences are unresolved. Here, we show that LPS and MPLA elicited CD25 expression on DCs, both *in vivo* and *in vitro*, concomitant with DC maturation as reflected by increased expression of MHCII and CD86. LPS-induced CD25 expression was unique to DCs as LPS exposure did not elicit CD25 expression on B cells or macrophages. This increase in CD25, MHCII, and CD86 was rapid and was detected 45 minutes after LPS exposure. This $CD25^+$ DC phenotype was stable for 3 days, even after removal of the stimulus. IL-2 bound to CD25 on the surface of DCs but did not induce signaling through phosphorylation of STAT5, and the IL-2 bound by these $CD25^+$ DCs generated a concentration gradient sufficient to induce IL-2-dependent proliferation of $CD25^+$ T cells. Altogether, we show that expression of functional CD25 induced by TLR-4 agonism is a unique feature of mature DCs.

3.2 RESULTS

LPS led to increased expression of CD25 on DCs coupled to increased CD86 and MHCII expression *in vitro*

We showed that LPS (50 ng/mL), when added to standard DC cultures, resulted in expression of CD25 on the surface of the DCs (Figure 3.1A-B). As a baseline control, we also showed LPS increased CD86 and MHCII expression on $CD11c^+$ DCs, which denotes classical DC maturation (Figure 3.1A-B) (243-245). With addition of LPS, an average of 52% of $CD11c^+$ DCs expressed CD25, compared to just 13% of DCs without LPS (Figure 3.1B) The same effect was seen with MHCII and CD86 expression, because CD86 expression increased from 6% to 58% and MHCII expression increased from 29% to 69% with LPS addition (Figure 3.1B). We also showed that increases in CD25, CD86 and MHCII expression were coupled, presumptively as part of a coordinated gene expression program. Of the $CD25^+$ DCs, 98% were $CD86^+$ and 95% were $MHCII^+$ (Figure 3.2A-B). These data revealed that CD25 is a marker of mature DCs much like CD86 and MHCII.

TLR-4 agonism was the main driver of CD25 expression on DCs *in vitro*

To show that TLR-4 agonism was the main driver of CD25 expression on DCs, we utilized a detoxified LPS derivative, MPLA, that also agonizes TLR-4. When immature DCs in culture were treated with LPS (50 ng/ mL) or MPLA (1 µg/ mL), DCs increased expression of CD25, CD86, and MHCII whereas immature DCs treated with the TLR-3 agonist Poly I:C (10 µg/ mL) exhibited a marginal increase in CD25 (Figure 3.3A). TLR-4 agonism led to an increased percentage of DCs expressing CD25 from 2% to 30% for LPS and 34% for MPLA,

whereas Poly I:C treatment resulted in 6% $CD25^+$ DCs, an insignificant increase from 2% of untreated DCs. We also showed that MPLA and LPS increased CD86 (Figure 3.3B) and MHCII (Figure 3.3C) expression on $CD11c^+$ DCs, while Poly I:C did not induce CD86 or MHCII expression. LPS led to higher CD86 levels than MPLA despite being at a 20-fold lower concentration. These data indicated TLR-4 agonism, but not TLR-3 agonism, is sufficient to induce high levels of CD25 on DCs by a mechanism coordinated with induction of the CD86 and MHCII maturation markers.

Other groups reported that a cocktail of LPS, PGE_2, and TNF-α induces CD25 expression on DCs, but this group did not dissect the individual actions of each mediator. We showed that LPS alone was the main driver of CD25 expression on DCs *in vitro*. LPS was able to drive CD25 expression from 9% to 36%, while PGE_2 (1 µg/mL) and TNF-α (20 ng/mL) alone did not drive an increase in CD25 expression on DCs (Figure 3.4A-B). Additionally, while all three mediators led to the highest CD25 expression (53%), the four groups with the highest percentage of $CD25^+$ DCs were all treated with LPS (Figure 3.4C). Thus, LPS, the main driver of CD25 expression, was utilized throughout the remaining experiments. These data together highlight the role of TLR-4 agonism in CD25 expression on DCs.

CD25 expression in response to TLR-4 agonism was unique to the DC lineage *in vitro*

We next hypothesized that CD25 expression in response to TLR-4 agonism was unique to DCs. Accordingly, when LPS (50 ng/mL) was added to splenocytes in culture, the DCs and not the B cells showed a significant elevation in CD25 expression (Figure 3.5A-B). In response to LPS, the percent of B cells expressing CD25 increased slightly but not significantly while the percent of DCs expressing CD25 increased significantly from 4% to 35% (Figure 3.5B).

Additionally, the CD25 MFI on LPS-stimulated $CD25^+$ DCs increased about 3-fold while the CD25 MFI on $CD25^+$ B cells was unaffected (Figure 3.5C). Although B cells did not show an increase in CD25 expression, they did show an increase in CD19 expression, as well as an increase in size indicating they were activated by LPS (Figure 3.5A) (246).

CD25 was also largely absent on other APCs of the myeloid lineage (Figure 3.6A-C). M-CSF was used to derive macrophages from the bone marrow while GM-CSF was used to derive DCs (247). In M-CSF cultures, $CD25^+$ percentages and MFI values were not impacted by LPS treatment while GM-CSF cultures showed increases in $CD25^+$ DC percentage from 3% to 30% (Figure 3.6B) and a 2-fold increase in CD25 MFI (Figure 3.6C) in response to LPS. To further test whether TLR4-induced CD25-expression is unique to DCs, we replaced GM-CSF with Flt3-L, another DC differentiating factor (248, 249), and observed similar results (Figure 3.7A-B) in that addition of LPS to Flt3-L-treated cells caused an elevation in CD25, CD86, and MHCII expression compared to untreated controls (Figure 3.7B). In addition to differences in expression of observed markers, LPS-treatment of DCs (both Flt3-L and GM-CSF differentiated DCs) impacted the light scatter properties of the cells. When treated with LPS, cells displayed increased autofluorescence and increased internal complexity, presenting as a difference in fluorescence of the "negative" cells (Figure 3.6A (bottom) and 3.7A). These differences were more pronounced for DCs compared to macrophages. However, when single-stained controls were used for each treatment, the "positive" cells presented at the same fluorescence cut-off. Taken together, these data indicated that LPS treatment has a unique impact on DCs compared to other APCs, namely that LPS selectively induces CD25 expression on DCs and not on other APC subsets, at least under these culture conditions.

The CD25$^+$ DC phenotype was induced rapidly and reflected a stable phenotype *in vitro*

The importance of CD25 on DCs was supported by the rapid expression of CD25, MHCII, and CD86 after exposure to 100 ng/mL of LPS (Figure 3.8A-D). After just 30 minutes of exposure, all three markers increased above those levels noted at "zero" minutes. Statistical significance was reached at 45 minutes (Figure 3.8A-D). At the 45-minute time point, CD25$^+$, CD86$^+$ and MHCII$^+$ cell percentages and MFIs increased above levels seen prior to LPS stimulation. This increasing expression of CD25, CD86 and MHCII plateaued around 3 hours after LPS treatment and remained steady for the remainder of the 8.5-hour experiment (Figure 3.8B). This rapid increase in surface expression may reflect an initial mobilization from intracellular stores rather than new protein synthesis. Furthermore, the rapid increase of CD25, CD86, and MHCII together further support that these gene expression profiles are coupled together, likely in a protein expression and/or in intracellular storage. In addition to rapid expression, these markers were stably expressed on DCs. When LPS was removed from the culture after 1 day, cells remained positive for CD25, CD86, and MHCII for 2 additional days (Figure 3.9A-B). In fact, despite LPS being removed from the culture, CD25 and CD86 expression increased on CD25$^+$ cells increasing from 40% on Day 1 to 55% on Day 3 and CD86$^+$ cells increasing from 68% to 85% (Figure 3.9B). MHCII expression stayed relatively stable. This finding suggested that the CD25$^+$ CD86$^+$ MHCII$^+$ DC phenotype represented a stable, differentiated phenotype.

DCs classically lose proliferative capacity in their mature state (250). We hypothesized TLR-4 agonism-based activation would inhibit proliferation of the DCs in response to GM-CSF. We found both TLR-4 agonists, MPLA (10 ng/ mL – 10 µg/ mL) and LPS (1 ng/ mL – 10 µg/ mL), inhibited DC proliferation in comparison to no treatment (Figure 3.10A). At 100 ng/ mL,

LPS inhibited DC proliferation about 20-fold compared to blank while MPLA inhibited DC proliferation by over 5-fold. MPLA inhibited DC proliferation in a more gradual manner compared to LPS which showed no inhibition at 100 pg/ mL and 8-fold inhibition at 1ng/ mL. This indicated LPS is a more potent inhibitor of DC proliferation, consistent with other data indicating LPS is a more potent DC activator compared to MPLA. Overall, these data indicated that TLR-4 agonism induces a rapid and stable increase of CD25, CD86 and MHCII expression that reflected a mature DC phenotype.

CD25$^+$ DCs exhibited specific binding to IL-2 *in vitro*

We next wanted to explore the role of CD25 on LPS-treated DCs *in vitro*. First, we explored the ability of CD25 on DCs to bind to its ligand, IL-2. DCs were pulsed with His-tagged IL-2 then stained for surface bound IL-2 with a fluorescently labeled anti-His antibody. We found that LPS-treated DCs pulsed with IL-2 showed detectable binding of IL-2 to the surface (Figure 3.11A-B). When pulsed with IL-2, about 16% of LPS-treated DCs showed detectable IL-2 binding compared to about 3% of untreated DCs. Additionally, the MFI of IL-2 bound to the surface was 1.4-fold higher on LPS-treated DCs compared to untreated DCs which strongly trended toward significance indicating LPS-treated DCs can bind more IL-2 (Figure 3.11C). In a separate experiment, IL-2 and CD25 were co-stained via use of the anti-His-tag and anti-CD25 antibody clone 3C7, respectively. 3C7 antibody is an anti-CD25 mAb that does not disrupt IL-2/ CD25 interactions but binds CD25 near the binding pocket of IL-2. In this experiment, CD25 expression and IL-2 binding levels showed a strong positive correlation (Figure 3.12A). 55% of CD25$^+$ DCs had IL-2 bound to the surface while under 3% of CD25$^-$ DCs had IL-2 bound (Figure 3.12B). The same trend was observed for IL-2 MFI, with CD25$^+$

DCs displaying nearly 3-fold higher MFI of bound IL-2 compared to $CD25^-$ DCs (Figure 3.12C). Together these data provided evidence that CD25 on LPS-treated DCs bound to IL-2.

We next sought to determine if the DCs signal in response to IL-2. Using pSTAT5 as an indicator of canonical IL-2 signaling, we did not detect signal transduction in response to IL-2 in LPS-treated DCs (Figure 3.13A-C). IL-2 stimulation did not lead to an increase in either pSTAT5 MFI of $pSTAT5^+$ positive cells (Figure 3.13B) or percentages of $pSTAT5^+$ cells (Figure 3.13C) in LPS-treated or untreated DCs. Positive controls of pSTAT5 signal transduction included GM-CSF-induced pSTAT5 signaling in DCs and IL-2-induced pSTAT5 signaling in an SJL derived IL-2 dependent T cells line. Both GM-CSF stimulated DCs and IL-2 stimulated T cells showed high levels of detectable pSTAT5 (Figure 3.13.A). These data provide evidence that IL-2 binds but does not efficiently signal in $CD25^+$ DCs.

We next hypothesized that the bound IL-2 could be utilized by responder T cells. We found that IL-2 bound to LPS-treated DCs elicited IL-2-dependent proliferation of responder T cells, even when it was the only source of IL-2 in culture (Figure 3.14A). When IL-2 was bound to the surface of LPS-treated DCs, responder T cell proliferation increased 16-fold compared to proliferation with no IL-2 present. In comparison, T cells did not proliferate when cultured with IL-2 pulsed untreated-DCs that lacked CD25. These results indicated that IL-2 bound to $CD25^+$ DCs and that this IL-2 pool was accessible for T cell utilization and growth. The SJL T cell proliferation observed was independent of antigen recognition. Therefore, the IL-2-induced proliferation is likely a result of IL-2 released from CD25 on DCs. Likewise, these results suggest that $CD25^+$ DCs can act as a source of IL-2 to support local T cell growth.

3.3 CONCLUSIONS

LPS and MPLA elicit CD25 expression concomitant with DC maturation. CD25 is coregulated with antigen presentation machinery such as MHCII and the costimulatory molecule CD86. Additionally, CD25 on DCs can bind IL-2 and supply IL-2 to T cells, highlighting a possible role in the immunological synapse for CD25 expression on DCs in regulating T cell proliferation.

FIGURE 3.1 | TLR4 agonism elicited CD25 expression on DCs together with CD86 and MHCII expression. DCs were generated as described in the Materials and Methods. (A-B) LPS (50 ng/ mL) was added for 24 hours to LPS-treated groups on day 6 of culture. Cells were removed from petri dishes with 2.5 mM EDTA release buffer and stained for CD11c, CD86, MHCII, and CD25. (A) Shown are representative dot plots comparing CD25, CD86 and MHCII expression. Plots are gated on $CD11c^+$ cells. Bar graphs were generated from replicate experiments. Each experimental replicate represents DC cultures derived from different individual mice. Shown are the average percentage of $CD11c^+$ cells expressing CD25 (LPS-treated n=23, untreated n=25), CD86 (LPS-treated n=9, untreated n=9) or MHCII (LPS-treated n=16, untreated n=16). Statistical significance was determined by use of a two-tailed t-test comparing LPS-treated vs. untreated for each marker. (***$p < 0.001$)

Figure 3.1

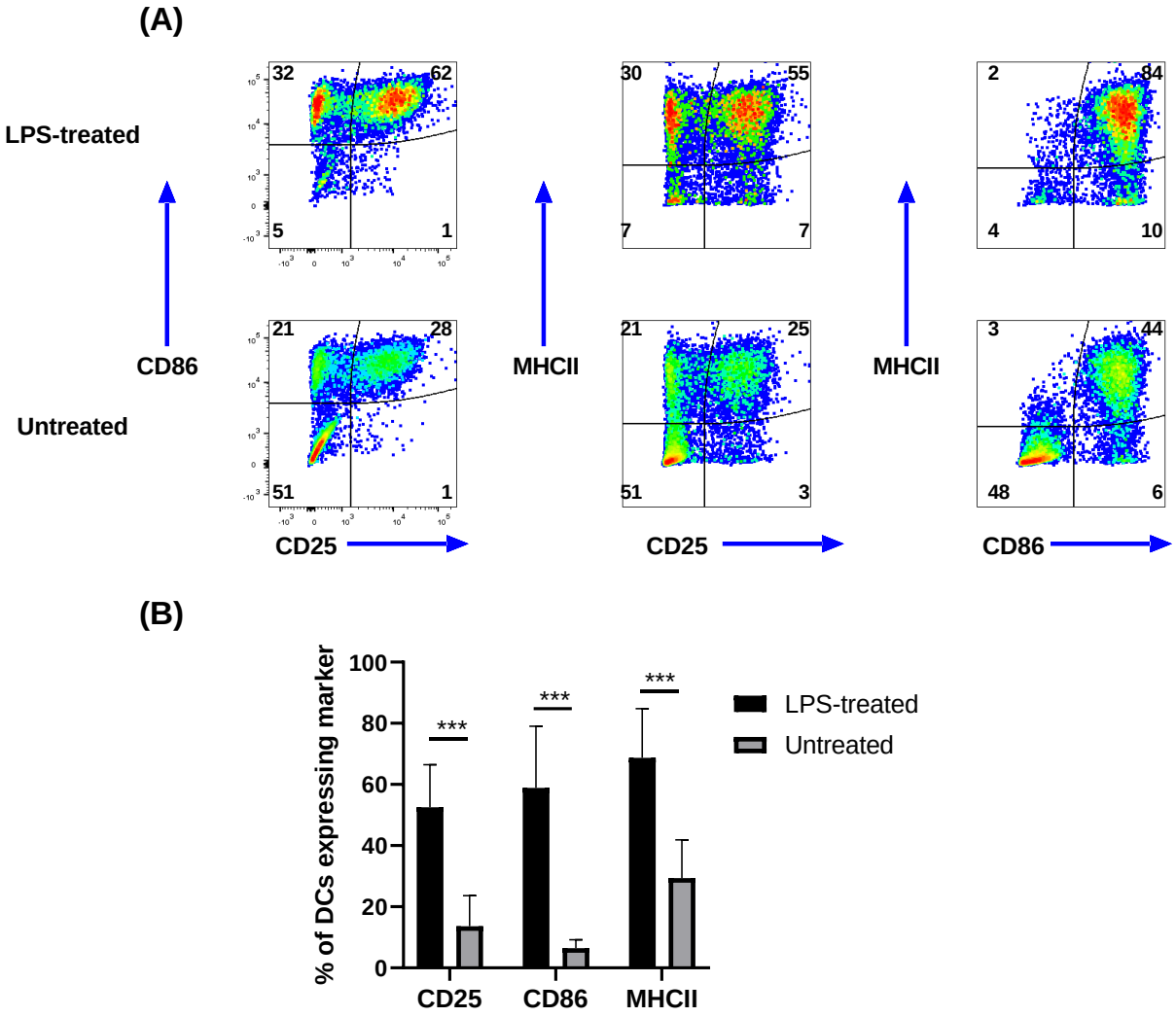
(A)
LPS-treated
Untreated
CD86
CD25
MHCII
CD25
MHCII
CD86
32
62
5
1
30
55
7
7
2
84
4
10
21
28
51
1
21
25
51
3
3
44
48
6
(B)
% of DCs expressing marker
100
80
60
40
20
0
***
***
***
CD25
CD86
MHCII
LPS-treated
Untreated

FIGURE 3.2 | CD25 expression was coupled to CD86 and MHCII expression. DCs were generated as described in the Materials and Methods. LPS (50 ng/ mL) was added for 24 hours to LPS-treated groups. Cells were removed from petri dishes with 2.5 mM EDTA release buffer and stained for CD11c, CD86, MHCII and CD25. (A) Shown is a representative dot plot of CD86 and MHCII expression gated on $CD11c^{+}CD25^{+}$ cells. (B) Shown are bar graphs also gated on $CD25^{+}$ $CD11c^{+}$ cells in the LPS-treated group (n=2). Replicate experiments represent DC cultures derived from individual mice.

Figure 3.2

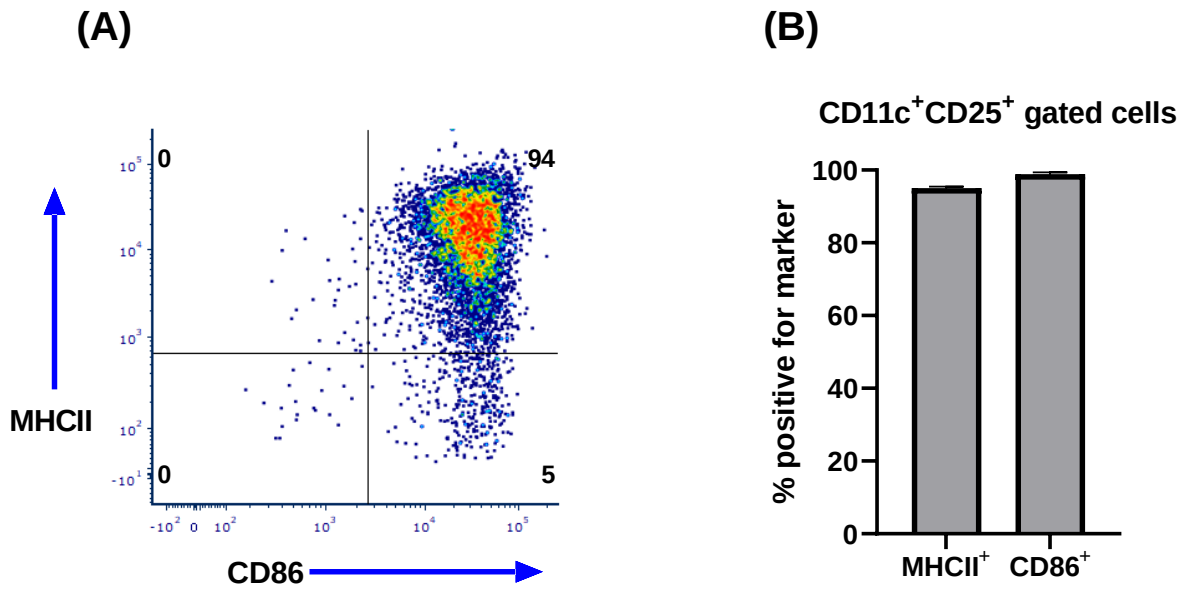
(A)
(B)
MHCII
CD86
0
94
0
5
CD11c+CD25+ gated cells
% positive for marker
100
80
60
40
20
0
MHCII+
CD86+

FIGURE 3.3 | TLR-4 but not TLR-3 agonism increased CD25 on DCs. DCs were generated as described in the Materials and Methods. Concentrations of 50 ng/ mL LPS, 1 μg/ mL MPLA, or 10 μg/ mL Poly I:C were added to DC cultures for 24 hours. (A-C) Representative dot plots show (A) CD25, (B) CD86 and (C) MHCII expression on $CD11c^+$ DCs together with respective corresponding bar graphs (n=3) to highlight differences between treatment groups. Replicates represent DC cultures derived from individual mice. Statistical significance was determined by use of a one-way ANOVA and post-hoc t-tests. (**$p < 0.01$ and ***$p < 0.001$)

Figure 3.3

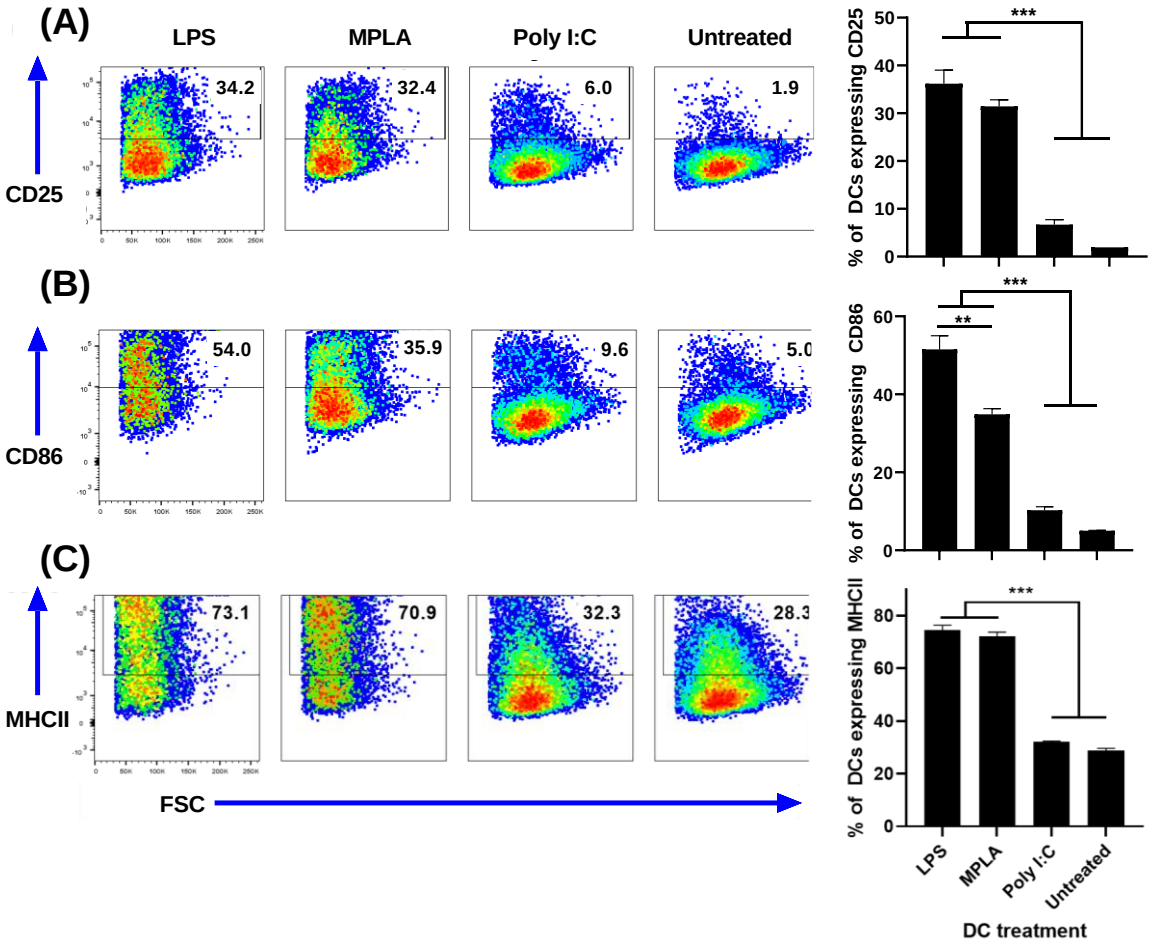
(A)
LPS
MPLA
Poly I:C
Untreated
34.2
32.4
6.0
1.9
CD25
(B)
54.0
35.9
9.6
5.0
CD86
(C)
73.1
70.9
32.3
28.3
MHCII
FSC
% of DCs expressing CD25
% of DCs expressing CD86
% of DCs expressing MHCII
***
**
LPS
MPLA
Poly I:C
Untreated
DC treatment

FIGURE 3.4 | LPS was the main driver of $CD25^+$ DCs. DCs were generated as described in the Materials and Methods. Every combination of 50 ng/ mL LPS, 20 ng/ mL TNF-α, or 1 μg/ mL PGE_2 was added for 24 hours. Representative dot plots (A) and compiled bar graphs (B-C) are gated on $CD11c^+$ DCs to highlight the impact of each individual mediator on CD25 expression (n=2). Replicates represent DC cultures derived from individual mice. Statistical significance was determined by use of a one-way ANOVA and post-hoc t-tests. (**$p < 0.01$)

Figure 3.4

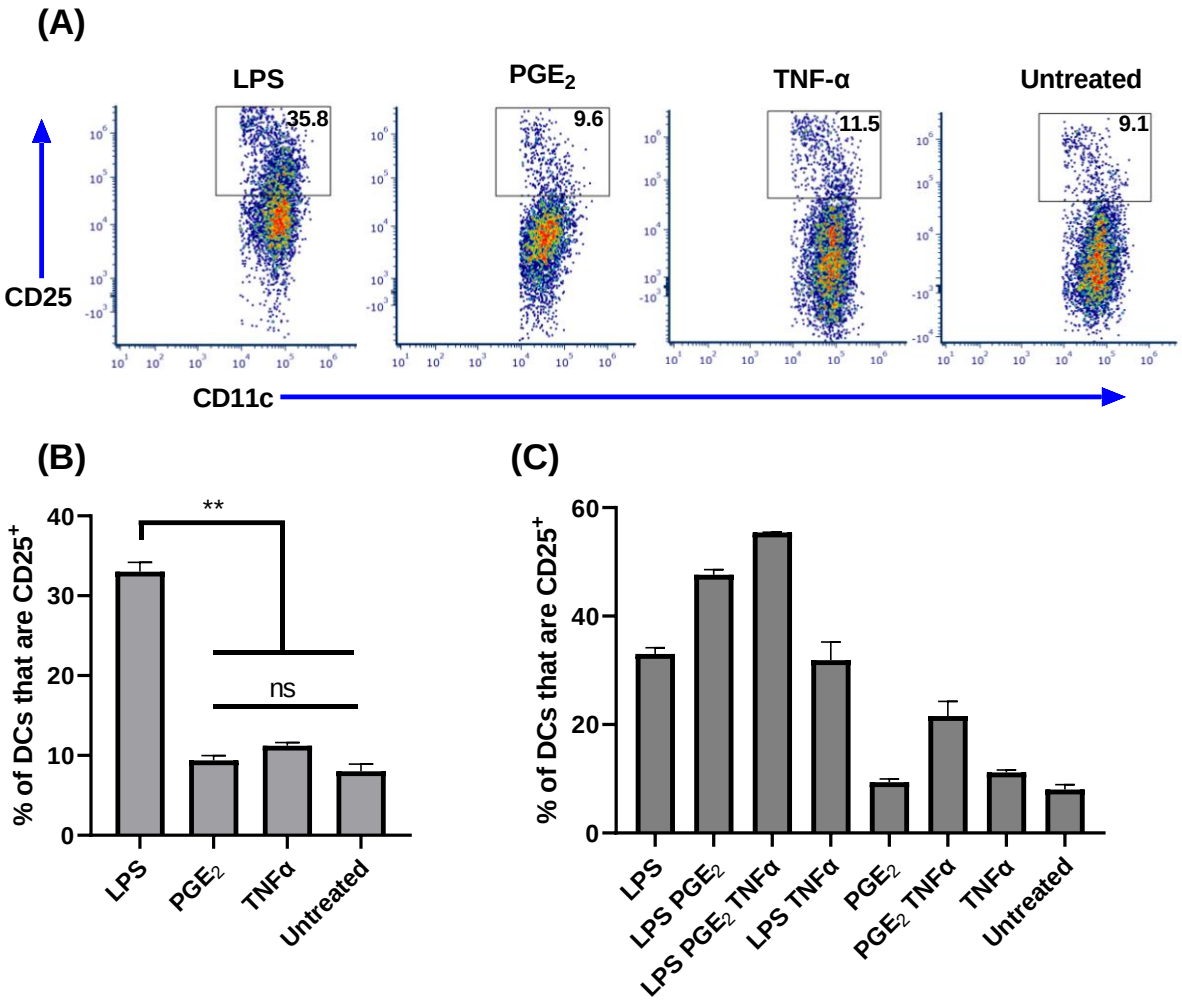
(A)
LPS
PGE2
TNF-α
Untreated
35.8
9.6
11.5
9.1
CD25
CD11c
(B)
% of DCs that are CD25+
**
ns
LPS
PGE2
TNFα
Untreated
(C)
% of DCs that are CD25+
LPS
LPS PGE2 TNFα
LPS PGE2 TNFα
LPS TNFα
PGE2
PGE2 TNFα
TNFα
Untreated

FIGURE 3.5 | TLR-4 agonism led to CD25 expression on DCs but not B cells. Splenocytes were harvested from C57BL/6 mice and pressed though a 70 µm cell strainer to obtain a single cell suspension. Cells were then plated at 1 x 10^6 cells/ mL in cRPMI with or without 50 ng/ mL LPS in the presence of murine GM-CSF and IL-4. Cells were cultured for 3 days and then harvested and stained for CD11c, CD19 and CD25. (A) Representative dot plots shown are gated on $CD19^+$ cells (top) or $CD11c^+$ cells (bottom). (B) Bar graphs are shown depicting the percentage of CD25-expressing cells with B cells (n=2) defined as $CD19^+$ and DCs (n=2) defined as $CD11c^+$. (C) MFI is shown gated on $CD25^+$ cells for B cells ($CD19^+$) and DCs ($CD11c^+$). Replicates represent DC cultures derived from individual mice. Statistical significance was determined by use of two-tailed t-tests comparing LPS-treated and untreated for each cell type. (*$p < 0.05$)

Figure 3.5

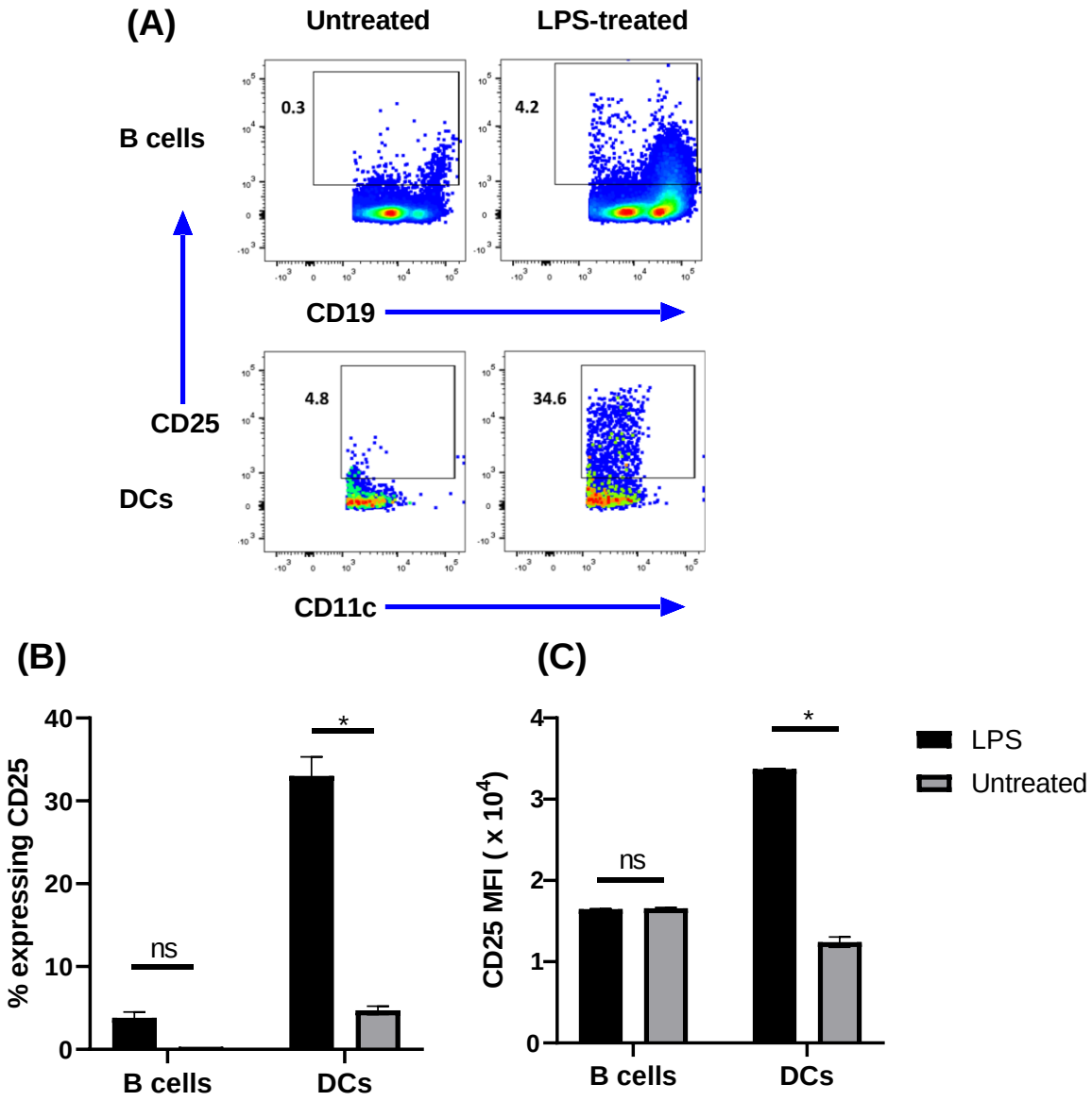
(A)
Untreated
LPS-treated
B cells
0.3
4.2
CD19
CD25
4.8
34.6
DCs
CD11c
(B)
% expressing CD25
40
30
20
10
0
ns
*
B cells
DCs
(C)
CD25 MFI (x 10^4)
4
3
2
1
0
ns
*
B cells
DCs
LPS
Untreated

FIGURE 3.6 | TLR-4 agonism elicited CD25 expression on DCs but not macrophages. DC and macrophage cultures were generated as described in the Materials and Methods. DCs were derived with GM-CSF and macrophages were derived with M-CSF. For both groups, 50 ng/ mL LPS was added for 24 hours before cells were removed with 2.5 mM EDTA release buffer and stained for CD11b, CD11c, F4/80 and CD25. (A) Representative dot plots shown are gated on $CD11b^+$ $F4/80^+$ cells representing macrophages (top) or $CD11b^+$ $CD11c^+$ DCs (bottom). (B) Bar graphs are shown depicting the percentage of CD25-expressing macrophages (n=2) and DCs (n=2). CD25 MFI is shown (C) gated on $CD25^+$ cells for M-CSF cultures ($F4/80^+$) and GM-CSF cultures ($CD11c^+$). Replicates represent cultures derived from individual mice. Statistical significance was determined by used of two-tailed t-tests comparing LPS-treated and untreated samples for each cell type. (**$p < 0.01$ and ***$p < 0.001$)

Figure 3.6

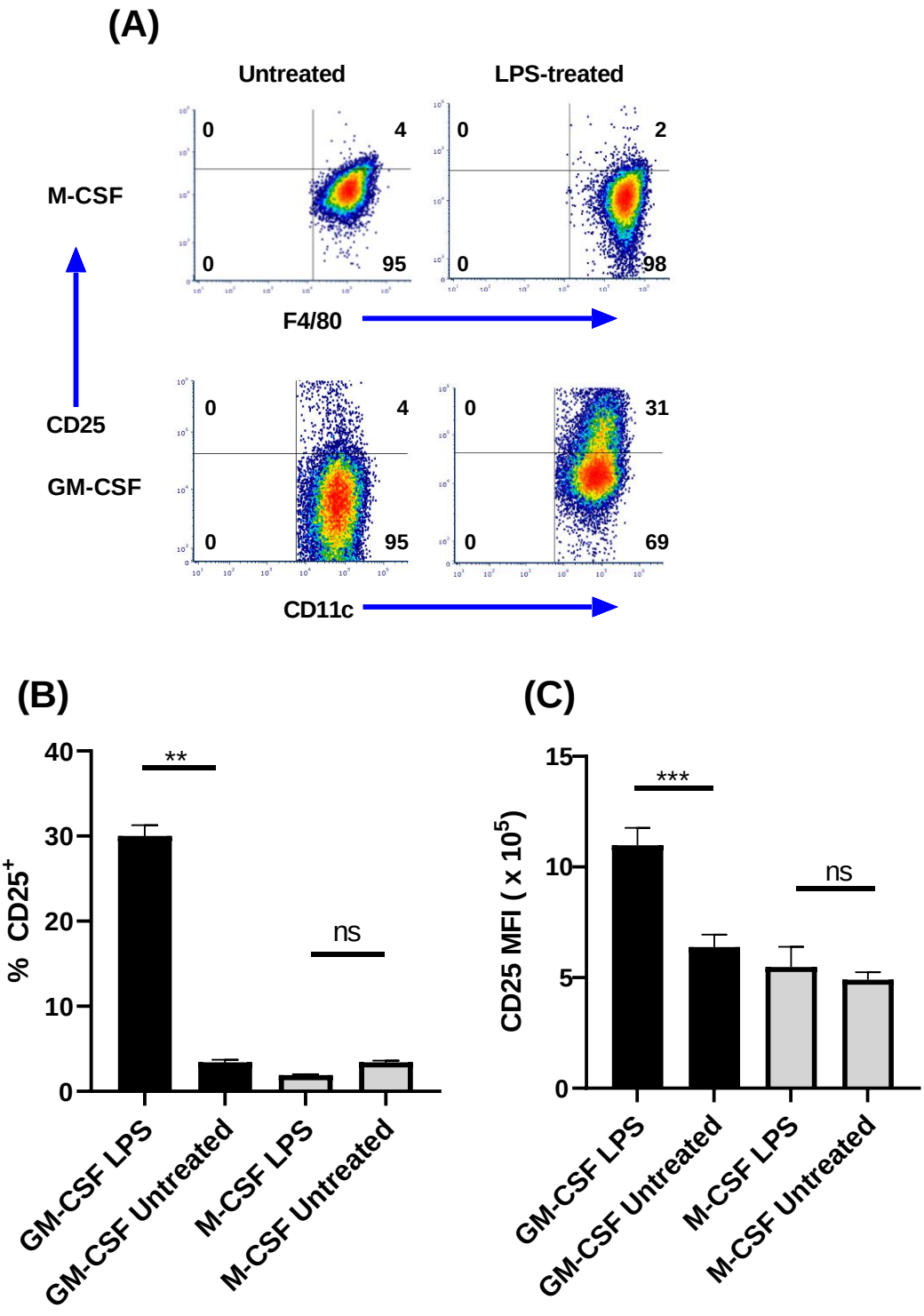
(A)
Untreated
LPS-treated
M-CSF
F4/80
CD25
GM-CSF
CD11c
0
4
95
2
98
31
69
(B)
% CD25+
**
ns
GM-CSF LPS
GM-CSF Untreated
M-CSF LPS
M-CSF Untreated
(C)
CD25 MFI (x 10^5)
***
ns

FIGURE 3.7 | TLR-4 agonism stimulated CD25 expression on FLT3-L-differentiated DCs.

DCs were obtained from bone marrow cultures as described in Materials and Methods. For this experiment, 100 ng/ mL FLT3-L rather than GM-CSF was used as a DC differentiation factor. Cells were cultured for 6 days, and then 50 ng/ mL LPS was added for 24 hours before cells were removed with 2.5 mM EDTA release buffer and stained for CD11c, F4/80, CD25, CD86 and MHCII. (A) Representative dot plots of CD25 and MHCII expression are gated on $CD11c^+$ DCs. (B) Bar graphs depict the percentage of cells positive for each marker gated on $CD11c^+$ cells (n=3). Replicate experiments represent DC cultures derived from individual mice. Statistical significance was determined by use of two-tailed t-tests comparing LPS-treated and untreated samples for each marker. (***$p < 0.001$)

Figure 3.7

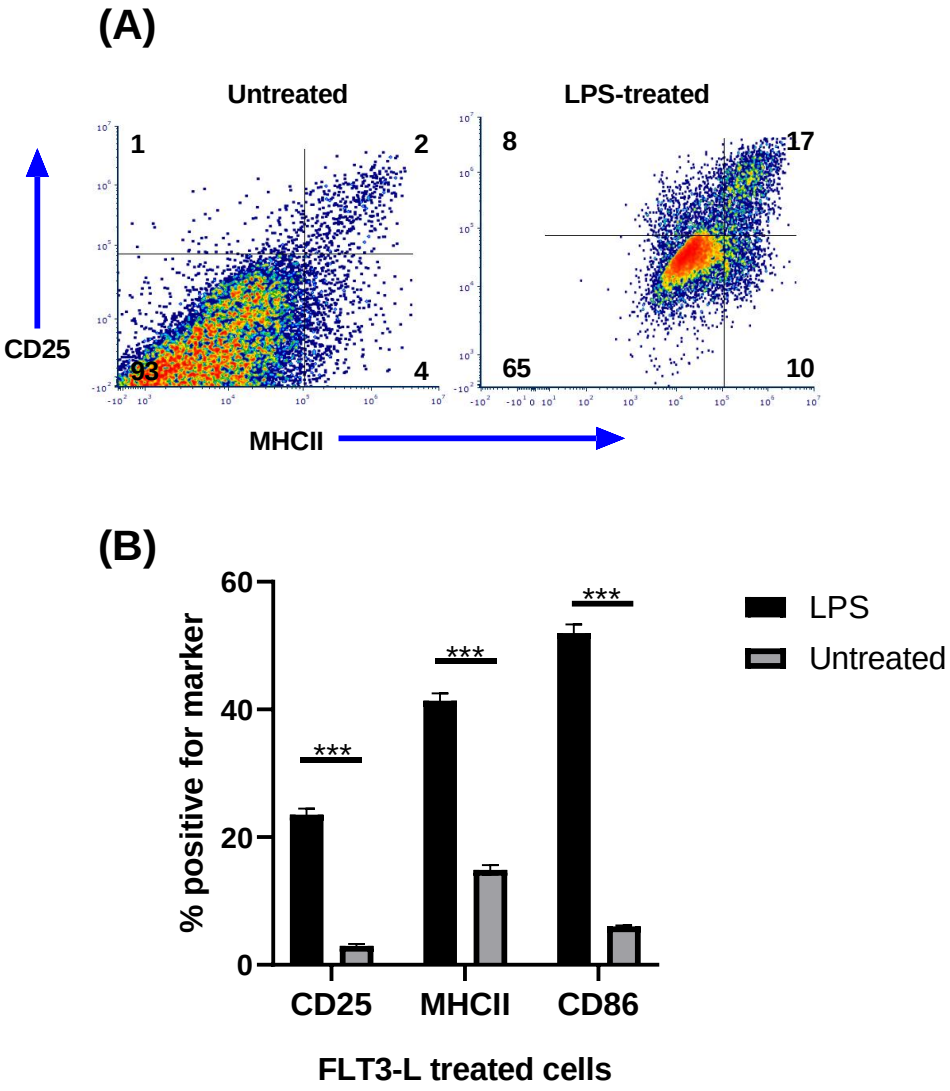
(A)
Untreated
LPS-treated
1
2
93
4
8
17
65
10
CD25
MHCII
(B)
% positive for marker
60
40
20
0
***
***
***
LPS
Untreated
CD25
MHCII
CD86
FLT3-L treated cells

FIGURE 3.8 | TLR-4 agonism led to rapid expression of CD25 coupled to CD86 and MHCII. DCs were cultured as described in the Materials and Methods section. LPS (100 ng/ mL) was added to DCs in pre-warmed media in petri dishes. Cells were incubated at 37°C until the designated time point had elapsed. Cells were then removed from the petri dish with cold 2.5 mM EDTA release buffer and washed twice with cold media to remove LPS. Cells were kept on ice for the remaining duration of the experiment. Cells in the "0 Minutes" group were immediately washed with cold media following LPS addition. Cells were stained for CD11c, CD25, MHCII and CD86. (A) Shown are representative dot plots of CD25 and FSC-A expression gated on $CD11c^+$ DCs. (B) Shown is a cumulative timecourse graph gated on $CD11c^+$ cells that are positive for CD25, CD86, and MHCII at each timepoint from time 0 to 480 minutes. (C-D) Differences at the "45 minutes" timepoint are highlighted for percentages (C) and MFI (D) for CD25, CD86 and MHCII. (B) Statistical significance was assessed for differences at each time point compared to "0 minutes" with a two-tailed t-test at each timepoint. Significance indicated highlights difference in CD25 expression (*a*), CD86 expression (*b*), and MHCII expression (*c*) as defined by $p<0.05$, compared to the "0 minutes" baseline control. (C-D) Statistical significance was determined by use of two-tailed t-test. (*$p < 0.05$, **$p < 0.01$, ***$p < 0.001$)

Figure 3.8

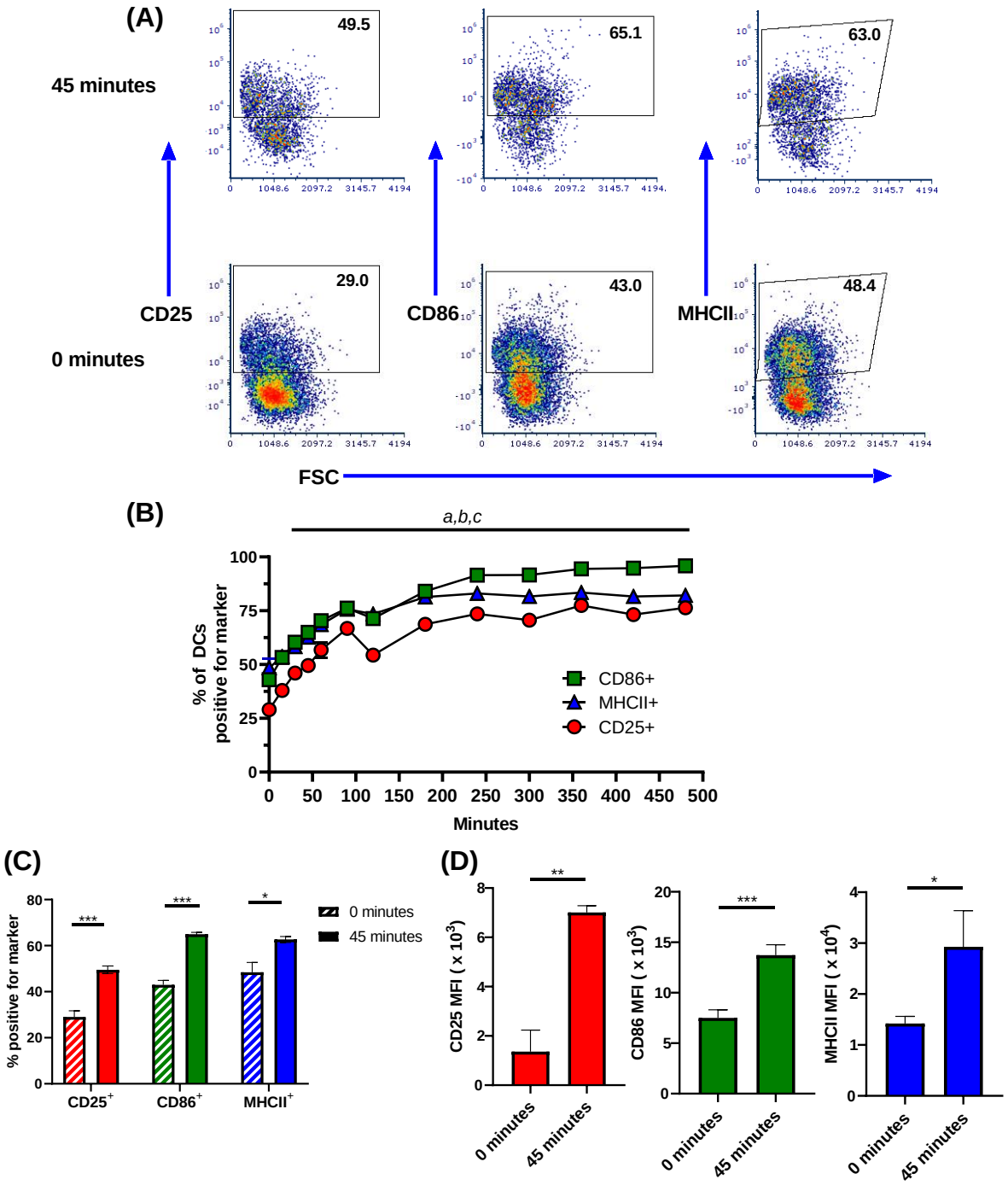
(A)
45 minutes
0 minutes
CD25
CD86
MHCII
49.5
65.1
63.0
29.0
43.0
48.4
FSC
(B)
a,b,c
% of DCs positive for marker
CD86+
MHCII+
CD25+
Minutes
(C)
% positive for marker
0 minutes
45 minutes
CD25+
CD86+
MHCII+
(D)
CD25 MFI (x 10^3)
CD86 MFI (x 10^3)
MHCII MFI (x 10^4)
0 minutes
45 minutes

FIGURE 3.9 | CD25$^+$ DCs exhibited a stable mature DC phenotype. DCs were cultured as described in the Materials and Methods section. DCs were analyzed before any LPS addition on Day 0. LPS (100 ng/ mL) was added to designated cultures and after 24 hours, all cells were washed. Half of the DCs were analyzed that day as the "Day 1" groups while the other half were put back in incubation for 2 more days in only cRPMI. After 2 more days of culture, the remaining cells were analyzed as the "Day 3" groups. (A) Shown are representative dot plots of CD25, CD86 and MHCII expression gated on CD11c$^+$ DCs for each indicated timepoint. (B) Shown are quantified timecourse graphs for expression of CD25, CD86 and MHCII (n=2). Replicates represent DC cultures derived from individual mice. Statistical significance was determined via two-tailed t-tests comparing each treatment group on each day. (*$p < 0.05$ and **$p < 0.01$)

Figure 3.9

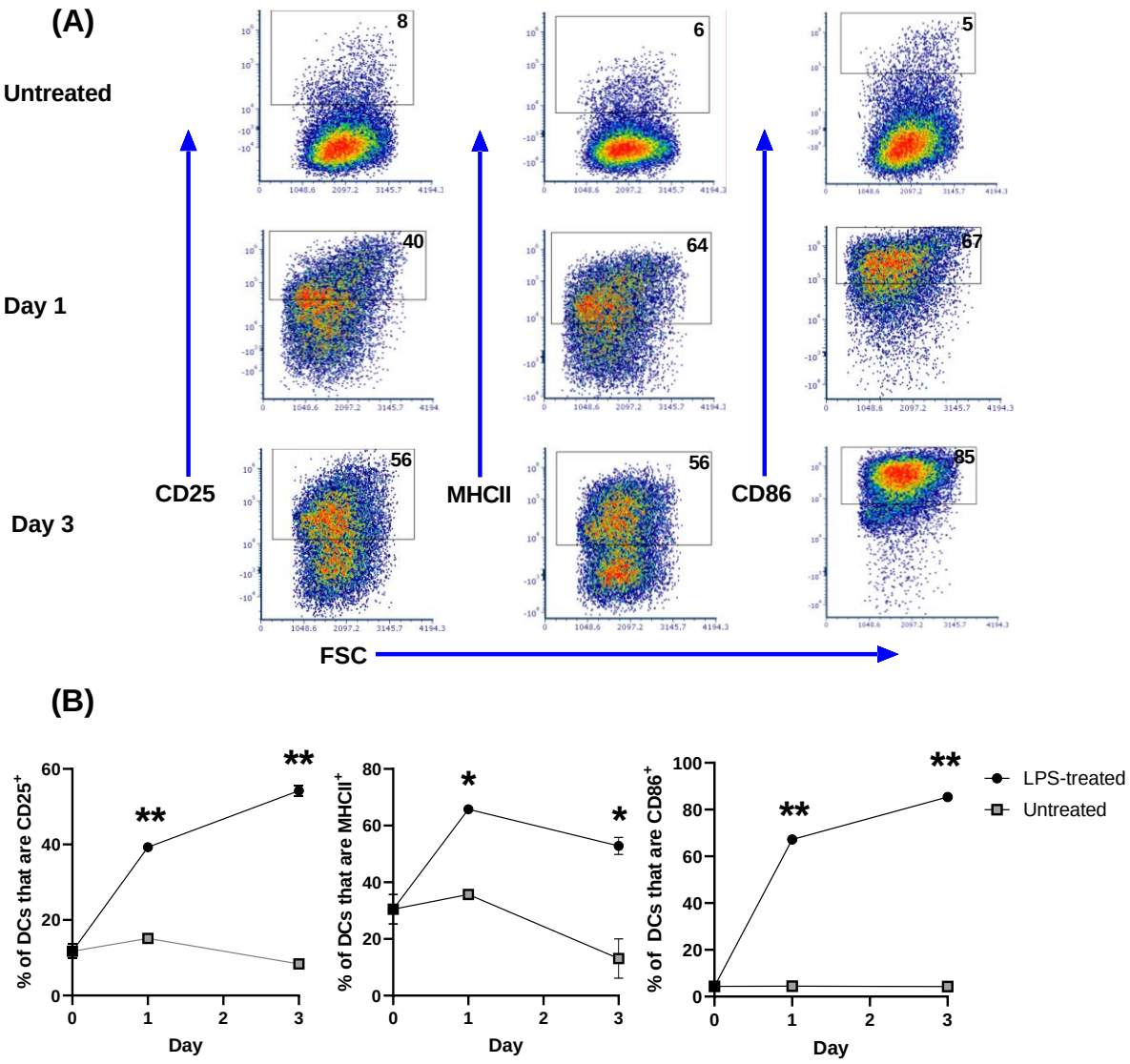
(A)
Untreated
Day 1
Day 3
CD25
MHCII
CD86
FSC
8
6
5
40
64
67
56
56
85
(B)
% of DCs that are CD25+
% of DCs that are MHCII+
% of DCs that are CD86+
Day
LPS-treated
Untreated

FIGURE 3.10 | TLR-4 agonism inhibited DC proliferation. DCs were cultured as described in the Materials and Methods section. DCs were placed in a 96 well plate with 1 μM GM-CSF in all wells. A full-log titration of LPS and MPLA was applied to the DCs ranging from 10 pg/ mL to 10 μg/ mL. Cells were cultured for 48 hours, then 1μC of [^{3}H]thymidine was added to each well. Cells were cultured for another 24 hours before being harvested onto a filtermat and analyzed via a scintillation counter. (A) Shown is a titration curve showing proliferation based on thymidine incorporation at each concentration of each agonist (n=3). Replicates represent DC cultures derived from individual mice. Statistical significance is calculated by a two-tailed t-test comparing each concentration to the blank (i.e., the "0" group). The "*" indicates statistical significance for the LPS group compared to the blank and "^" indicated statistical significance for the MPLA group. Both significance markers are defined by $p < 0.05$.

Figure 3.10

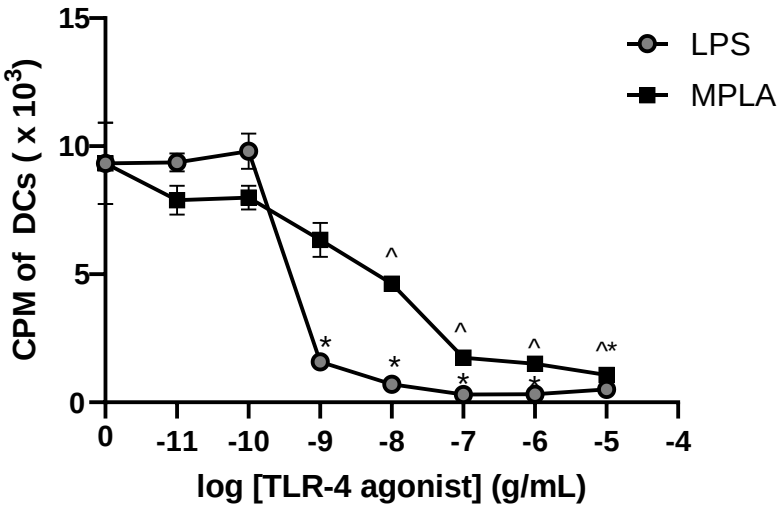
15
10
5
0
CPM of DCs (x 10^3)
LPS
MPLA
^
^
^
^*
*
*
*
*
0
-11
-10
-9
-8
-7
-6
-5
-4
log [TLR-4 agonist] (g/mL)

FIGURE 3.11 | LPS-treated CD25$^+$ DCs exhibited specific binding to IL-2. DCs were cultured as described in the Materials and Methods section. DCs were treated with 50 ng/ mL LPS for 2 days. DCs were then pulsed with 100 nM His-tagged IL-2 for 1 hour at 4°C and washed extensively at 4°C to remove excess IL-2. Cells were then stained for the presence of surface bound His-tag and CD11c. (A) Shown are representative dot plots gated of surface bound IL-2 and FSC-A on CD11c$^+$ DCs. (B) Shown are bar graphs of cell percentages that exhibited surface bound IL-2 (n=2). (C) Shown are bar graphs comparing MFI of His-tag IL-2 from the "IL-2 pulsed" group of each DC treatment. Replicate experiments represent DC cultures derived from individual mice. Statistical significance was calculated by use of a (B) one-way ANOVA or (C) a one-tailed t-test. (*$p < 0.05$)

Figure 3.11

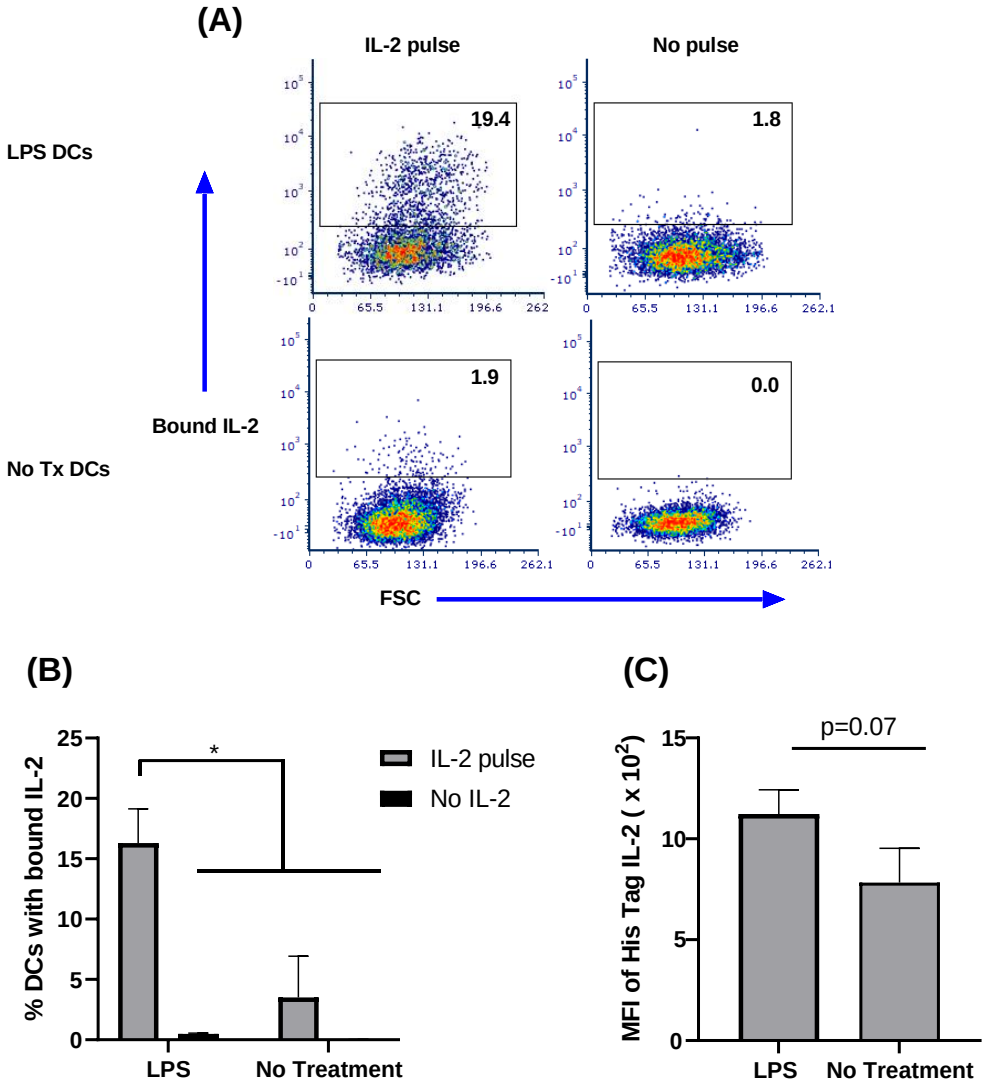
(A)
IL-2 pulse
No pulse
LPS DCs
No Tx DCs
Bound IL-2
19.4
1.8
1.9
0.0
FSC
(B)
% DCs with bound IL-2
IL-2 pulse
No IL-2
*
LPS
No Treatment
(C)
MFI of His Tag IL-2 (x 10²)
p=0.07
LPS
No Treatment

FIGURE 3.12 | In LPS-treated DC cultures, binding of IL-2 was positively correlated with CD25 expression. DCs were cultured as described in the Materials and Methods section. DCs were treated with 50 ng/ mL LPS for 2 days. DCs were then pulsed with 100 nM His-tagged IL-2 for 1 hour at 4°C and washed extensively at 4°C to remove excess IL-2. Cells were then stained for presence of His-tag and CD11c as well as with the non-competing anti-CD25 antibody 3C7. (A) Shown is a representative dot plot of LPS-treated DCs pulsed with IL-2. The inset graph is a linear regression of IL-2 binding levels compared to CD25 expression levels of $CD11c^+$ gated cells. (B-C) Shown are bar graphs, quantifying the percent (B) or MFI (C) of DCs with bound IL-2 gated on either $CD25^+$ or $CD25^-$ cells. All cells are gated on $CD11c^+$. Replicates represent duplicate wells in the same experiment. Statistical significance was calculated by use of a one-tailed t-test. (**$p < 0.01$ and ***$p < 0.001$)

Figure 3.12

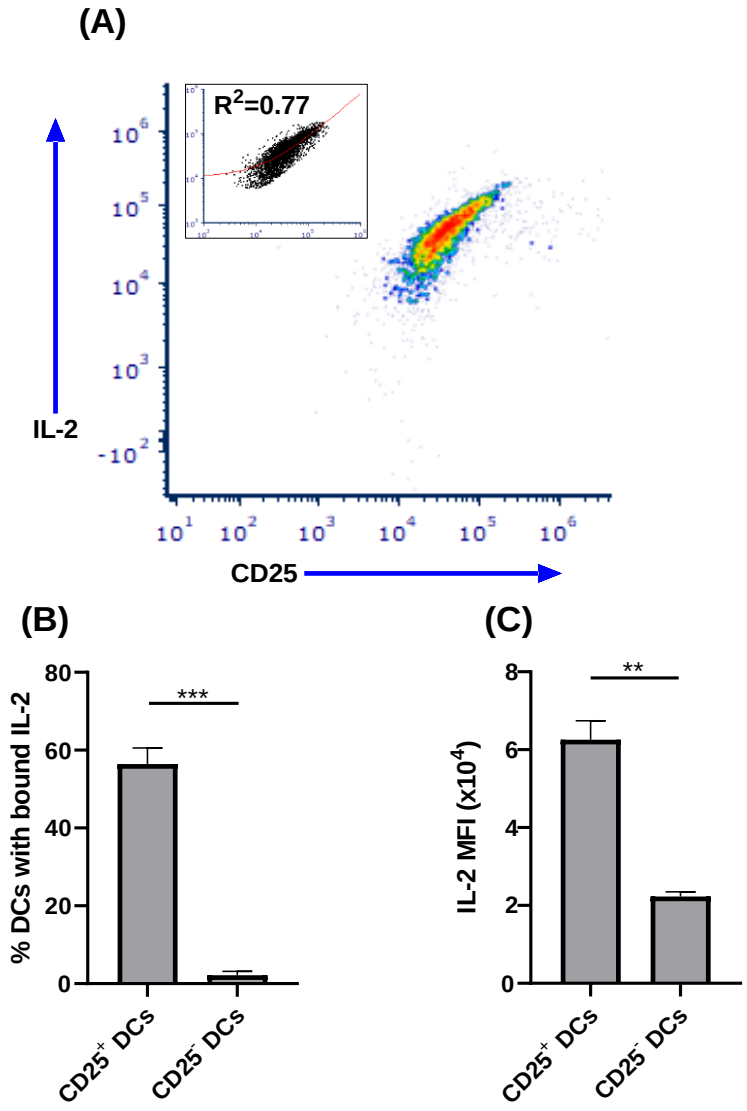
(A)
R2=0.77
IL-2
CD25
(B)
% DCs with bound IL-2
***
CD25+ DCs
CD25- DCs
(C)
IL-2 MFI (x10^4)
**
CD25+ DCs
CD25- DCs

FIGURE 3.13 | IL-2 stimulation did not elicit detectable phosphorylation of STAT5 in CD25$^+$ DCs. DCs were cultured as described in the Materials and Methods section. DCs were kept in media without GM-CSF for 24 hours, while SJL-PLP T cells were starved of IL-2 for 24 hours. Cells were then stimulated with 2 μM GM-CSF or 100 nM IL-2 at 37°C for 40 minutes. Cells were fixed as described in materials and methods and stained for CD11b, CD11c, and pSTAT5. (A) Shown are representative histograms of CD11b$^+$ CD11c$^+$ DCs for pSTAT5 expression for each treatment group and ungated SJL T cells. Samples stimulated with the cytokine (light blue) are compared to the respective unstimulated cells (red). (B-C) Shown are compiled bar graphs for each group (n=2) gated on CD11b$^+$ CD11c$^+$ DCs depicting (B) MFI of pSTAT5$^+$ cells and (C) percent pSTAT5 positive cells. Replicates represent DC cultures derived from individual mice. Statistical significance was calculated by use of One-Way ANOVA comparing all stimulations in a treatment group. (*$p < 0.05$ and **$p < 0.01$)

Figure 3.13

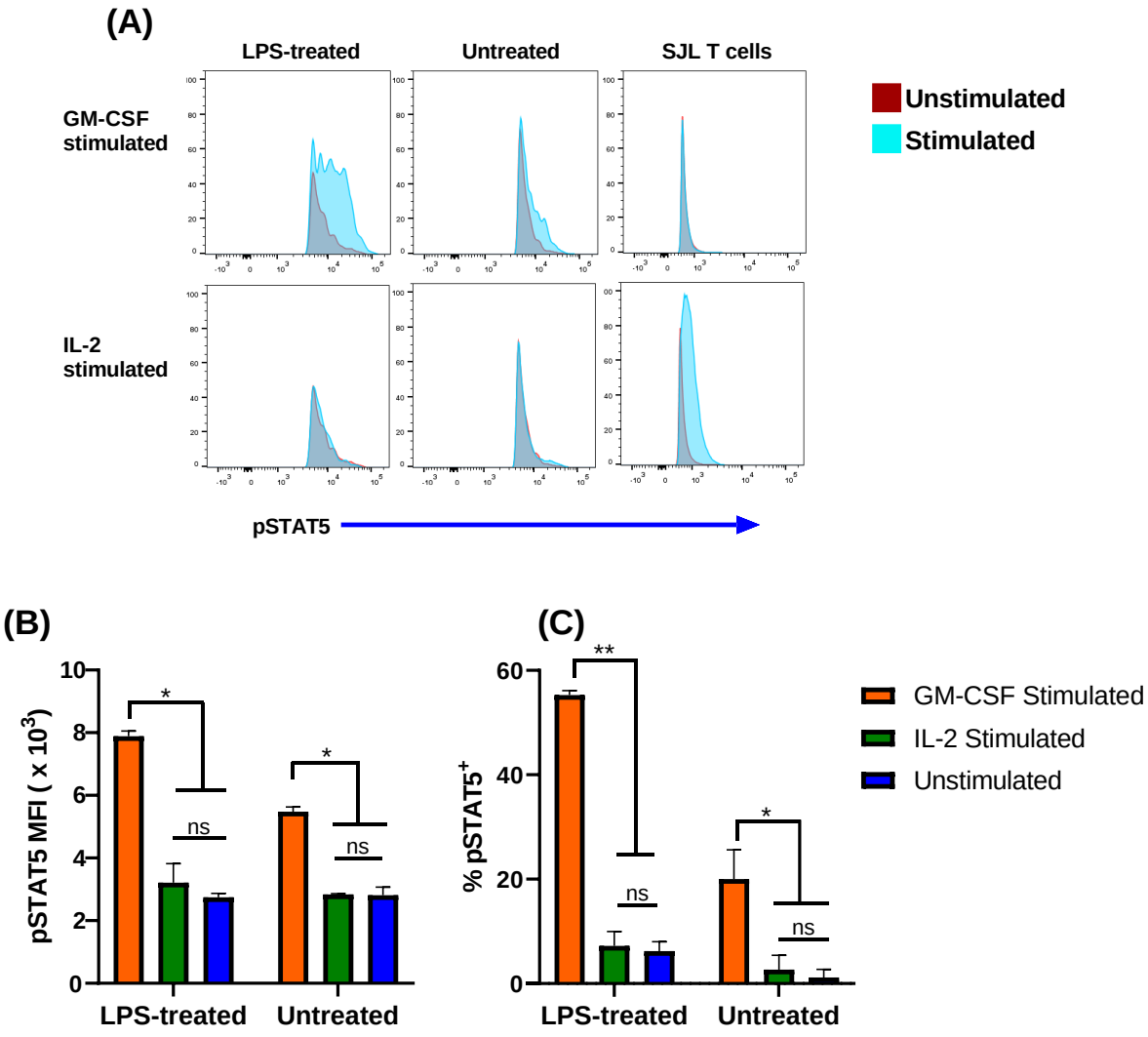
(A)
LPS-treated
Untreated
SJL T cells
GM-CSF stimulated
IL-2 stimulated
Unstimulated
Stimulated
pSTAT5
(B)
pSTAT5 MFI (x 10^3)
10
8
6
4
2
0
*
ns
*
ns
LPS-treated
Untreated
(C)
% pSTAT5+
60
40
20
0
**
ns
*
ns
LPS-treated
Untreated
GM-CSF Stimulated
IL-2 Stimulated
Unstimulated

FIGURE 3.14 | IL-2 bound to CD25^{+} DCs stimulated proliferation of IL-2 dependent SJL.PLP T cells. DCs were cultured as described in the Materials and Methods section. DCs were treated for 1 day with 100 ng/ mL LPS. DCs were then pulsed with 100 nM IL-2 at 4°C for 1 hour. Cells were washed thoroughly to remove excess IL-2. DCs were placed at a 5:1 ratio with SJL T cells that had been starved overnight of IL-2. DCs and SJL T cells were cultured together for 2 days, and then 1 μCi/ well [^{3}H]thymidine was added to each well. Cells were incubated for 24 more hours and harvested onto a filtermat and analyzed via a scintillation counter. (A) Shown is a bar graph (n=3) of DC treatment effects on the proliferation of responder T cells. Replicates represent DC cultures derived from individual mice. Statistical significance was calculated by use of a two-tailed t-test. (**$p < 0.01$)

Figure 3.14

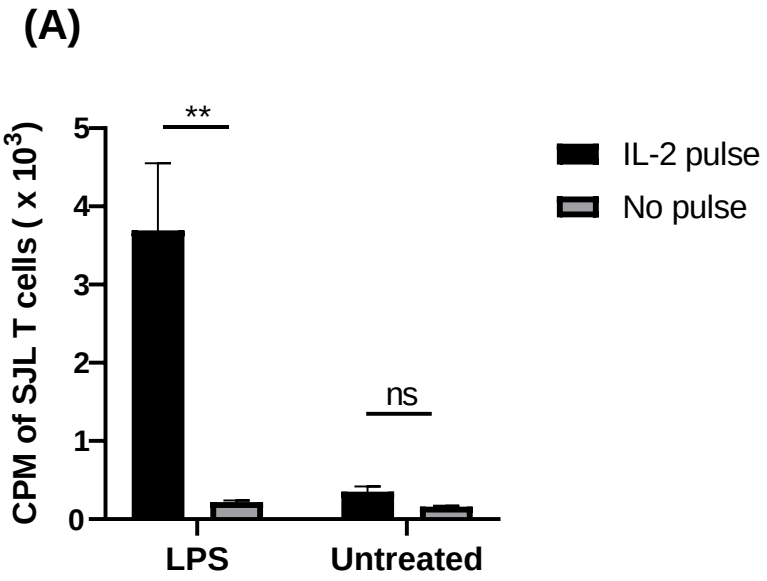
(A)
**
ns
CPM of SJL T cells (x 10^3)
5
4
3
2
1
0
LPS
Untreated
IL-2 pulse
No pulse

CHAPTER 4

TLR-4 AGONISM POTENTIATES TOLEROGENIC T CELL RESPONSES

4.1 ABSTRACT

Here, we show that TLR-4 agonism is beneficial to tolerogenic T cell responses. LPS-treated DCs support a more suppressive Treg phenotype by increasing CD25 expression on responder Tregs. These DCs preferentially activate Tregs over Tcons. Likewise, MPLA addition to splenocyte cultures enriches the $CD25^+$ Treg population in the culture, and MPLA injection into wild-type mice leads to an increase in Treg percentage. Because of its ability to potentiate tolerogenic T cell responses, MPLA was an effective tolerogenic adjuvant when combined with GMCSF-MOG, a DC-targeting tolerogenic vaccine. MPLA increased the Treg levels induced by GMSCF-MOG, and this increase was detectable out to day 78. MPLA also potentiated the loss of Tcons seen with the GMCSF-MOG vaccine. An observed increase in CD44 on Tcons indicated MPLA was leading to an enhanced T cell response and possible extended presence of cognate antigen which responder T cells can experience. Lastly, we show that MPLA was an effective tolerogenic adjuvant when combined with GMCSF-MOG that led to increased suppression of EAE. MPLA increased the rate at which paralytic symptoms resolved and prevented a relapse seen with the GMSCF-MOG vaccine alone. Altogether, we show that TLR-4

agonism can potentiate tolerogenic T cell responses by promoting tolerogenic antigen recognition events.

4.2 RESULTS

CD25^{+} DCs supported responder Tregs *in vitro*

We found that LPS-treated DCs elicited higher CD25 expression on responder Tregs compared to untreated DCs (Figure 4.1A-C). Because cultured Tregs are CD25^{+}, we measured increases in CD25 expression by denoting a superlative CD25^{high} gate on the FOXP3^{+} Treg population. About 45% of responder 2D2-FIG Tregs exhibited a superlative CD25^{high} phenotype when I-A^{b}/ MOG was presented by LPS-treated DCs compared to control values of approximately 10% when MOG was presented by untreated DCs (Figure 4.1A and C). As expected, this increase in CD25 expression on Tregs was dependent on antigen recognition because only DCs presenting MOG elicited the superlative CD25^{high} Treg phenotype (Figure 4.1A and C). This same pattern was seen with CD25 MFI of responder Tregs in that LPS-treated DCs induced 1.6-fold higher CD25 expression upon cognate antigen recognition compared to untreated DCs (Figure 4.1B). Higher CD25 levels are associated with a more activated and suppressive Treg phenotype (251, 252).

We also found that LPS-treated DCs favored blastogenesis (increased cell size as measured by FSC-A) of MOG-responsive Tregs compared to Tcons while untreated DCs showed no preference (Figure 4.2A-B). Forward scatter, a measurement of cell size, is a reliable marker of T cell activation (253, 254). Specifically, when MOG was presented by LPS-treated DCs, Tregs displayed higher forward scatter MFI compared to Tcons. This difference in MFI was not seen when MOG was presented on untreated DCs indicating that LPS-treated DCs more efficiently support the activation of MOG-reactive Tregs.

We next hypothesized that IL-2 on the surface of DCs is beneficial for responder Tregs by providing selective access to IL-2 during cell-cell contact and formation of the immunological synapse during antigen presentation. To test this possibility, we pulsed MOG-presenting DCs with IL-2 which were then cocultured with Tregs. We found that IL-2-pulsed DCs induced higher CD25 expression on responder Tregs that trended towards significance (Figure 4.3A-C). LPS-treated DCs pulsed with IL-2 induced "high" expression of CD25 on 54% of responder Tregs compared to 46% when DCs were not pulsed with IL-2 (Figure 4.3B). The IL-2 pulse of DCs also increased CD25 MFI on responder Tregs that trended towards statistical significance (Figure 4.3C). These data indicated that IL-2 bound to CD25 on the surface of DCs may be utilized by responder Tregs upon persistent cell-cell conjugation catalyzed via TCR/MHCII-Ag recognition. This DC-sequestered pool of IL-2 may assist in activation of these Tregs.

TLR-4 agonism enriched Treg populations *in vitro* and *in vivo*

We found that LPS added directly to naïve, wildtype splenocyte cultures enriched the $CD25^+$ Treg pool. The overall percentages of $CD25^+$ T cells remained unchanged upon addition of LPS. However, the makeup of the $CD25^+$ T cell population was skewed toward $FOXP3^+$ Tregs and a more tolerogenic phenotype (Figure 4.4A-E). Specifically, upon LPS addition, the CD25 MFI of $CD25^+$ T cells was increased 1.4-fold (Figure 4.4C). LPS addition also increased the CD25 MFI of Tregs in the culture 3.3-fold which is indicative of a more suppressive Treg phenotype (Figure 4.4D). Additionally, the $CD25^+$ T cell pool was enriched with Tregs as Tregs made up 42% of the $CD25^+$ T cell population with the addition of LPS compared to just 21% without LPS (Figure 4.4E).

Given these results, we next hypothesized that the LPS-derivative, MPLA, could elicit Tregs *in vivo*. We found that subcutaneous injection of MPLA leads to a slight increase in Treg

percentage in the blood measured 5-days and 8-days post injection (Figure 4.5A-B). On Day 5, in MPLA-treated mice, Tregs made up 7.2% of the circulating $CD4^+$ T cell pool compared to 5.9% in saline-treated mice (Figure 4.5B). This difference increased on Day 8 as Tregs made up an average of 9.7% of circulating T cells in MPLA-injected mice compared to 6.8% in saline-injected mice. On both days, the difference trended towards statistical significance (Figure 4.5B).

MPLA was an effective tolerogenic adjuvant when combined with the tolerogenic GMCSF-MOG vaccine *in vivo*

We hypothesized that in an antigen-independent system of Treg induction, T cells recognizing endogenous self-antigen/MHCII complexes on the surface of DCs were expanding, resulting in the observed Treg enrichment of the circulating T cell pool. Given this possible mechanism, we hypothesized that MPLA could function as an adjuvant when coupled with a DC-targeting, antigen-based tolerogenic vaccine. We hypothesized that MPLA would enhance the responses induced by a tolerogenic vaccine containing self-antigens by enhancing antigen presentation on DCs as observed in *in vitro* cultures (Chapter 3). To test this, we utilized the GMCSF-MOG tolerogenic vaccine, which has been shown to ameliorate EAE and induce robust Treg expansion in a MOG-specific FOXP3-GFP reporter, 2D2-FIG mice (225, 226, 229). When MPLA (20 μg) was combined with GMCSF-MOG (2 nanomoles), we found that the Treg inductive potential was increased (4.6A-B). Vaccination of 2D2-FIG mice with GMSCF-MOG alone, resulted in the increased circulation of $FOXP3^+$ Tregs (21% of the total T cells in blood) compared to 1% $FOXP3^+$ Tregs in saline-treated mice. However, when MPLA was included in the vaccine formulation, mean Treg percentages increased to 43% on day 8 after injection (Figure 4.6A-B). In this study, MPLA alone once again led to a modest increase in Treg levels, as Tregs made up 6% of the T cell pool compared to 1% in saline-treated mice.

In a separate experiment, we confirmed that MPLA increased the Treg inductive capacity of GMSCF-MOG, and this increase was persistent for 78 days. On each day measured from day 12 to day 78, MPLA + GMCSF-MOG resulted in higher levels of Tregs compared to GMCSF-MOG alone and saline (Figure 4.7B). On day 54 post-injection, Tregs made up 15% of the T cell population when MPLA was included in the vaccination compared to 5% when GMCSF-MOG alone was administered (Figure 4.7A, C). Treg counts were also higher when MPLA was included in the vaccine (Figure 4.7D-E). On day 16, there were 112 Tregs/ µL of blood when MPLA was included in the vaccine compared to 63 Tregs/ µL when GMCSF-MOG alone was administered (Figure 4.7E). This increase in absolute Treg numbers (Figure 4.7D) was short-lived compared to the increase in Treg percentages (Figure 4.7B).

These differences may reflect GMCSF-MOG-induced decreases in the total numbers of $CD4^+$ T cells (Figure 4.8A-E). When MPLA was included with GMCSF-MOG vaccination, $CD4^+$ T cells comprised lower percentages of circulating leukocytes compared to GMSCF-MOG alone. This decrease was similar for the first 16 days post-vaccination before the T cell pool steadily rebounded in the GMSCF-MOG group while remaining low in the MPLA + GMCSF-MOG group. This difference was noted throughout the entire 78-day timecourse (Figure 4.8B). On day 54, $CD4^+$ T cells made up only 6% of the circulating leukocyte pool with MPLA included in the vaccine. However, mice that received GMSCF-MOG alone showed $CD4^+$ T cell levels had rebounded to baseline with $CD4^+$ T cells comprising 16% of circulating leukocytes compared to 17% in the saline control group (Figure 4.8C). This trend was also seen in total $CD4^+$ T cell count data. On day 38, MPLA + GMCSF-MOG mice averaged 439 T cells/ µL of blood compared to 1,360 T cells/ µL of blood for mice that received only GMCSF-MOG (Figure 4.8D-E). Hypothetically, this decrease in absolute $CD4^+$ T cell numbers may reflect two related

mechanisms, including the possibilities that MPLA-matured persistent DCs may facilitate the MOG-dependent entrapment of T cells in the lymph nodes by preventing their egress into circulation coupled with enhanced Tcon deletion due to MOG-induced Tcon death. These mechanisms, together with induction of Tcon anergy due to Treg-dominance may contribute to the increased reduction in $CD4^+$ T cells. (122, 255).

The persistence of elevated Treg percentages and decreased total T cell numbers provided suggestive evidence that a persistent pool of vaccine-dependent I-A^b/ MOG antigen provides continuing MOG-specific T cell stimulation thereby favoring $CD44^+$ memory T cells, which would include prominent populations of $FOXP3^+$ $CD44^+$ memory Tregs. A persistent antigenic MOG pool may also support $CD44^+$ memory Tcons. To assess this possibility, we used CD44 as a downstream marker of extended T cell activation and memory (256, 257). We found that CD44 expression on Tcons (defined as $FOXP3^-$ T cells) was higher when MPLA was included in the vaccine. Over the course of 78 days, the CD44 expression on Tcons in mice that received GMCSF-MOG alone steadily decreased to levels similar to the saline-treated group (Figure 4.9B). Specifically, mice that received GMCSF-MOG alone, CD44 expression on Tcons decreased from 42% on day 16 to 13% on day 54, similar to the mean 10% values of $CD44^+$ Tcons seen in mice receiving saline (Figure 4.9A). These two groups remained low at baseline levels for the remainder of the experiment (Figure 4.9B). In contrast, mice that received GMCSF-MOG + MPLA maintained high levels of CD44 expression on Tcons with 39% of Tcons expressing CD44 on day 54.

Tcons were used as a measurement of persistent antigen presentation, T cell activation, and memory because Tregs require continual self-antigen recognition for long-term maintenance (258, 259) unlike memory Tcons (260). Thus, Tregs predominantly express a $CD44^+$ memory

phenotype. In accordance with this concept, Tregs from all groups showed consistently high CD44 expression, ranging from 96-97% on Day 54 (Figure 4.10A, C). All groups also showed decrease in CD44 expression on Tregs starting on day 61 (Figure 4.10B). The reason for this was unknown, although a reason may relate to the extended nature of the experiment and repeated bleeding and associated stress on the mice. Altogether, the CD44 expression pattern on T cells, the extended levels of Tregs, and the extended lymphocytopenia provided suggestive evidence that the MPLA adjuvant conferred extended DC-mediated antigen presence throughout the time-course.

We also show that MPLA was an effective tolerogenic adjuvant paired with GMCSF-MOG in an EAE model (Figure 4.11). Mice were treated at peak disease with either GMCSF-MOG (4 nanomoles) + MPLA (10 µg), GMSCF-MOG (4 nanomoles) alone, or saline. When MPLA was included in the vaccine, symptoms resolved more quickly as mice started to improve about 3 days earlier compared to mice injected with GMCSF-MOG vaccine alone. On day 22, mice that received MPLA + GMCSF-MOG averaged a clinical score of 0.8, while mice that received GMCSF-MOG alone averaged a clinical score of 2.1, reaching statistical significance. Furthermore, mice that received only GMCSF-MOG as a treatment showed a relapse in symptoms around day 32 in contrast to mice that received MPLA + GMCSF-MOG which exhibited sustained remission. These data provide additional evidence that the MPLA adjuvant may confer persistent DC-mediated MOG/ I-A^b presentation and a longer lasting Treg pool in the context of tolerogenic vaccination. Mice that received the negative control treatment of saline exhibited a mean clinical score of 2.7 for the 50-day duration of the experiment. Overall, these data indicated that the MPLA adjuvant extends the duration of a single tolerogenic vaccination.

4.3 CONCLUSIONS

We showed that TLR-4 agonism potentiates tolerogenic T cell responses. LPS-treated DCs elicited a more suppressive $CD25^{high}$ Treg phenotype and favored blastogenesis of Tregs over Tcons. Importantly, MPLA elicited Tregs in combination with the DC-targeting vaccine, GMCSF-MOG. MPLA enhanced the tolerogenic response elicited by GMCSF-MOG, including the increased Treg persistence for 78 days. Based on CD44 expression, MPLA extended T cell activation which, in the context of tolerogenic vaccination, was favorable to Tregs over Tcons. When combined with the GMSCF-MOG tolerogenic vaccine, MPLA prevented disease relapse in a model of Multiple Sclerosis, indicating the extended presence of tolerogenic antigen presentation and a functional, disease-relevant Treg pool.

FIGURE 4.1 | LPS-treated DCs elicited superlative CD25 expression on responder Tregs.

DCs were cultured as described in the Material and Methods section. DCs were treated with 100 ng/ mL LPS for 1 day. DCs were then pulsed with 10 μM MOG35-55 at 37°C for 2 hours and washed thoroughly to remove excess MOG35-55. DCs were then placed at a 1:5 ratio with 2D2-FIG Tregs that had been cultured as described in the Materials and Methods section. Tregs and DCs were cocultured overnight at 37°C and then washed and stained for CD4 and CD25. (A) Shown are representative dot plots of CD25 expression and FSC-A gated on $CD4^+$ $FOXP3^+$ Tregs. The gate drawn is for $CD25^{high}$ Tregs because all Tregs in the culture were $CD25^+$. (B) Shown are bar graphs for each treatment group (n=2) comparing CD25 MFI on $CD4^+FOXP3^+$ Tregs. (C) Shown are bar graphs comparing percentages of $CD25^{high}$ of $CD4^+$ $FOXP3^+$ Tregs in each treatment group (n=2). Replicate experiments represent cultures derived from individual mice. Statistical significance was calculated by use of one-tailed t-tests comparing the indicated groups on the graphs. (*$p < 0.05$)

Figure 4.1

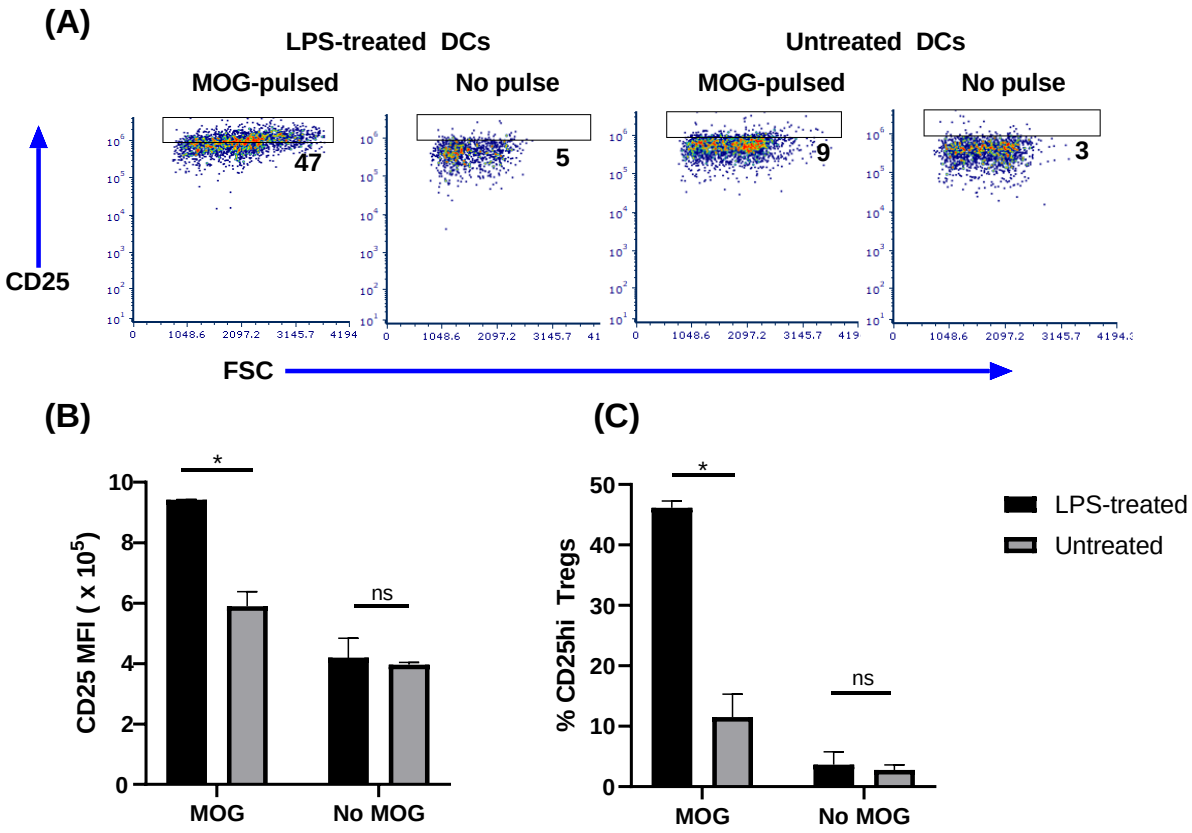
(A)
LPS-treated DCs
Untreated DCs
MOG-pulsed
No pulse
MOG-pulsed
No pulse
47
5
9
3
CD25
FSC
(B)
CD25 MFI (x 10^5)
*
ns
MOG
No MOG
(C)
% CD25hi Tregs
*
ns
MOG
No MOG
LPS-treated
Untreated

FIGURE 4.2 | LPS-treated DCs favored blastogenesis of Tregs. DCs were cultured as described in the Material and Methods section. DCs were treated with 100 ng/ mL LPS for 1 day. DCs were then pulsed with 10 μM MOG35-55 at 37°C for 2 hours and washed thoroughly to remove excess MOG35-55. DCs were then cultured at a 1:5 ratio with 2D2-FIG T cells (~85% Tregs) that were derived as described in the Materials and Methods section. Tregs and DCs were cocultured overnight at 37°C. Cells were then washed and stained for CD4 and CD25. (A) Shown are representative dot plots of FOXP3 expression and FSC-A gated on $CD4^+$ T cells. (B) Shown are bar graphs comparing the cell size of responder T cells as a function of LPS treatment of DCs. Replicates are duplicate wells in the same experiment. Statistical significance was calculated by use of one-tailed t-tests comparing the indicated groups on the graphs.

Figure 4.2

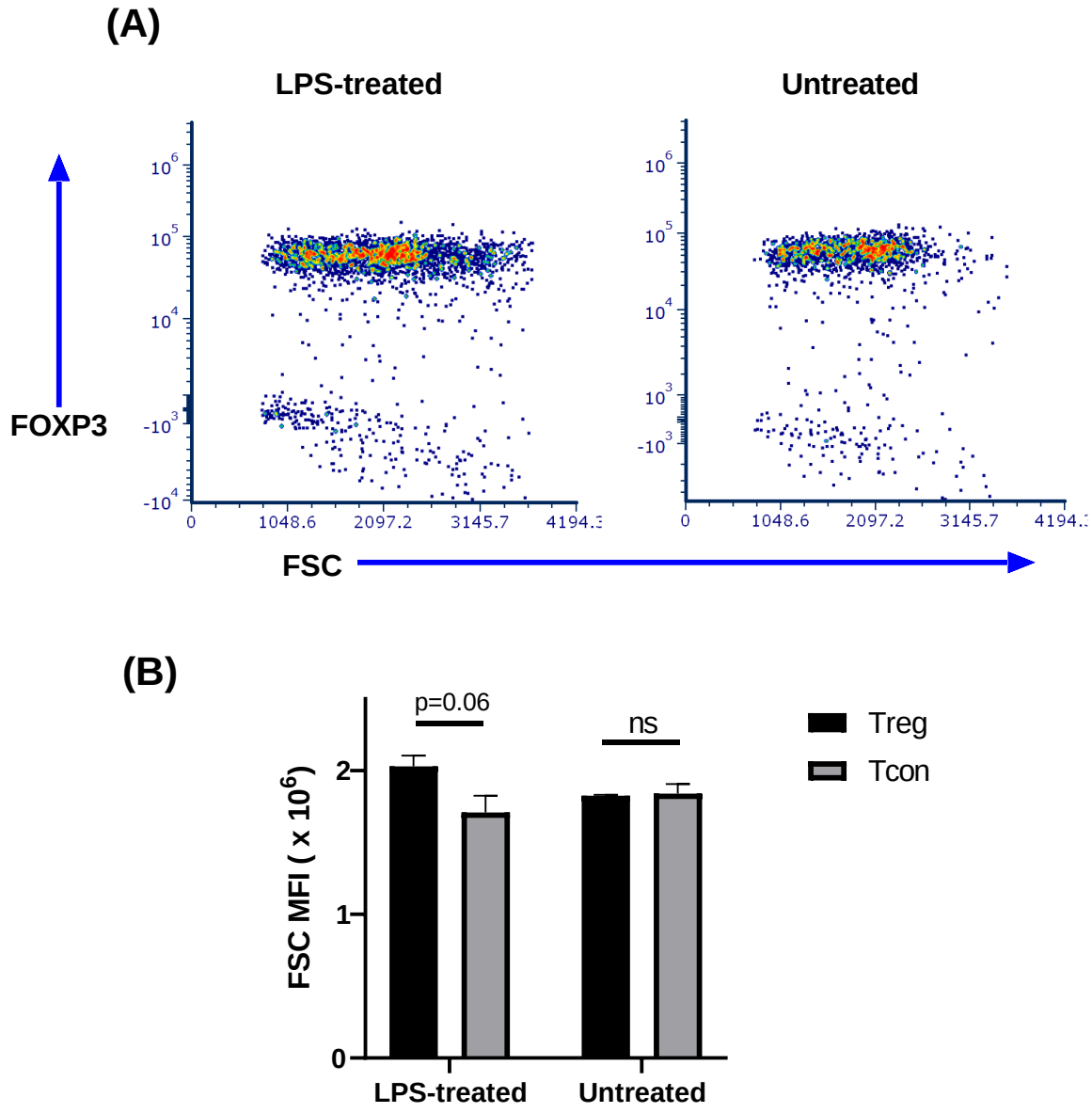
(A)
LPS-treated
Untreated
FOXP3
FSC
0
1048.6
2097.2
3145.7
4194.3
(B)
p=0.06
ns
Treg
Tcon
FSC MFI (x 10^6)
LPS-treated
Untreated

FIGURE 4.3 | Presence of IL-2 on $CD25^+$ DCs caused an increased trend in CD25 expression on responder Tregs. DCs were cultured as described in the Material and Methods section. DCs were treated with 100 ng/ mL LPS for 1 day. DCs were then pulsed with 10 μM MOG35-55 at 37°C for 2 hours and washed thoroughly to remove excess MOG35-55. DCs were then pulsed with 100 nM IL-2 for 1 hour at 4°C. DCs were thoroughly washed again to remove excess IL-2. DCs were then placed at a 1:5 ratio with 2D2-FIG T cells (~85% Tregs) that were derived as described in the Materials and Methods section. DCs/ Tregs were cocultured overnight at 37°C and were then washed and stained for CD4 and CD25. (A) Shown are representative dot plots of CD25 expression and FSC-A gated on $CD4^+$ $FOXP3^+$ Tregs. The gate drawn is for $CD25^{high}$ Tregs because all Tregs in the culture were $CD25^+$. (B) Shown are bar graphs for each treatment group (n=2) comparing percentages of $CD25^{high}$ Tregs (B) and CD25 MFI (C) on $CD4^+FOXP3^+$ gated cells. Replicates represent cultures derived from individual mice. Statistical significance was calculated by use of one-tailed t-tests comparing the indicated groups on the graphs and p values are indicated in graph.

Figure 4.3

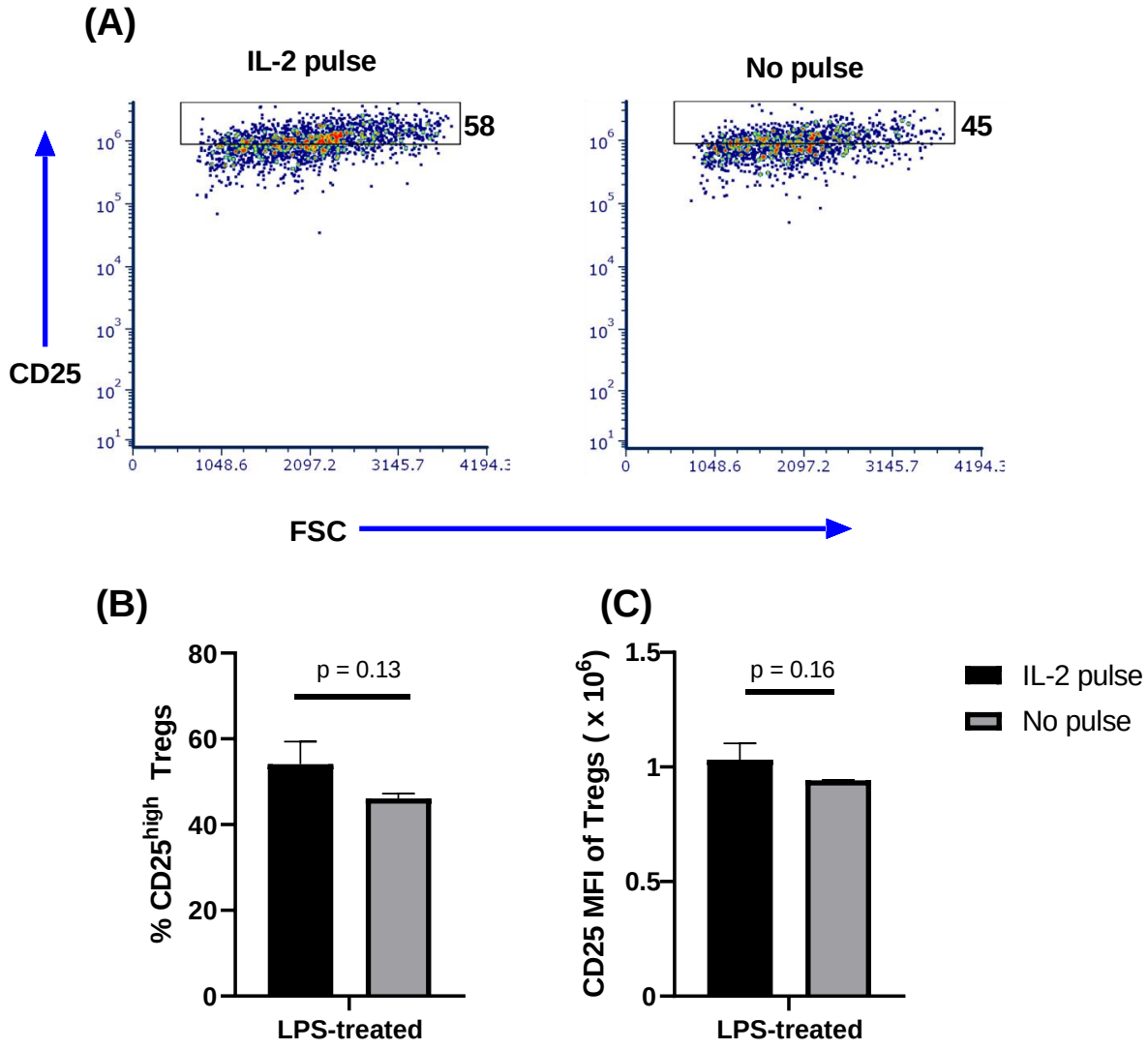
(A)
IL-2 pulse
No pulse
58
45
CD25
FSC
0
1048.6
2097.2
3145.7
4194.3
(B)
% CD25high Tregs
p = 0.13
LPS-treated
(C)
CD25 MFI of Tregs (x 10^6)
p = 0.16
LPS-treated
IL-2 pulse
No pulse

FIGURE 4.4 | LPS added to splenocyte cultures enriched the $CD25^+$ Treg pool. Splenocytes from FIG mice were pressed through a 70 μm cell strainer to obtain a single cell suspension. Cells were plated at 1 x 10^6 cells/ mL and cultured with or without 50 ng/ mL LPS for 3 days. Cells were washed and stained for CD3, CD4, and CD25. (A) Shown are representative dot plots of CD25 expression and FSC-A of $CD4^+$ $CD3^+$ T cells. (B) Shown are representative dot plots of $FOXP3^+$ expression in the $CD25^+$ T cells. (C) Shown are bar graphs (n=2) quantifying the CD25 MFI of $CD25^+$ T cells. (D) Shown are bar graphs of the CD25 MFI of Tregs. (E) Shown are the quantified bar graphs (n=2) of Treg percentages in the total $CD4^+$ $CD3^+$ T cell pool. Statistical significance was calculated by use of one-tailed t-tests. (*$p < 0.05$, **$p < 0.01$ and ***$p < 0.001$)

Figure 4.4

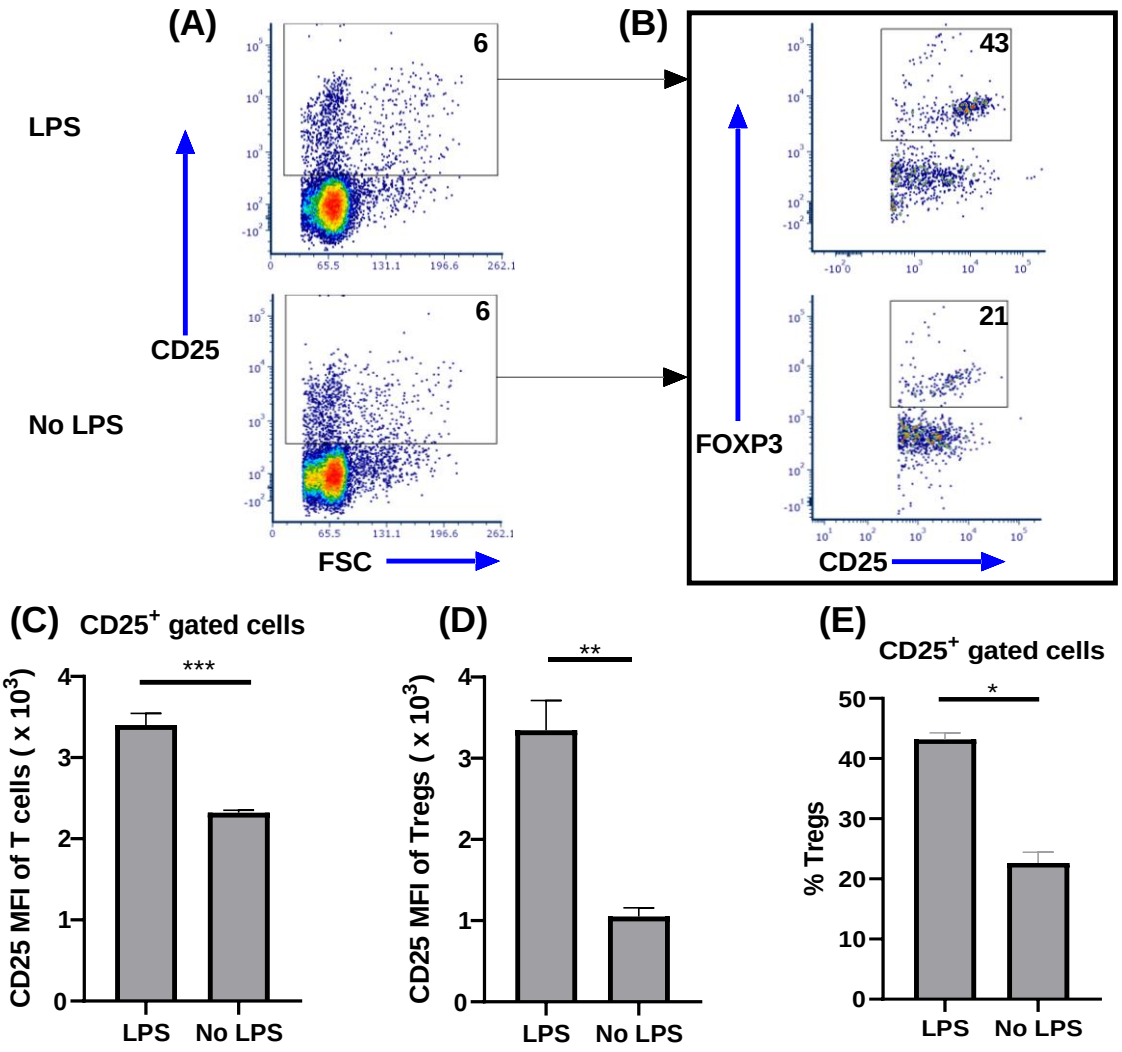
(A)
LPS
No LPS
CD25
FSC
6
6
(B)
43
21
FOXP3
CD25
(C) CD25+ gated cells
CD25 MFI of T cells (x 10^3)
***
LPS
No LPS
(D)
CD25 MFI of Tregs (x 10^3)
**
LPS
No LPS
(E)
CD25+ gated cells
% Tregs
*
LPS
No LPS

FIGURE 4.5 | Injection of MPLA in wild-type mice caused an increased trend of Treg percentages in vivo. C57BL/6 mice (n=6/ group) were injected subcutaneously with 20 µg MPLA or saline (100 µL total). Blood was collected via submandibular vein puncture on Day 5 and Day 8 post-injection. Blood was washed and stained for surface expression of CD3, CD4, and CD25 and intracellularly stained for FOXP3 as described in the Materials and Methods section. Erythrocytes were lysed and cells were analyzed. (A) Shown are representative dot plots of CD25 and FOXP3 expression of total $CD4^+$ $CD3^+$ T cells from mice Day 8 post-injection. (B) Shown are compiled data from all days showing $FOXP3^+$ percentages in the $CD3^+$ $CD4^+$ T cell pool. Statistical significance was calculated via one-tailed t-test at each time point. Error bars represent SEM.

Figure 4.5

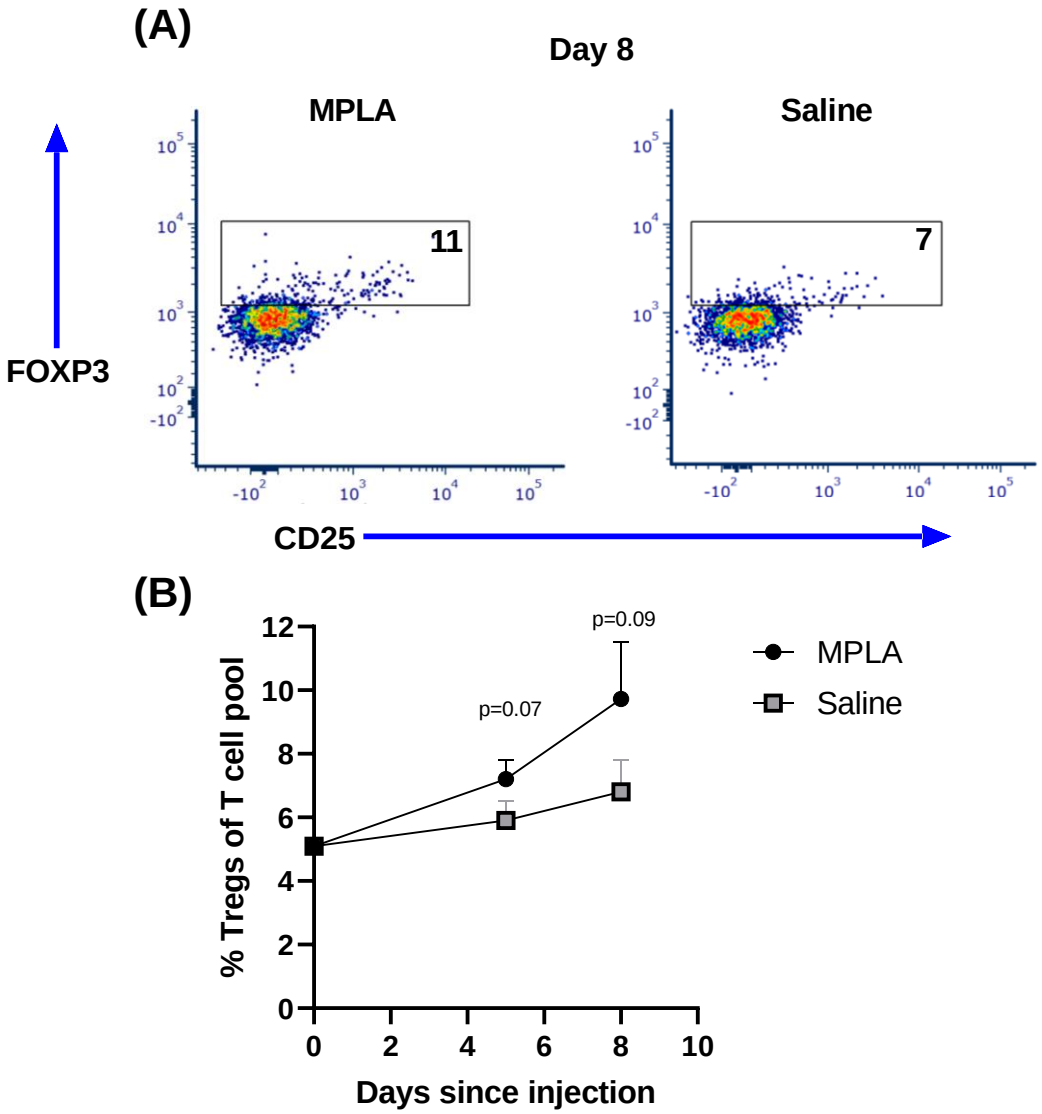
(A)
Day 8
MPLA
Saline
11
7
FOXP3
CD25
(B)
% Tregs of T cell pool
Days since injection
p=0.09
p=0.07
MPLA
Saline

FIGURE 4.6 | MPLA increased the Treg-inductive potential of GMCSF-MOG. 2D2-FIG mice were injected with 2 nmoles GMCSF-MOG (n=3), 2 nmoles GMCSF-MOG + 20 µg MPLA (n=3), 20 µg MPLA (n=2), or saline (n=3). Detailed vaccine formulation is described in the Materials and Methods section. Blood was collected via submandibular vein puncture on day 8 post-injection. Blood was washed and stained for CD3, CD4 and CD25. Erythrocytes were lysed and cells were analyzed using flow cytometry. (A) Shown are representative dot plots of FOXP3 and CD25 expression of $CD3^+$ $CD4^+$ T cells in the circulating PBMC pool. (B) Shown are the compiled data showing $FOXP3^+$ percentages of the $CD3^+$ $CD4^+$ T cell pool. Statistical significance was calculated via one-way ANOVA. Error bars represent SEM. (*$p < 0.05$ and **$p < 0.01$)

Figure 4.6

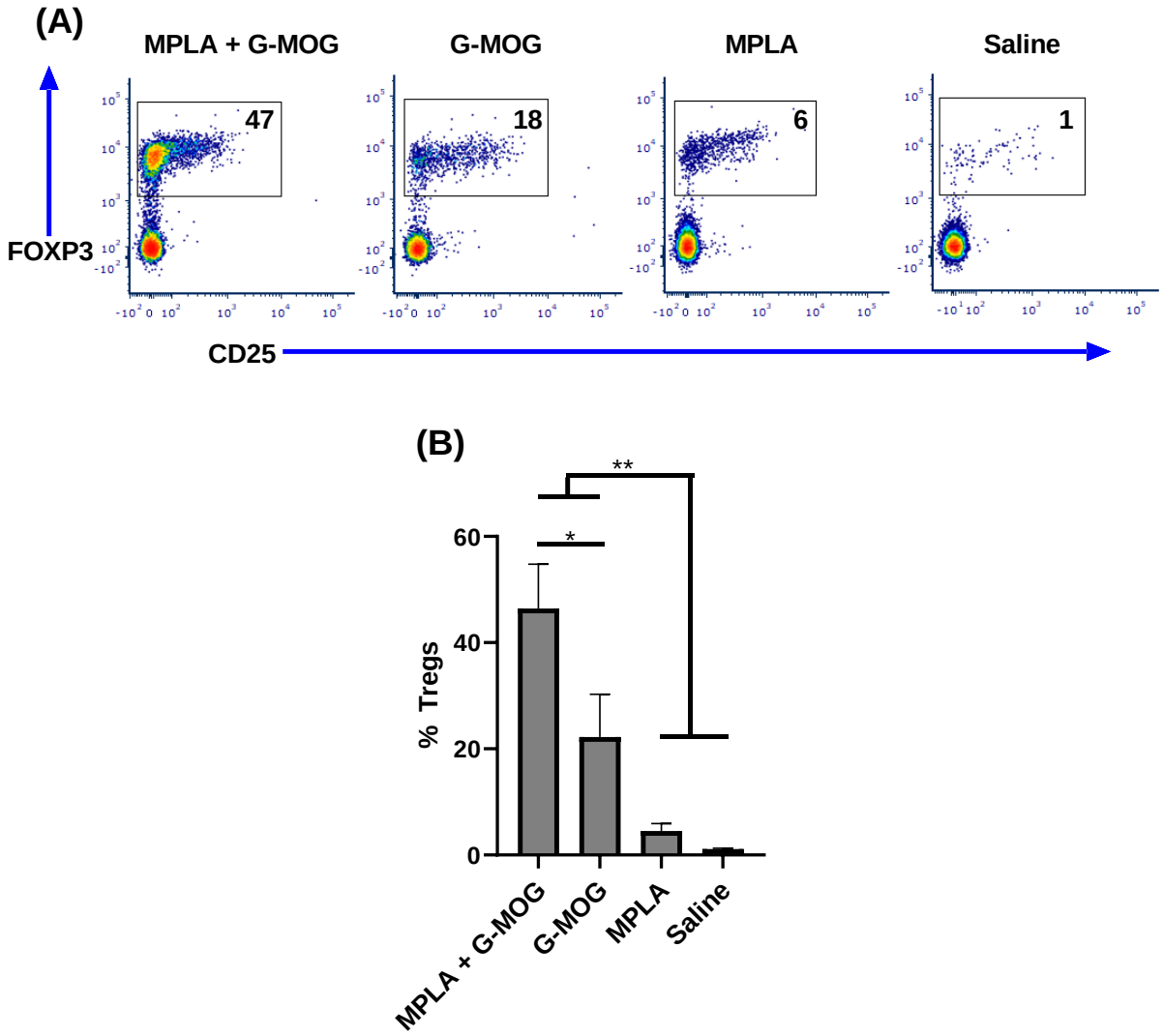
(A)
MPLA + G-MOG
G-MOG
MPLA
Saline
47
18
6
1
FOXP3
CD25
(B)
% Tregs
60
40
20
0
*
**
MPLA + G-MOG
G-MOG
MPLA
Saline

FIGURE 4.7 | Administration of MPLA augmented tolerogenic vaccination manifest as increased and extended Tregs levels in the PBMC pool. 2D2-FIG mice were injected with 2 nmoles GMCSF-MOG (n=8), 2 nmoles GMCSF-MOG + 80 µg MPLA (n=4), or saline (n=4). Formulation of vaccines is given in detail in the Materials and Methods section. Blood was collected via submandibular vein puncture on all indicated days. On each day, blood was washed and stained for CD3, CD4, CD44, Vβ11 (2D2 TCR), and CD25. Erythrocytes were lysed and cells were analyzed using flow cytometry. (A) Shown are representative dot plots of CD25 and FOXP3 expression of $CD3^+$ $CD4^+$ $V\beta11^+$ T cells that were obtained day 54 post-injection. (B) Shown are the compiled data of $FOXP3^+$ percentages in the $CD3^+$ $CD4^+$ $V\beta11^+$ T cell pool. The symbol '*' indicates statistical significance between "MPLA + G-MOG" and "G-MOG" groups calculated via repeated-measures ANOVA. (C) Shown are cumulative bar graphs of percent Tregs of $CD3^+$ $CD4^+$ $V\beta11^+$ T cells on day 54 for each treatment. (D) Shown are the compiled numbers of $FOXP3^+$ Tregs/ µL of blood. Note that the symbol '*' indicates statistical significance between "MPLA + G-MOG" and "G-MOG" groups calculated via one-tailed t-tests at each timepoint. (E) Shown is a bar graph of number of $FOXP3^+$ Treg/ µL of blood on day 16 for each treatment. Statistical significance was calculated via one-way ANOVA. Error bars represent SEM. ($*p < 0.05$)

Figure 4.7

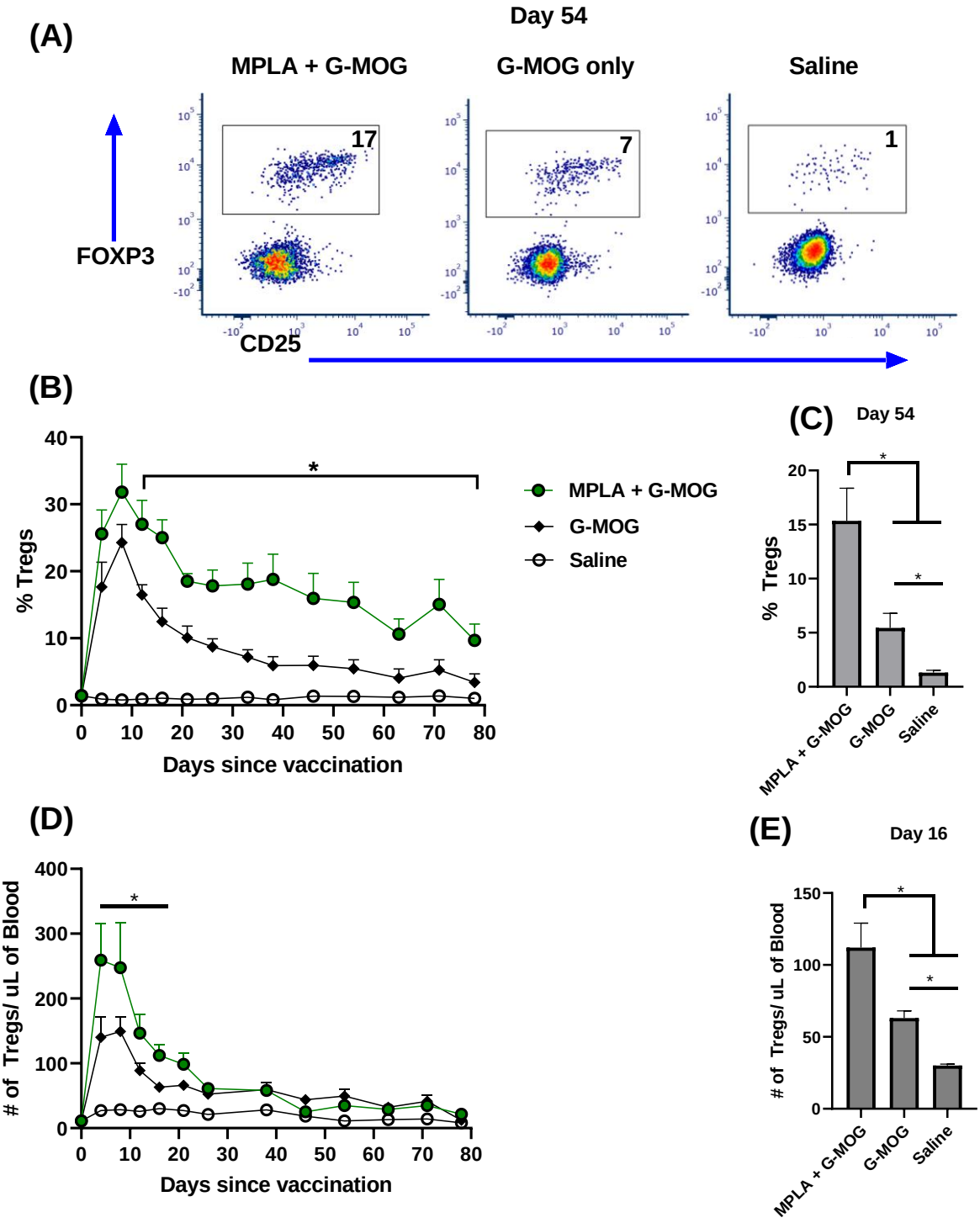
(A)
Day 54
MPLA + G-MOG
G-MOG only
Saline
17
7
1
FOXP3
CD25
(B)
% Tregs
Days since vaccination
MPLA + G-MOG
G-MOG
Saline
(C)
Day 54
% Tregs
MPLA + G-MOG
G-MOG
Saline
(D)
# of Tregs/ uL of Blood
Days since vaccination
(E)
Day 16
# of Tregs/ uL of Blood
MPLA + G-MOG
G-MOG
Saline

FIGURE 4.8 | MPLA potentiated T cell lymphocytopenia caused by tolerogenic vaccination in vivo. 2D2-FIG mice were injected with 2 nmoles GMCSF-MOG (n=8), 2 nmoles GMCSF-MOG + 80 µg MPLA (n=4), or saline (n=4). Formulation of vaccines is given in detail in the Materials and Methods section. Blood was collected via submandibular vein puncture on the indicated days. On each day, blood was washed and stained for CD3, CD4, CD44, Vβ11 (2D2 TCR) and CD25. Erythrocytes were lysed and cells were analyzed using flow cytometry. (A) Shown are representative dot plots of CD4 and CD3 expression of total viable blood leukocytes from day 54 post-injection. (B) Shown are compiled data of $CD4^+$ $CD3^+$ T cell percentages of the total leukocyte pool. The symbol '*' indicates statistical significance between "MPLA + G-MOG" and "G-MOG" groups calculated via repeated-measures ANOVA. (C) Shown is a bar graph of the percent T cells of total viable leukocytes on day 54 for each treatment group. Statistical significance is calculated by use of one-way ANOVA. (D) Shown are compiled data of total number of $CD4^+CD3^+$ T cells per µL of blood over the course of 78 days for each treatment group. The symbol '*' indicates statistical significance between "MPLA + G-MOG" and "G-MOG" groups calculated via one-tailed t-tests on each day. (E) Shown is a bar graph of the total T cell count on day 38 for each treatment group. Statistical significance was calculated by use of one-tailed t-tests comparing each group. Error bars represent SEM. ($*p < 0.05$)

Figure 4.8

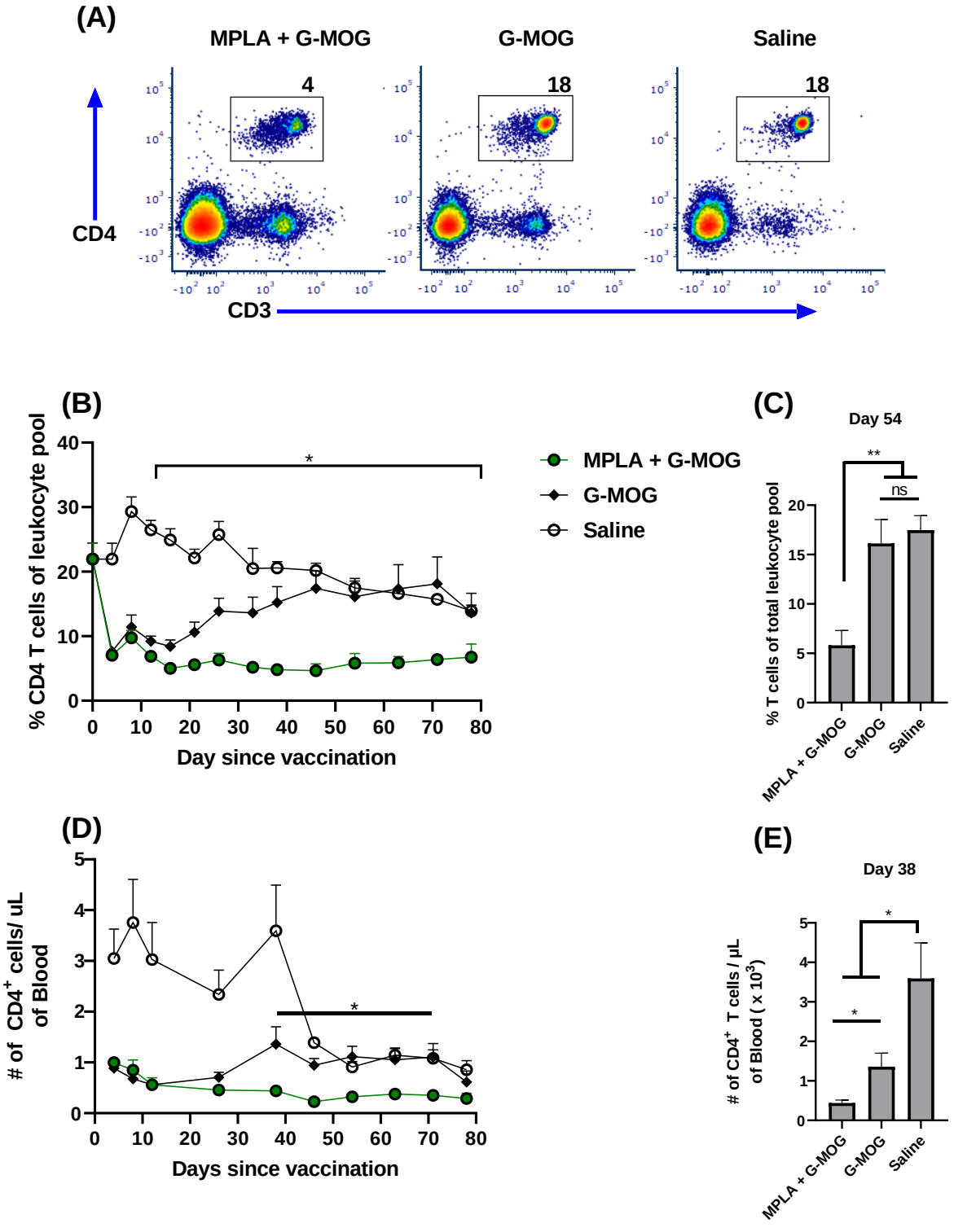
(A)
MPLA + G-MOG
G-MOG
Saline
4
18
18
CD4
CD3
(B)
% CD4 T cells of leukocyte pool
Day since vaccination
MPLA + G-MOG
G-MOG
Saline
(C)
Day 54
% T cells of total leukocyte pool
ns
MPLA + G-MOG
G-MOG
Saline
(D)
# of CD4+ cells/ uL of Blood
Days since vaccination
(E)
Day 38
# of CD4+ T cells / µL of Blood (x 10^3)
MPLA + G-MOG
G-MOG
Saline

FIGURE 4.9 | MPLA extended CD44 expression on Tcons. 2D2-FIG mice were injected with 2 nmoles GMCSF-MOG (n=8), 2 nmoles GMCSF-MOG + 80 µg MPLA (n=4), or saline (n=4). Formulation of vaccines is given in detail in the Materials and Methods section. Blood was collected via submandibular vein puncture on the indicated days. On each day, blood was washed and stained for CD3, CD4, CD44, Vβ11 (2D2 TCR) and CD25. Erythrocytes were lysed and cells were analyzed using flow cytometry. (A) Shown are representative dot plots of CD44 expression and FSC-A of $CD3^+$ $CD4^+$ $V\beta11^+FOXP3^-$ T cells on day 54 post vaccination for each treatment group. (B) Shown is a time course graph of the percent $FOXP3^-$ Tcons expressing CD44 across 78 days for each treatment group. The symbol '*' indicates statistical significance between "MPLA + G-MOG" and "G-MOG" groups calculated via repeated-measures ANOVA. (C) Shown is a bar graph of CD44 expression on $FOXP3^-$ Tcons on day 54 for each treatment group. Statistical significance is calculated via one-way ANOVA. Error bars represent SEM. (*$p < 0.05$)

Figure 4.9

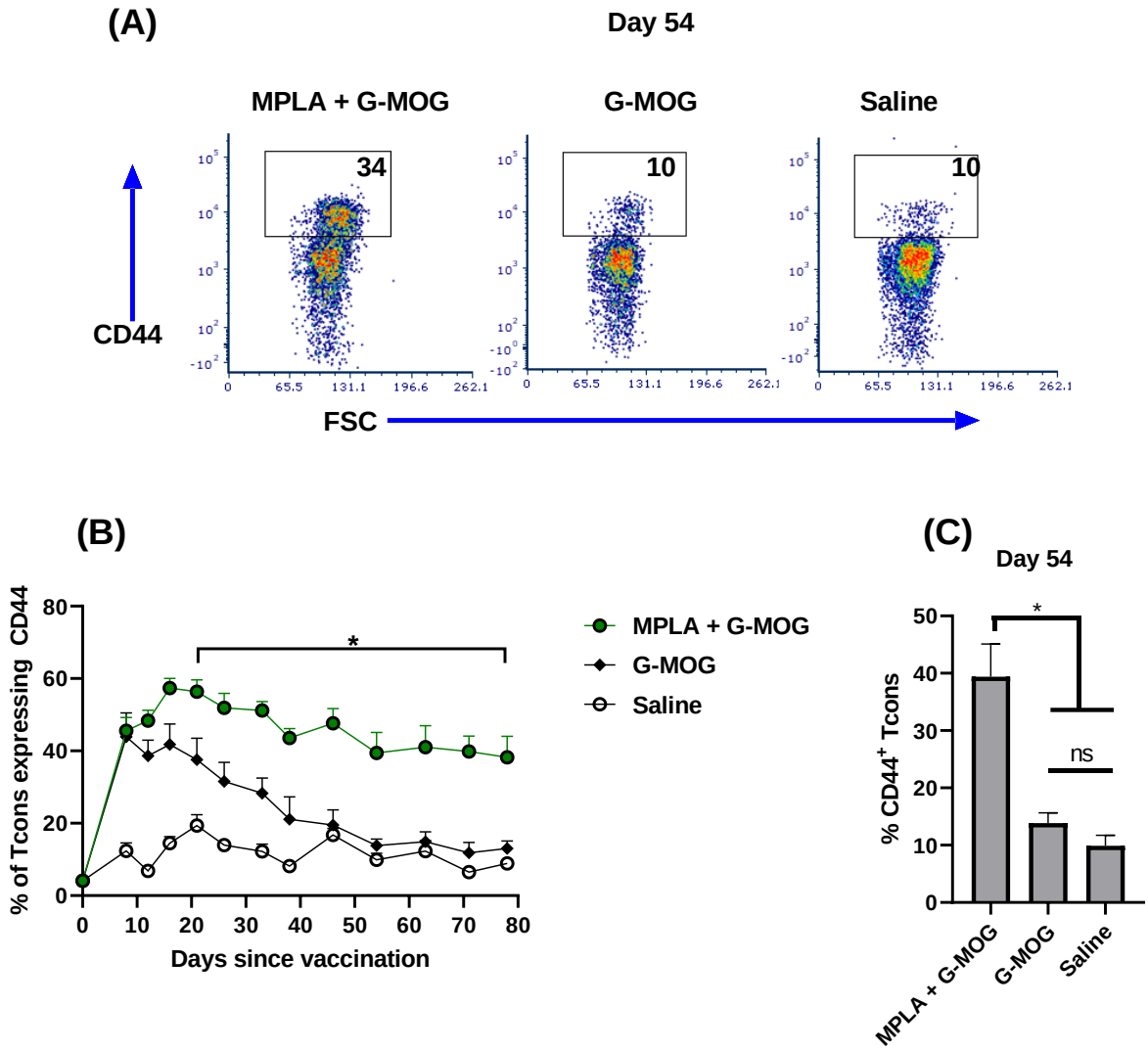
(A)
Day 54
MPLA + G-MOG
G-MOG
Saline
34
10
10
CD44
FSC
(B)
% of Tcons expressing CD44
Days since vaccination
MPLA + G-MOG
G-MOG
Saline
*
(C)
Day 54
% CD44+ Tcons
*
ns
MPLA + G-MOG
G-MOG
Saline

FIGURE 4.10 | Tregs expressed high levels of CD44 regardless of MPLA adjuvanticity. 2D2-FIG mice were injected with 2 nmoles GMCSF-MOG (n=8), 2 nmoles GMCSF-MOG + 80 µg MPLA (n=4), or saline (n=4). Formulation of vaccines is given in more detail in the Materials and Methods section. Blood was collected via submandibular vein puncture on all indicated days. On each day, blood was washed and stained for CD3, CD4, CD44, Vβ11 (2D2 TCR) and CD25. Erythrocytes were lysed and cells were analyzed using flow cytometry. (A) Shown are representative dot plots for day 54 post-injection showing cells gated on $CD3^+$ $CD4^+$ $V\beta11^+$ $FOXP3^+$ Tregs. (B) Shown are compiled time course graph of the percent $FOXP3^+$ Tregs expressing CD44 across 78 days for each treatment group. Not significant (ns) refers to statistical comparison between "MPLA + G-MOG" and "G-MOG" groups calculated via repeated-measures ANOVA. (C) Shown is a bar graph of the percent Tregs that are $CD44^+$ in each treatment group on day 54. Statistical significance is calculated via one-way ANOVA. Error bars represent SEM.

Figure 4.10

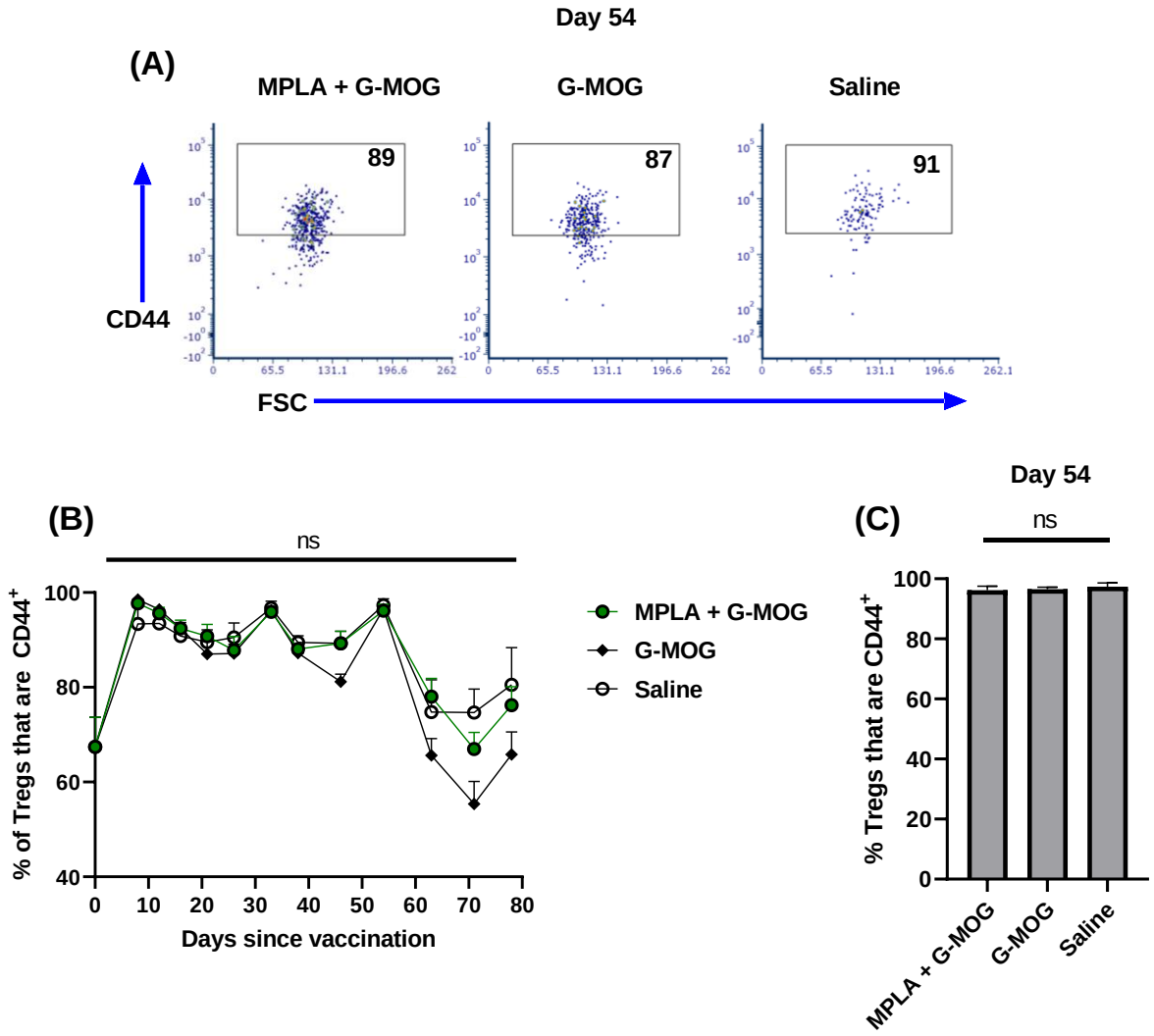
Day 54
(A)
MPLA + G-MOG
G-MOG
Saline
89
87
91
CD44
FSC
(B)
ns
% of Tregs that are CD44+
Days since vaccination
MPLA + G-MOG
G-MOG
Saline
Day 54
(C)
ns
% Tregs that are CD44+
MPLA + G-MOG
G-MOG
Saline

FIGURE 4.11 | MPLA was an effective tolerogenic adjuvant in EAE. EAE was induced as described in the Materials and Methods section. Mice were treated with 4 nmoles GMCSF-MOG (n=6), 4 nmoles GMCSF-MOG + 10 μg MPLA (n=6), or saline (n=6) on day 13 as indicated by an arrow. Mice were weighed and scored each day. Statistical significance was calculated by a one-way ANOVA on each day. The symbol "*" indicates statistical differences between "GMCSF-MOG + MPLA" and "GMCSF-MOG" groups. Error bars represent SEM. (*$p < 0.05$)

Figure 4.11

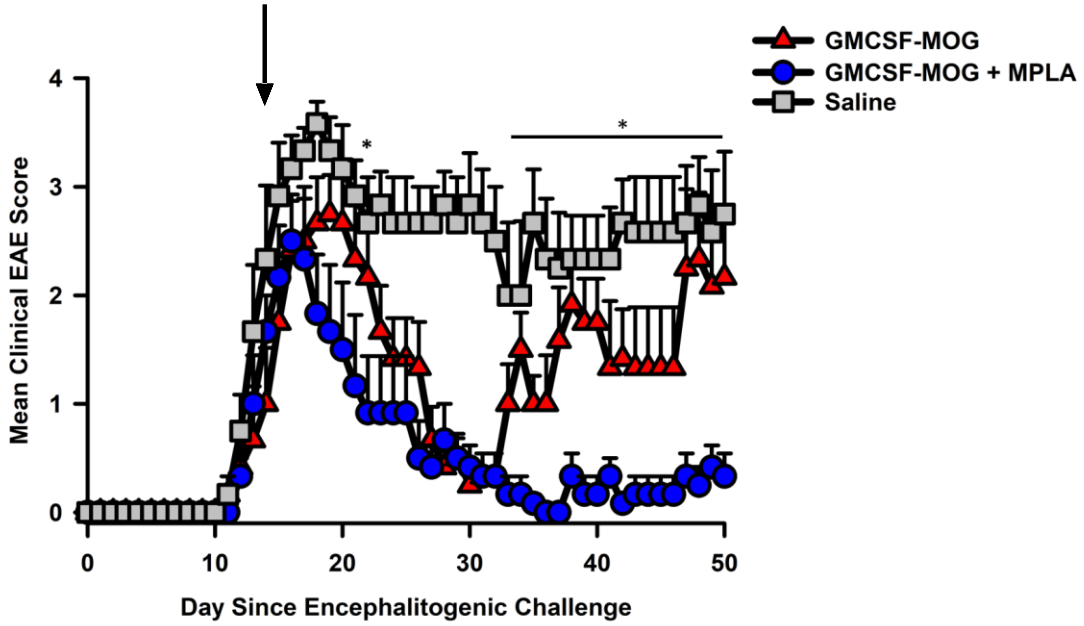
GMCSF-MOG
GMCSF-MOG + MPLA
Saline
Mean Clinical EAE Score
Day Since Encephalitogenic Challenge
0
1
2
3
4
0
10
20
30
40
50
*
*

CHAPTER 5

LOW-EFFICIENCY ANTIGEN RECOGNTION EVENTS FAVORS TOLEROGENIC T CELL RESPONSES

5.1 ABSTRACT

Here, we show that the efficiency of TCR antigen recognition was formative in determining the fate of responder T cells. TCR transgenic 2D2 T cells recognizing the low-affinity antigen MOG exhibited elevated expression of the immunoregulatory molecule PD-1 compared to 2D2 T cells recognizing high-affinity antigen NFM. In addition, we show that low-affinity MOG recognition led to lower CD40L levels on responder 2D2 T cells compared to high-affinity NFM recognition. These data indicate that lower-efficiency antigen recognition events lead to lower immunogenicity via decreased co-stimulatory (CD40L) and increased co-inhibitory (PD-1) molecule induction on responder 2D2 T cells. Additionally, MPLA treatment of DCs increased the CD40L inductive potential only in the context of the high-affinity antigen (NFM), further highlighting the importance of antigen recognition efficiency in determining T cell fate. We also show that inhibiting the CD40L/CD40 axis increased Tregs *in vitro* and led to a more stable and suppressive Treg phenotype. Altogether we show that low-efficiency antigen recognition events support tolerogenic T cell responses at least partly through lower CD40L/CD40 interaction.

5.2 RESULTS

Low-affinity antigen led to less immunogenic T cell responses compared to high-affinity antigens *in vivo* and *in vitro*

We compared NFM and MOG antigens to test the concept that low-efficiency antigen recognition events support tolerogenic T cell responses. The approach utilized the 2D2 TCR transgenic mouse strain that recognizes NFM as a higher affinity antigen and MOG as a lower affinity antigen (261). First, we injected 2D2-FIG mice with GMCSF-MOG or GMCSF-NFM and analyzed responder T cell phenotype. We found that, in comparison to GMCSF-NFM injection, GMCSF-MOG injection led to higher PD-1 expression, a major immunoregulatory molecule on the surface of T cells (Figure 5.1A-C) (262, 263). Over the course of 19 days, T cells from mice that received GMCSF-MOG had higher PD-1 expression compared to those from mice that received GMCSF-NFM (Figure 5.1B). On day 5 specifically, 38% of T cells from GMSCF-MOG-vaccinated mice were PD-1^+ compared to 18% of T cells from GMCSF-NFM-vaccinated mice (Figure 5.1A-C). Increased PD-1 on T cells indicated a lower immunogenic state of responder T cells following low-efficiency antigen recognition.

In addition to PD-1, CD40L expression is a major costimulatory molecule that drives immunogenic T cell responses. We have previously shown that low-efficiency antigen recognition are typically below threshold for triggering the CD40L/CD40 axis (264). Here, we show that NFM leads to higher CD40L expression than MOG on responder 2D2-FIG T cells (Figure 5.2A-C). At every concentration measured ranging from 10 nM to 10 μM, NFM stimulated higher CD40L expression compared to MOG (Figure 5.2B). At 10 μM, NFM stimulated CD40L expression on 26% of T cells whereas MOG stimulated 7% of T cells to express a CD40L^+ phenotype (Figure 5.2A-C). Indeed, MOG was an effective inducer of CD40L

expression only at concentrations of 320 nM or above. The data indicated that the efficiency of TCR antigen recognition is proportional to the efficiency of CD40L induction. These data highlight the importance of low-efficiency antigen recognition in limiting immunogenicity of responder T cells, which in turn may enable more efficient tolerogenic responses.

Antigen presentation by CD25^{+} DCs stimulates CD40L on T cells by a mechanism contingent upon high-affinity antigen recognition *in vitro*

We next tested whether MPLA-treatment of DCs impacted the CD40L expression of responder T cells. Interestingly, we found that MPLA-treated DCs, which have higher MHCII, CD86 and CD25 expression, elicited higher levels of CD40L on responder T cells only in the context of high-affinity antigen. When NFM was presented by MPLA-treated DCs, responder 2D2 T cells exhibited higher levels of CD40L expression compared to when NFM was presented by untreated DCs (Figure 5.3A-C). At 1 µM, MPLA-treated DCs presenting NFM led to CD40L expression on 19% of T cells compared to 13% when NFM was presented on untreated DCs. This difference was not seen in the context of MOG, as MPLA-treated and untreated DCs induced similar levels of CD40L on responder T cells. At 1 µM, MPLA-treated DCs presenting MOG led to 3% of T cells expressing CD40L in comparison to MPLA-treated DCs presenting NFM which induced 19% of T cells to express CD40L. These data highlight the impact of the antigen-recognition efficiency in the induction of the co-stimulatory molecule CD40L.

DCs displayed less CD40 compared to macrophages *in vitro*

To support the hypothesis that lower CD40/CD40L interactions facilitates DC induction of tolerogenic T cells, we assessed CD40 expression on APCs to determine which APC subset

may best support T cell interactions with lower CD40/CD40L engagement. We compared CD40 expression of DCs and macrophages and found that macrophages expressed higher CD40 levels compared to DCs (Figure 5.4A-C). In addition, LPS-treatment increased CD40 expression on both DCs and macrophages, but macrophage CD40 levels were higher compared to that of DCs in both the presence and absence of LPS. Following LPS-treatment, 99% of macrophages expressed CD40 compared to 76% of DCs (Figure 5.4A-B). Following LPS-treatment, $CD40^+$ macrophages had a 3-fold higher CD40 MFI than $CD40^+$ DCs (Figure 5.4C). In addition, higher percentages of untreated macrophages expressed CD40 (56%) than untreated DCs (8%), and untreated macrophages had a higher CD40 MFI than untreated DCs. The lower CD40 expression of DCs compared to macrophages may be indicative of their ability to act as fine-tuned APCs that support tolerogenic or immunogenic T cell responses.

Inhibiting the CD40/CD40L axis favored Treg dominance *in vitro*

Since tolerogenic T cell responses were favored through low-efficiency recognition events and consequentially, low-efficiency CD40/CD40L interactions, we hypothesized that antagonizing this interaction would favor Treg responses. To test this hypothesis, we utilized MR-1, an antagonistic anti-CD40L mAb (265). In an initial Treg activation, we found that the addition of MR-1 to the culture increased the resulting percentage of Tregs (Figure 5.5A-B). With MR-1, Tregs comprised 85% of the T cell culture compared to 52% without MR-1 (Figure 5.5A-B). In a separate experiment, MR-1 was found to increase Treg percentages with either MOG or NFM as the activating antigen (Figure 5.5C). Additionally, the resulting Tregs in cultures with MR-1 were found to have higher FOXP3 MFI values compared to cultures without MR-1 (Figure 5.5D). This observed increase in Treg percentages and FOXP3 MFI indicated that

inhibiting CD40L/CD40 interactions favors dominance of Tregs and stability of the resulting Tregs.

We also found that MR-1 antagonism increased CD25 expression during Treg activation. When MR-1 was present, Tregs bearing a $CD25^{high}$ phenotype increased in frequency in both MOG-activated and NFM-activated 2D2 T cell cultures (Figure 5.6A-C). With MOG as the antigen, MR-1 antagonism increased Treg frequencies featuring high levels of CD25 (57%) in comparison to no antibody (25%) (Figure 5.6A-B). In NFM-stimulated cultures, MR1 antagonism increased Treg frequencies featuring high levels of CD25 (43%) compared to controls without antibody (34%). The finding that MOG induced higher levels of CD25 than NFM in the presence of MR-1 is consistent with the idea that less efficient CD40/CD40L interactions drives higher CD25 expression on Tregs. The same trends are seen for CD25 MFI values of Tregs (Figure 5.6A-B). In conclusion, when either MOG or NFM were used as activating antigens, MR-1 led to higher CD25 MFI on 2D2 Tregs compared to cultures without MR-1. Taken together, inhibition of the CD40/CD40L interactions during antigen recognition facilitates a more stable and suppressive Treg phenotype.

5.3 CONCLUSIONS

As noted previously, enhancing antigen presentation via MPLA or LPS appeared to represent an amplifier, whereas high or low efficiency TCR-antigen ranges appeared to control functional outcomes (i.e., tolerance versus immunogenicity). For example, low-efficiency antigen recognition led to lower immunogenicity of responder T cells as measured by increased immunosuppressive PD-1 expression and decreased immunogenic CD40L expression. Specifically, increased antigen presentation of high-affinity antigen NFM led to increased CD40L expression on responder T cells, while increased antigen presentation of a low-affinity antigen, MOG, had little or no effect on CD40L levels. The differential immunogenicity of T cell responses effected T cell fate because, CD40L antagonism increased Treg levels and led to an enhanced Treg phenotype. Altogether, these data show the importance of the efficiency of the antigen recognition event in determining responder T cell fate.

FIGURE 5.1 | Low-affinity antigens led to higher PD-1 expression levels on responder T cells *in vivo*. 2D2-FIG mice (n=5/ group) were injected subcutaneously with 4 nmoles GMCSF-MOG, 4 nmoles GMCSF-NFM, or saline in 100 µL. Blood was collected via submandibular vein puncture on days 5, 12 and 19 post-injection. Blood was washed and stained for surface expression of CD3, CD4, and PD-1. Erythrocytes were lysed, and cells were analyzed. (A) Shown are representative dot plots of PD-1 expression and FSC-A on $CD3^+$ $CD4^+$ T cells on day 5 days post-injection. (B) Shown are compiled data from all days showing the percentages of $CD3^+$ $CD4^+$ T cells that are positive for PD-1. The symbol "**" indicates differences between "G-MOG" and "G-NFM" as calculated by one-way ANOVA on each day. (C) Shown are bar graphs highlighting the difference in the percent of $PD\text{-}1^+$ T cells on day 5 among the treatment groups. Statistical significance was calculated via one-way ANOVA. (**$p < 0.01$)

Figure 5.1

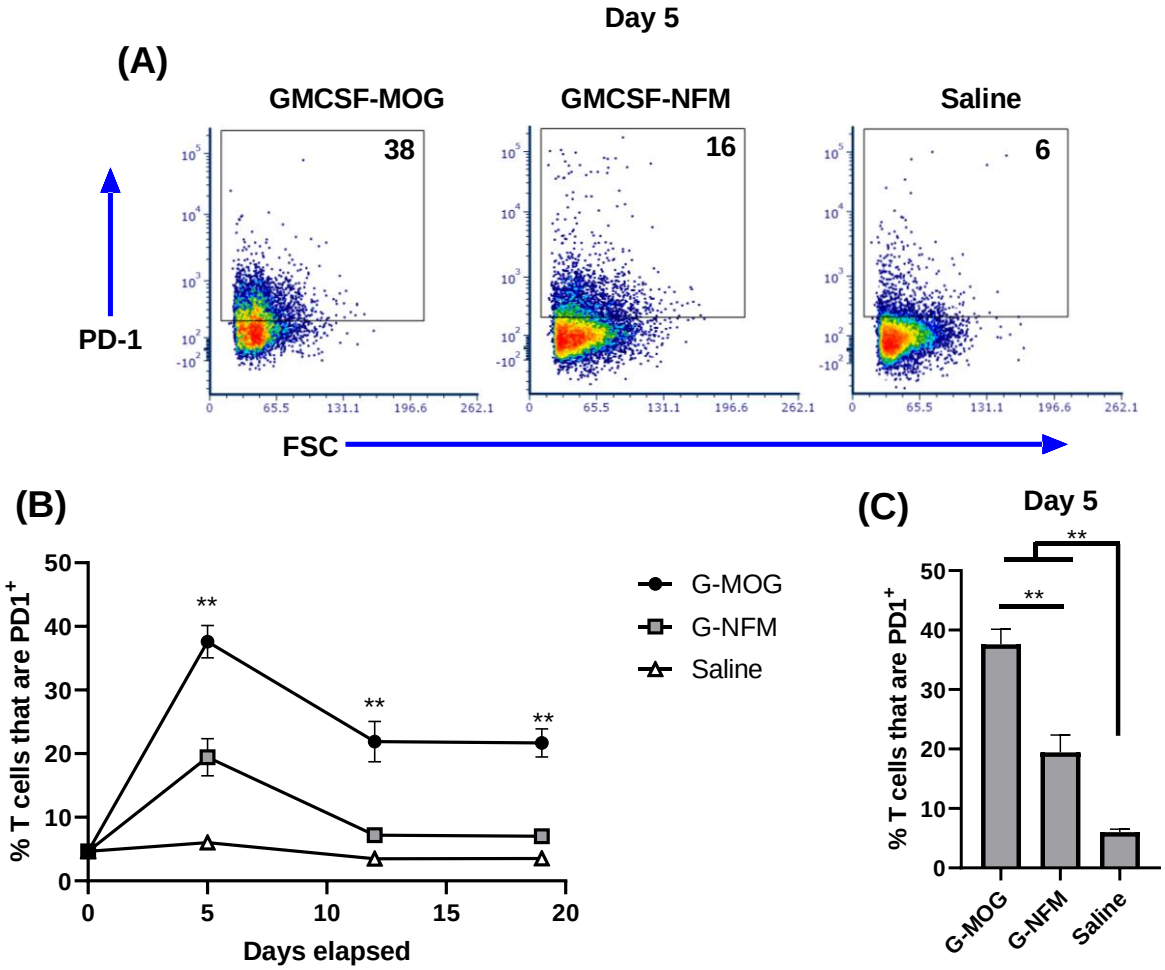
Day 5
(A)
GMCSF-MOG
GMCSF-NFM
Saline
38
16
6
PD-1
FSC
(B)
% T cells that are PD1+
Days elapsed
G-MOG
G-NFM
Saline
(C)
Day 5
% T cells that are PD1+
G-MOG
G-NFM
Saline

FIGURE 5.2 | Low-efficiency antigen recognition was associated with inefficient induction of CD40L on responder T cells *in vitro*. DCs were cultured as described in the Materials and Methods section. DCs were added at a 1:10 ratio to $CD4^+$ 2D2-FIG T cells sorted via magnetic-activated cell sorting. Antigen was added via half-log titration of MOG or NFM with concentrations ranging from 10 μM to 10 nM. Cells were co-cultured for 4 hours at 37°C before addition of fluorescently labeled anti-CD40L antibody. Cells were cultured for an additional 2 hours at 37°C and then were washed and stained for CD3 and CD4. Cells were then analyzed via flow cytometry. (A) Shown are representative dot plots at 10 μM for CD40L expression on $CD3^+$ $CD4^+$ T cells. (B) Shown are compiled data from the entire titration curve highlighting percentages of $CD3^+$ $CD4^+$ T cells that are $CD40L^+$. The symbol "*" indicates the difference between "NFM" and "MOG" as calculated via two-tailed t-tests at each concentration. (C) Shown are bar graphs of the percent $CD3^+$ $CD4^+$ T cells that are $CD40L^+$ at 10 μM for each treatment group. Statistical significance was calculated via two-tailed t-tests comparing each group. (*$p < 0.05$ and **$p < 0.01$)

Figure 5.2

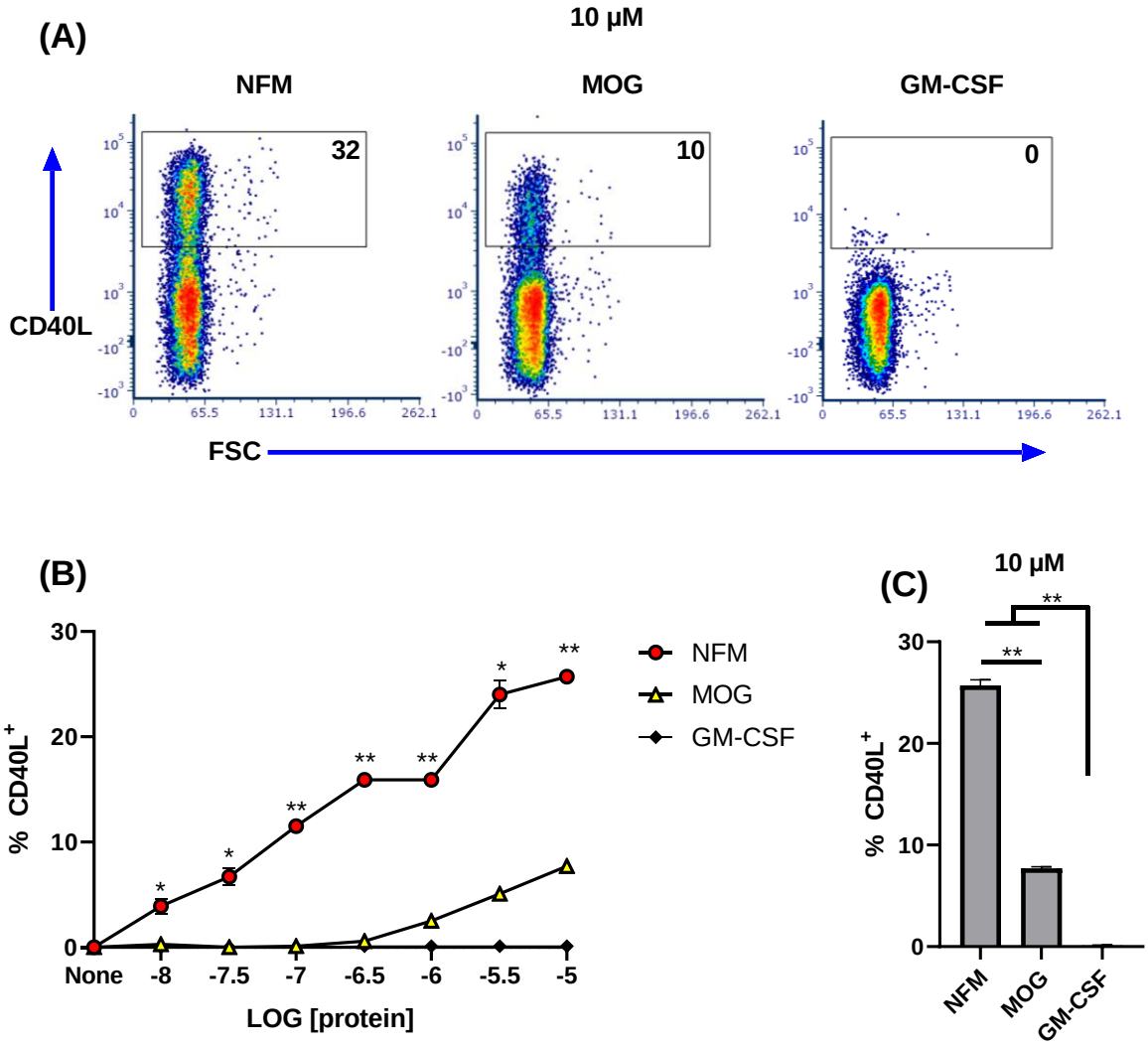
(A)
10 µM
NFM
MOG
GM-CSF
32
10
0
CD40L
FSC
(B)
% CD40L+
LOG [protein]
None
-8
-7.5
-7
-6.5
-6
-5.5
-5
NFM
MOG
GM-CSF
(C)
10 µM
% CD40L+
NFM
MOG
GM-CSF

FIGURE 5.3 | MPLA treatment of DCs predominantly augmented CD40L expression in the context of high-efficiency antigen recognition. DCs were cultured as described in the Materials and Methods section, and 1 µg/ mL MPLA was added to DCs for 24 hours. DCs were added at a 1:10 ratio to $CD4^+$ 2D2-FIG T cells purified via magnetic-activated cell sorting. Antigen was added via full-log titration of MOG or NFM with concentrations ranging from 1 µM to 10 pM. Cells were co-cultured for 4 hours at 37°C before addition of fluorescently labeled anti-CD40L antibody. Cells were cultured for an additional 2 hours at 37°C then washed and stained for CD3 and CD4. Cells were then analyzed via flow cytometry. (A) Shown are representative dot plots representing $CD3^+$ $CD4^+$ gated T cells stimulated with 1 µM NFM or MOG antigen and measured for CD40L expression. (B) Shown are compiled data from the entire titration curve showing percentages of $CD3^+$ $CD4^+$ T cells that were $CD40L^+$. The symbol "*" indicates differences between "MPLA-treated DCs NFM" versus "Untreated DCs NFM". Not significant "ns" compares "MPLA-treated DCs MOG" and "Untreated DCs MOG" as calculated via one-tailed t-tests at each concentration. (C) Shown are $CD40L^+$ T cell percentages in the T cell pool for each treatment group (1 µM MOG or NFM). Statistical significance was calculated via one-tailed t-tests comparing each group. (*$p < 0.05$, **$p < 0.01$)

Figure 5.3

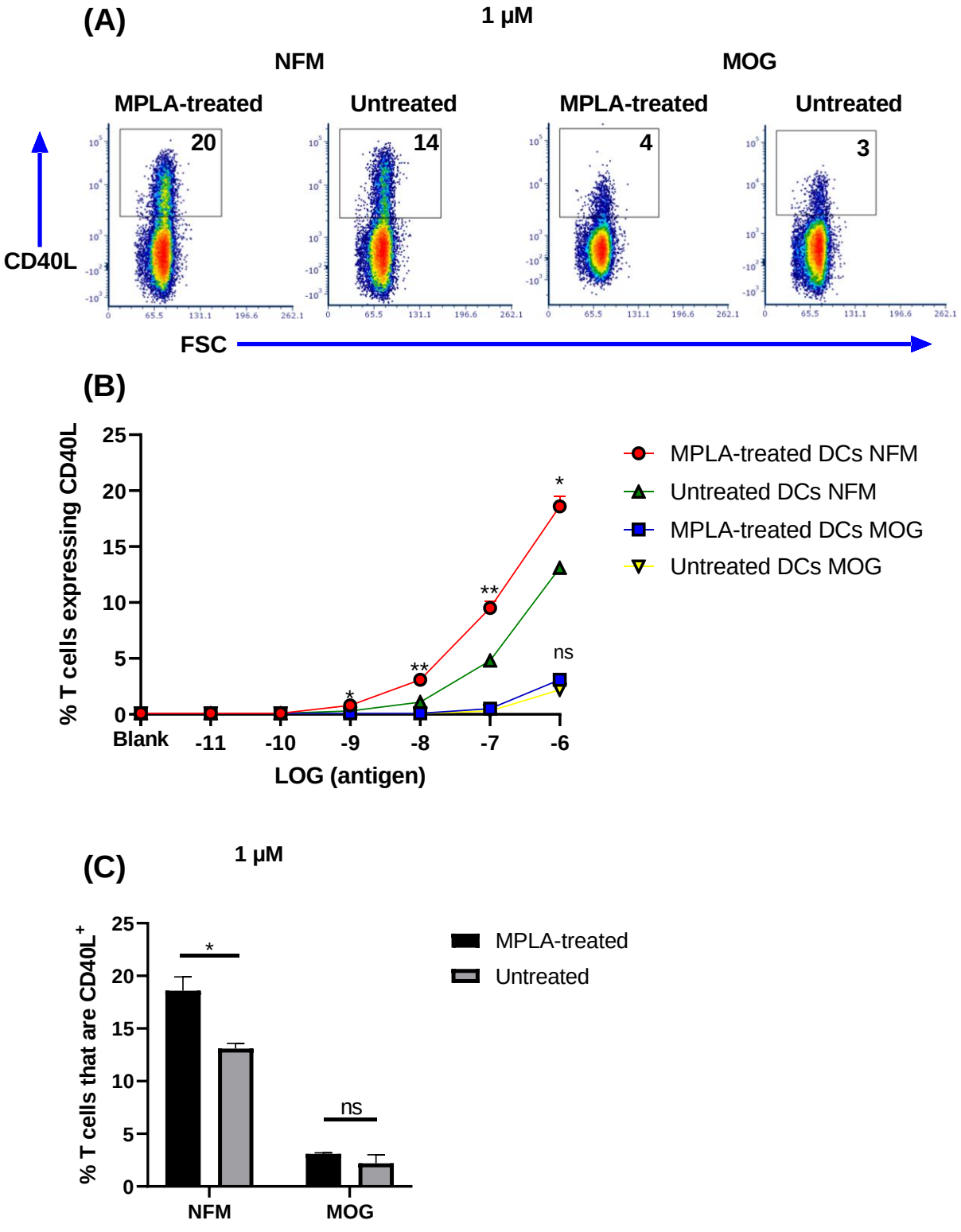
(A)
1 µM
NFM
MOG
MPLA-treated
Untreated
MPLA-treated
Untreated
20
14
4
3
CD40L
FSC
(B)
% T cells expressing CD40L
MPLA-treated DCs NFM
Untreated DCs NFM
MPLA-treated DCs MOG
Untreated DCs MOG
Blank
-11
-10
-9
-8
-7
-6
LOG (antigen)
ns
(C)
1 µM
% T cells that are CD40L+
MPLA-treated
Untreated
ns
NFM
MOG

FIGURE 5.4 | DCs express less CD40 than macrophages *in vitro*. DCs were cultured as described in the Materials and Methods section. GM-CSF was used to derive DCs, and M-CSF was used to derive macrophages. To induce maturation, 50 ng/ mL LPS was added to DCs or macrophages for 24 hours. Cells were released from plastic adherence via 2.5 mM EDTA release buffer and then were washed and stained for F4/80, CD11c, and CD40. Cells were then analyzed via flow cytometry. (A) Shown are representative dot plots highlighting CD40 expression. Macrophages were gated as $F4/80^+$ cells, whereas DCs were gated as $CD11c^+$ cells. Because macrophages and DCs displayed different autofluorescence and scatter properties, the positive gates shown were drawn based on unstained controls from the corresponding cell type. Shown are compiled bar graphs for each group (n=2) showing (B) percent $CD40^+$ cells and (C) MFI of $CD40^+$ macrophages or DCs simulated with or without LPS. Replicates indicate duplicate wells in the same experiment. Statistical significance was determined by use of two-tailed t-tests comparing each group. (**$p < 0.01$)

.

Figure 5.4

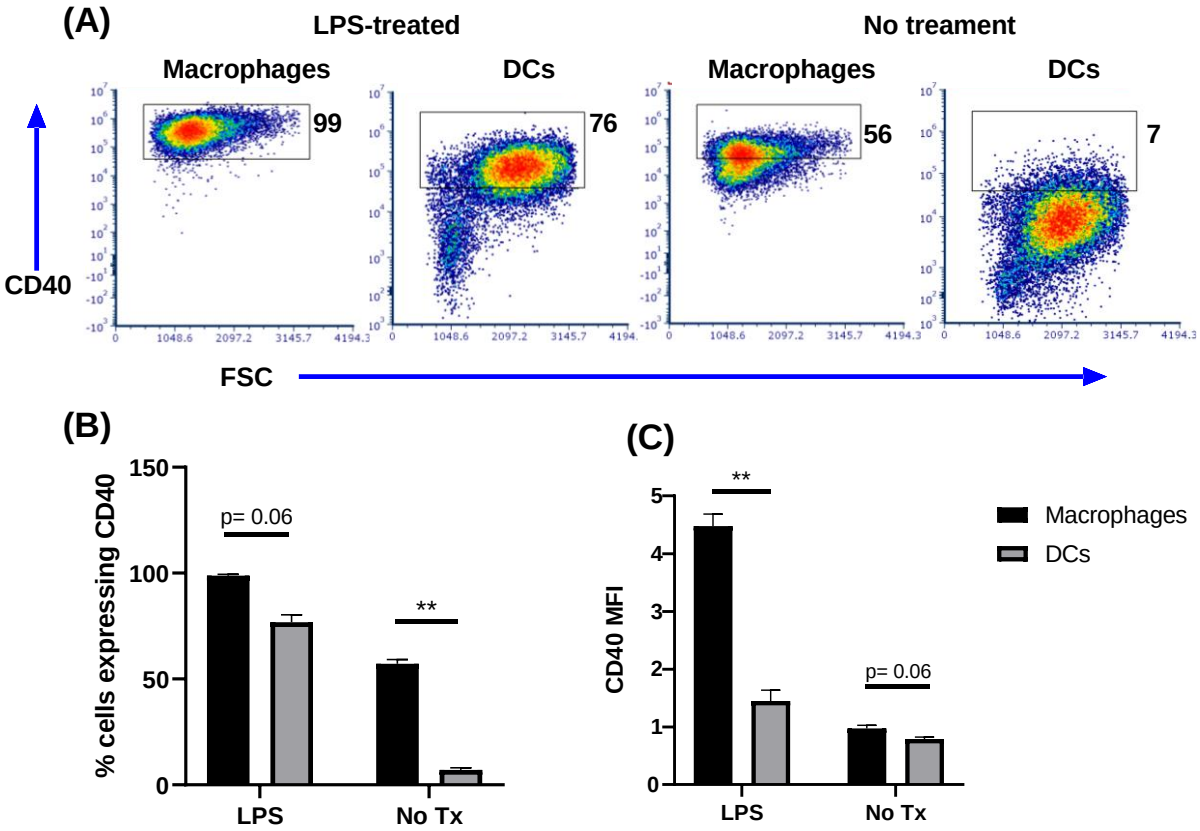
(A)
LPS-treated
No treament
Macrophages
DCs
Macrophages
DCs
99
76
56
7
CD40
FSC
(B)
% cells expressing CD40
p= 0.06
**
LPS
No Tx
(C)
CD40 MFI
**
p= 0.06
LPS
No Tx
Macrophages
DCs

FIGURE 5.5 | Inhibition of the CD40L/CD40 axis favored Treg differentiation *in vitro*. (A-B) MOG-stimulated Treg activation was performed as described in the Materials and Methods section. (C-D) In a separate experiment, 100 nM NFM was used in addition to 1 µM MOG in respective cultures. (A-D) Treg activation was performed in the presence or absence of 80 µg/ mL of the antagonistic anti-CD40L antibody MR-1. (A) Shown are representative dot plots of FOXP3 expression and FSC-A gated on MOG-stimulated $CD4^+$ T cells. (B) Shown are bar graphs representing Treg percentages for each treatment group (n=3). (C) Shown are compiled data of Treg percentages gated on $CD4^+$ T cells for each group with the added variable of antigen affinity (MOG and NFM = low and high TCR recognition efficiency respectively) (n=3/ group). (D) Shown is a bar graph of FOXP3 MFI of cells gated on $CD4^+$ $FOXP3^+$ Tregs for various treatment groups. Replicates indicate triplicate wells in the same experiment. Statistical significance was calculated via two-tailed t-tests. (*$p < 0.05$, **$p < 0.01$ and ***$p < 0.001$)

Figure 5.5

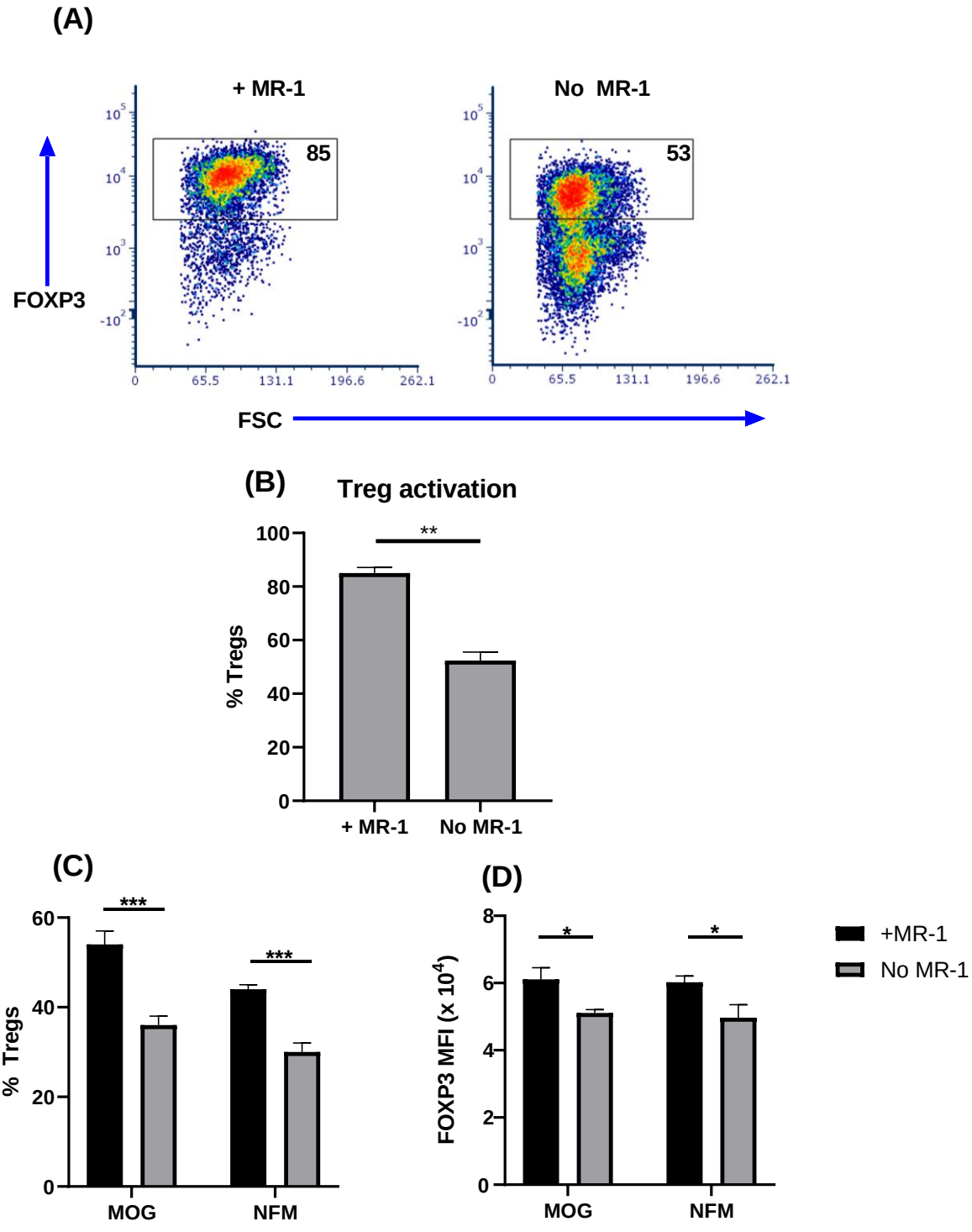
(A)
+ MR-1
No MR-1
85
53
FOXP3
FSC
(B)
Treg activation
% Tregs
+ MR-1
No MR-1
(C)
% Tregs
MOG
NFM
(D)
FOXP3 MFI (x 10^4)
MOG
NFM
+MR-1
No MR-1

FIGURE 5.6 | Inhibition of the CD40L/CD40 axis increased CD25 on Tregs *in vitro*. Treg activation was performed as described in the Materials and Methods section with 100 nM NFM used in place of 1 µM MOG in respective cultures. Additionally, 80 µg/ mL of the antagonistic MR-1 anti-CD40L antibody was or was not added to respective cultures. (A) Shown are representative dot plots of FOXP3 and CD25 expression gated on $CD4^+$ T cells. (B) Shown are compiled data of $CD25^{high}$ Treg percentages of $CD4^+$ T cells for each group (n=3/ group). (C) Shown is a bar graph of CD25 MFI gated on $CD4^+$ $FOXP3^+$ Tregs. Statistical significance was calculated via one-tailed t-tests. ($*p < 0.05$)

Figure 5.6

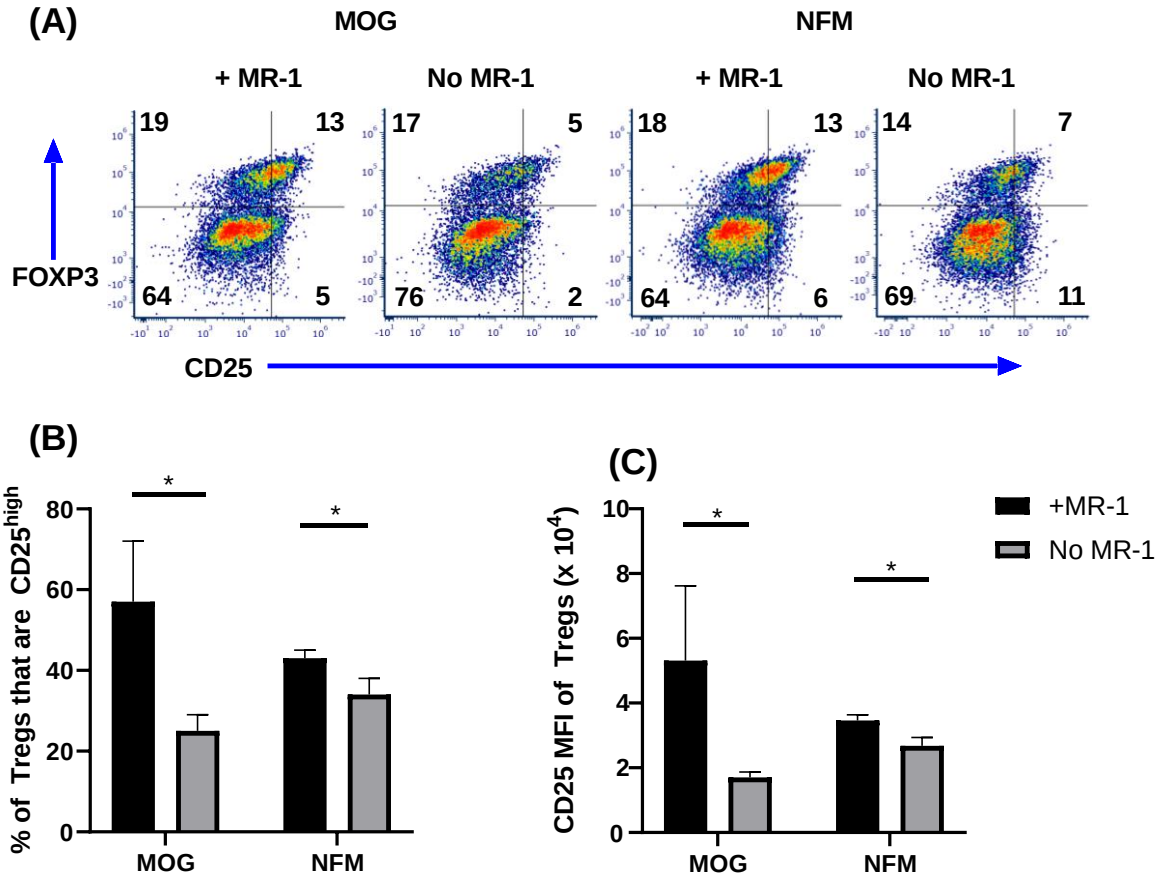
(A)
MOG
NFM
+ MR-1
No MR-1
+ MR-1
No MR-1
19
13
64
5
17
5
76
2
18
13
64
6
14
7
69
11
FOXP3
CD25
(B)
% of Tregs that are CD25high
80
60
40
20
0
*
*
MOG
NFM
(C)
CD25 MFI of Tregs (x 10^4)
10
8
6
4
2
0
*
*
MOG
NFM
+MR-1
No MR-1

CHAPTER 6

DISCUSSION

6.1 CD25 is part of the expression profile of mature DCs

The consistent and robust increase of CD25 expression on DCs in response to LPS treatment indicates CD25 is a marker of mature DCs. In this study, we show that TLR-4 agonism preferentially induces CD25 expression on DCs rather than other APC subsets including B cells and macrophages (Figures 3.1-3.7). We also highlight the coupling of CD25 expression to MHCII and CD86, known markers of DC maturation (Figure 3.2). The coupled expression of CD25 with known maturation markers indicates CD25 is part of the maturation gene expression profile (266). The rapid upregulation of CD25, CD86, and MHCII indicates possible mobilization from intracellular endosome storage of these markers (Figure 3.8). Frequent cycling of surface molecules during an immature state is a hallmark of DCs (134). Activation of DCs has been shown to activate mobilization of MHCII from endosomes to the surface of the DC. Other receptors are also known to be shuttled via endosomes to cellular locations where they mediate signaling (267). Given the known mobilization of surface markers through endosomes in DCs, it is reasonable to hypothesize that coupled mobilization may take place with MHCII, CD86, and as we show, CD25 upon activation through TLR-4 agonism (268).

Several previous studies have noted the expression of CD25 on DCs. For example, a subset of regulatory $CD25^+$ DCs expresses indoleamine 2, 3-dioxygenase (IDO), a suppressive

molecule secreted by DCs that converts tryptophan, a T cell stimulating factor, into kynurenine, a T cell inhibitory factor (151). In addition, CD25 is expressed on IFN-β-producing plasmacytoid DCs (pDCs) without the need for TLR-4 agonism (156). CD40L stimulation also induced CD25 levels on human pDCs in the presence of IL-3. Altogether, our research unifies these diverse findings by indicating that CD25 expression may be part of the standard gene expression profile of mature DCs (244, 245, 269).

6.2 CD25 on DCs is a reservoir of paracrine IL-2

We show that IL-2 is preferentially captured on LPS-treated DCs and that captured IL-2 levels on DCs are correlated with CD25 expression on DCs (Figure 3.11-3.12). These findings suggest that IL-2 specifically binds to CD25 on the surface of DCs, in accordance with the idea that $CD25^+$ DCs may sequester paracrine IL-2 (152) and thereby limit IL-2 in the local environment. Other studies provided evidence that quenching of IL-2 is beneficial for follicular T helper cells (Tfh), which thrive in the absence of IL-2 (270-272). The differentiation of T cells into Tfh cells was favored by $CD25^+$ DCs, and IL-2 signaling in T cells decreased in the presence of $CD25^+$ DCs. The quenching of IL-2 presumably leads to a low-zone IL-2 environment which is also beneficial for Tregs (68, 242, 273). We propose a similar mechanism in which $CD25^+$ DCs limit the available pool of free IL-2 leading to a low-zone IL-2 environment where Tregs dominate access to IL-2 due to higher expression of CD25 compared to CD25 expression levels on naïve T cells and Tcons. This proposed mechanism varies from the concept of DCs quenching IL-2 from the environment because quenching IL-2 involves receptor mediated endocytosis and does not leave IL-2 in the immunological synapse.

Due to the relatively low-affinity of the interaction of CD25 and IL-2, we propose that CD25 on the surface of DCs binds paracrine IL-2 and maintains a low-zone pool in the immunological synapse (274). Our data showing responder T cells can utilize IL-2 bound to CD25 on DCs provides credence to this hypothesis (Figure 3.14). With IL-2 present in the immunological synapse of DCs, access to IL-2 may be coupled with antigen recognition. Because T cells spend more time on the surface of DCs during MHC-restricted antigen recognition, TCR-engaged T cells may have preferential access to the IL-2 in the immunological synapse which will assist T cell activation. This mechanism may also benefit Tregs that competitively dominate the DC-localized pool of IL-2 (275, 276). Tregs are known to have higher affinity for cognate autoantigen compared to Tcons (277, 278), which may enable Tregs to dominate antigen recognition at the surface of the DCs at the expense of Tcons. In environments dominated by recognition of self-antigen, Tregs establish a larger area of interaction and a tighter physical opposition with DCs (276). In addition to dominating antigen recognition, Tregs also may dominate access to low levels of IL-2 in the immunological synapse. Higher levels of CD25 leads to higher levels of the heterotrimeric high affinity IL-2 receptor on Tregs compared to Tcons, allowing Tregs to dominate access to low levels of available IL-2. Overall, we propose a mechanism by which environmental IL-2 bound by CD25 on DCs preferentially binds to antigen-specific Tregs, assisting in their activation.

6.3 DCs induce diverse T cell responses

DCs are commonly thought of as the class of APC that specializes in antigen presentation to T cells. This specialized cell function is highlighted by diverse APC-focused mechanisms such as cross presentation of exogenous antigens to $CD8^+$ T cells and chemotactic migration to T cell-

enriched areas of lymph nodes. DCs induce a wide range of T cell responses. Under various conditions DCs have been shown to be instrumental in the differentiation of Th1, Th2, Th17, Tfh and Tregs highlighting a diverse niche as APCs (137, 279-284). This study particularly focuses on DCs ability to support Tregs. While other APC subsets play a role in the differentiation of $CD4^+$ T cells, Tregs are generally considered to be dependent on the DC lineage. DCs are known to maintain an antigen pool with an extended longevity compared to other APC classes (285-287). We used a DC-targeting vaccine (GMCSF-MOG) plus a DC maturation factor (MPLA) to show that T cells remain activated as measured by CD44 expression for 78 days, indicating a continued pool of cognate antigen for T cells to recognize (Figure 4.9). This continued activation is crucial to maintain the Treg pool as Tregs exhibit a mature, activated T cell phenotype that requires regular TCR ligation for survival in vivo. Accordingly, Tregs maintain a memory phenotype with high levels of CD44 (Figure 4.10) (258, 288, 289). Furthermore, lower affinity antigens persist for longer periods of time on APCs as higher affinity antigens are often removed from the surface through trogocytic membrane exchange (276, 290-292), further supporting the existence and persistence of the peripheral Treg pool.

For decades, the consensus was that lower levels of DC activation (i.e., immature DCs) supported tolerance while strongly activated mature DCs supported pathogenic T cell responses. More recently, this consensus has been revised in that mature DCs have been implicated in activation and maintenance of Treg populations (137, 151, 293). We corroborate the view that select mature DC subsets have a pronounced ability to support Treg responses. We provided evidence that activated $CD25^{high}$ DCs drove higher CD25 expression on responder Tregs, indicative of a more suppressive phenotype (Figure 4.1) wherein IL-2 binding to CD25 on presenting DCs may contribute to tolerogenic responses (Figure 4.3). We also show that these

mature DCs favor activation of Tregs over Tcons and enrich the $CD25^{+}$ Treg pool in mixed splenocyte cultures (Figure 4.2-Figure 4.4). We further show that including a DC activating factor (i.e., MPLA) in a Treg-inductive DC targeting vaccine further enhances Treg levels (Figures 4.6-4.7). Altogether our data support the idea that mature DCs facilitate Tregs under select conditions and elicit a more suppressive Treg phenotype compared to immature $CD25^{low}$ $MHCII^{low}$ $CD86^{low}$ DCs. While we focus on a mature DC/ Treg axis in tolerance in this project, we note that under different conditions, mature DCs potently induce immunogenic responses.

6.4 MPLA can function as a tolerogenic or immunogenic adjuvant

This study provides evidence that MPLA can increase tolerogenic responses driven by the tolerogenic GMCSF-MOG vaccine. Effective adjuvants accelerate, enhance, and prolong the immune response. In the context of tolerance, MPLA increased tolerogenic responses of the GMCSF-MOG vaccine by augmenting $FOXP3^{+}$ Tregs that persisted in circulation at higher frequencies through a 78-day time course (Figure 4.8). In the context of GMCSF-MOG vaccination, MPLA also conferred sustained remission in a chronic model of severe paralytic EAE (Figure 4.11) highlighting the ability of MPLA to potentiate tolerogenic vaccination. Conversely, MPLA is a clinically approved adjuvant for use in viral vaccines where the MPLA adjuvant increases antiviral immune responses (240, 294). We propose a mechanism of action by which MPLA as an adjuvant is not inherently tolerogenic or immunogenic. Rather, this study supports the concept that MPLA promotes immune responses that are consistent with the qualitative activities of particular antigens (Figures 5.2-5.3). Additionally, T cells are known to express TLR-4 so functional MPLA may also function through activation of T cells, which, in the context of self-antigen presentation, may further support Tregs (295, 296).

Similarly, the GM-CSF domain of GMCSF-antigen vaccines also has dual adjuvant potential in that the GM-CSF domain can augment tolerogenic or immunogenic activity dependent upon qualitative activities of antigens. In the context of GMCSF-MOG or GMCSF-OVA vaccination, low-efficiency TCR/ MHCII antigen recognition of a self-antigen such as MOG35-55 versus high-efficiency antigen recognition of a foreign antigen such as OVA favors tolerogenic versus immunogenic responses, respectively (226, 229, 264). Whereas GM-CSF domain potentiates tolerogenic responses when attached to MOG35-55, GM-CSF is an immunogenic adjuvant in cancer, viral, and bacterial vaccines (297-300). The adjuvant activity of GM-CSF and MPLA may be associated, at least in part, with the potential to drive DC maturation and thereby increase the efficiencies of antigen presentation together with enhanced long-term persistence of unique MHCII-peptide complexes on the surfaces of long-lived mature DCs. This study thereby supports an emerging consensus is that the efficiency of TCR recognition determines downstream signaling that sets the balance of immunogenic versus tolerogenic responses (197, 199, 301-304).

6.5 Antigen affinity determines responder T cell fate

As indicated above, the efficiency of the antigen recognition event is a major player in determining responder T cell fate with low-efficiency antigen recognition supporting tolerogenic responses and high-efficiency supporting immunogenic responses. The efficiency of the antigen recognition event integrates many events including affinity of TCR/MHC-Ag complexes, inductive conformational events, assembly of signaling complexes, and recruitment of costimulatory molecules and adhesion molecules (164, 305, 306). In this study, we provide evidence that low-efficiency antigen recognition of MOG35-55 leads to lower levels of

immunogenicity in responder T cells compared to high-efficiency recognition of NFM13-37. Recognition of MOG induced higher levels of the immunoregulatory molecule PD-1 compared to NFM (Figure 5.1) and induced lower levels of CD40L, a driver of immune activation (Figure 5.2). Even when cognate antigens were expressed on mature DCs presenting high levels of antigens, only NFM led to high levels of CD40L (Figure 5.3) highlighting the importance of the antigen recognition efficiency at driving T cell responses. We highlight the importance of the CD40/CD40L axis in driving T cell fate by specifically inhibiting this interaction with an antagonistic anti-CD40L antibody which increased Treg levels and favored a more suppressive Treg phenotype. This concept that has been proposed previously but not in the context of high- vs low-efficiency antigens (307, 308). Overall, this study supports the concept that in the immunological synapse, the efficiency of the antigen recognition is driven at least in part by TCR/MHCII-Ag affinity in combination with CD40L costimulatory interactions which are integrated by both the presenting APC and responder T cells to determine the balance between immunogenicity and tolerance.

6.6 Significance and conclusions

We show that CD25 induction is part of the maturation profile of DCs in response to TLR-4 agonism, highlighting a role for CD25 in the function of DCs. CD25 on DCs binds IL-2 which upon subsequent dissociation of IL-2 from DCs may be utilized by responder T cells to stimulate growth. Thus, CD25 on DCs may enable targeting of IL-2 to antigen-specific T cells during antigen presentation. The role of CD25 on mature DCs has not been fully elucidated yet but this study highlights the presence of CD25 on DCs and broaches the possibility of novel functional mechanisms.

In addition to CD25 induction on DCs, the TLR-4 agonist MPLA stimulated tolerogenic T cell responses when combined with GMCSF-MOG, a DC-targeting tolerogenic vaccine. This finding highlights the role of mature DCs in mediating tolerogenic T cell responses when presenting low-affinity self-antigens. Tolerogenic vaccination is an evolving field, and this study presents the novel finding that MPLA as an effective tolerogenic adjuvant. In the context of self-antigen presentation on DCs, MPLA enhances tolerance through increased percentages of Tregs as well as accelerated and sustained autoimmune disease amelioration. This idea could be utilized to theoretically enhance tolerogenic treatments that use self-peptide recognition to engender tolerogenic responses. There is a significant need for the development of tolerogenic treatments, as current clinical options consist of immunosuppressive and immunomodulatory treatments that are moderately efficacious and are often associated with adverse side effects due to their untargeted nature (213, 309).

In addition to the use MPLA as a tolerogenic adjuvant, this study reveals the importance of DC presentation of self-antigen in tolerogenic immunity. When presenting low-affinity myelin peptides, these DCs elicit robust tolerogenic T cell responses and ameliorate autoimmune-mediated CNS inflammation. In the context of other diseases, presentation of low-affinity antigen associated with other tissues may lead to amelioration of inflammation in that tissue. For example, presentation of low-affinity antigens from pancreatic beta cells may foster tolerogenic T cell responses leading to reduction in T1D.

Our data supports the model that the efficiency of the antigen recognition is an important parameter in determining responder T cell fate. We show lowering the efficiency of antigen recognition through CD40L blockade increases Treg percentage and the suppressive phenotype of these Tregs through elevated CD25 expression. Overall, our data contributes to the concept

that low-efficiency antigen recognition favors tolerance in responder T cells. MPLA-augmentation of these low antigen recognition events appears to potentiate tolerogenic T cell responses. This model provides a theoretical platform by which tolerance can be understood in T cell-mediated autoimmune disease.

CHAPTER 7

REFERENCES

1. Dempsey, P. W., S. A. Vaidya, and G. Cheng. 2003. The Art of War: Innate and adaptive immune responses. *Cellular and Molecular Life Sciences CMLS* 60: 2604-2621.

2. Gasteiger, G., A. D'Osualdo, D. A. Schubert, A. Weber, E. M. Bruscia, and D. Hartl. 2017. Cellular Innate Immunity: An Old Game with New Players. *Journal of Innate Immunity* 9: 111-125.

3. Rosales, C., and E. Uribe-Querol. 2017. Phagocytosis: A Fundamental Process in Immunity. *BioMed Research International* 2017: 1-18.

4. Trivedi, P. C., J. J. Bartlett, and T. Pulinilkunnil. 2020. Lysosomal Biology and Function: Modern View of Cellular Debris Bin. *Cells* 9: 1131.

5. Nguyen, J. A., and R. M. Yates. 2021. Better Together: Current Insights Into Phagosome-Lysosome Fusion. *Front Immunol* 12: 636078.

6. Mora, T., and A. M. Walczak. 2019. How many different clonotypes do immune repertoires contain? Cold Spring Harbor Laboratory.

7. da Gama Duarte, J., K. Woods, M. C. Andrews, and A. Behren. 2018. The good, the (not so) bad and the ugly of immune homeostasis in melanoma. *Immunol Cell Biol* 96: 497-506.

8. Kumar, B. V., T. J. Connors, and D. L. Farber. 2018. Human T Cell Development, Localization, and Function throughout Life. *Immunity* 48: 202-213.

9. Davenport, M. P., N. L. Smith, and B. D. Rudd. 2020. Building a T cell compartment: how immune cell development shapes function. *Nat Rev Immunol* 20: 499-506.

10. LeBien, T. W., and T. F. Tedder. 2008. B lymphocytes: how they develop and function. *Blood* 112: 1570-1580.

11. Mozes, E., R. Isac, and M. J. Taussig. 1975. Antigen-specific T-cell factors in the genetic control of the immune response to poly(Tyr,Glu)-polyDLAla--polyLys. Evidence for T- and B-cell defects in SJL mice. *J Exp Med* 141: 703-707.

12. Taussig, M. J. 1980. Antigen-specific T-cell factors. *Immunology* 41: 759-787.

13. Schatz, D. G., and Y. Ji. 2011. Recombination centres and the orchestration of V(D)J recombination. *Nat Rev Immunol* 11: 251-263.

14. Nemazee, D. 2000. Receptor selection in B and T lymphocytes. *Annu Rev Immunol* 18: 19-51.

15. Rahmanzadeh, R., W. Brück, A. Minagar, and M. A. Sahraian. 2018. Multiple sclerosis pathogenesis: missing pieces of an old puzzle. *Rev Neurosci* 30: 67-83.

16. Lassmann, H., and J. van Horssen. 2011. The molecular basis of neurodegeneration in multiple sclerosis. *FEBS Lett* 585: 3715-3723.

17. Lassmann, H. 2018. Multiple Sclerosis Pathology and its Reflection by Imaging Technologies: Introduction. *Brain Pathol* 28: 721-722.

18. Calabrese, M., and M. Castellaro. 2017. Cortical Gray Matter MR Imaging in Multiple Sclerosis. *Neuroimaging Clin N Am* 27: 301-312.

19. Hinman, R. M., and J. C. Cambier. 2014. Role of B lymphocytes in the pathogenesis of type 1 diabetes. *Curr Diab Rep* 14: 543.

20. Giwa, A. M., R. Ahmed, Z. Omidian, N. Majety, K. E. Karakus, S. M. Omer, T. Donner, and A. R. A. Hamad. 2020. Current understandings of the pathogenesis of type 1 diabetes: Genetics to environment. *World J Diabetes* 11: 13-25.

21. Prabhakar, B. S., R. S. Bahn, and T. J. Smith. 2003. Current perspective on the pathogenesis of Graves' disease and ophthalmopathy. *Endocr Rev* 24: 802-835.

22. McIver, B., and J. C. Morris. 1998. The pathogenesis of Graves' disease. *Endocrinol Metab Clin North Am* 27: 73-89.

23. Pelanda, R., and R. M. Torres. 2012. Central B-cell tolerance: where selection begins. *Cold Spring Harb Perspect Biol* 4: a007146.

24. Burger, M. L., K. K. Leung, M. J. Bennett, and A. Winoto. 2014. T cell-specific inhibition of multiple apoptotic pathways blocks negative selection and causes autoimmunity. *Elife* 3.

25. Tsubata, T. 2017. B-cell tolerance and autoimmunity. *F1000Res* 6: 391.

26. Breed, E. R., S. T. Lee, and K. A. Hogquist. 2018. Directing T cell fate: How thymic antigen presenting cells coordinate thymocyte selection. *Semin Cell Dev Biol* 84: 2-10.

27. Perniola, R. 2018. Twenty Years of AIRE. *Front Immunol* 9: 98.

28. Palmer, E. 2003. Negative selection--clearing out the bad apples from the T-cell repertoire. *Nat Rev Immunol* 3: 383-391.

29. Hogquist, K. A., T. A. Baldwin, and S. C. Jameson. 2005. Central tolerance: learning self-control in the thymus. *Nat Rev Immunol* 5: 772-782.

30. Yan, J., and M. J. Mamula. 2002. Autoreactive T cells revealed in the normal repertoire: escape from negative selection and peripheral tolerance. *J Immunol* 168: 3188-3194.

31. van der Vliet, H. J., and E. E. Nieuwenhuis. 2007. IPEX as a result of mutations in FOXP3. *Clin Dev Immunol* 2007: 89017.

32. Ramsdell, F., and S. F. Ziegler. 2014. FOXP3 and scurfy: how it all began. *Nat Rev Immunol* 14: 343-349.

33. Kim, J. M., J. P. Rasmussen, and A. Y. Rudensky. 2007. Regulatory T cells prevent catastrophic autoimmunity throughout the lifespan of mice. *Nat Immunol* 8: 191-197.

34. Lee, H. M., J. L. Bautista, and C. S. Hsieh. 2011. Thymic and peripheral differentiation of regulatory T cells. *Adv Immunol* 112: 25-71.

35. Shevach, E. M., and A. M. Thornton. 2014. tTregs, pTregs, and iTregs: similarities and differences. *Immunol Rev* 259: 88-102.

36. Moldenhauer, L. M., J. E. Schjenken, C. M. Hope, E. S. Green, B. Zhang, P. Eldi, J. D. Hayball, S. C. Barry, and S. A. Robertson. 2019. Thymus-Derived Regulatory T Cells Exhibit. *J Immunol* 203: 647-657.

37. Yadav, M., S. Stephan, and J. A. Bluestone. 2013. Peripherally induced tregs - role in immune homeostasis and autoimmunity. *Front Immunol* 4: 232.

38. Sharma, A., and D. Rudra. 2018. Emerging Functions of Regulatory T Cells in Tissue Homeostasis. *Front Immunol* 9: 883.

39. Commins, S. P. 2015. Mechanisms of Oral Tolerance. *Pediatric clinics of North America* 62: 1523-1529.

40. Duan, W., and M. Croft. 2014. Control of regulatory T cells and airway tolerance by lung macrophages and dendritic cells. *Ann Am Thorac Soc* 11 Suppl 5: S306-313.

41. Hasegawa, H., and T. Matsumoto. 2018. Mechanisms of Tolerance Induction by Dendritic Cells In Vivo. *Front Immunol* 9: 350.

42. Zegarra-Ruiz, D. F., D. V. Kim, K. Norwood, M. Kim, W. H. Wu, F. B. Saldana-Morales, A. A. Hill, S. Majumdar, S. Orozco, R. Bell, J. L. Round, R. S. Longman, T. Egawa, M. L. Bettini, and G. E. Diehl. 2021. Thymic development of gut-microbiota-specific T cells. *Nature* 594: 413-417.

43. Sawant, D. V., and D. A. Vignali. 2014. Once a Treg, always a Treg? *Immunol Rev* 259: 173-191.

44. Smigiel, K. S., S. Srivastava, J. M. Stolley, and D. J. Campbell. 2014. Regulatory T-cell homeostasis: steady-state maintenance and modulation during inflammation. *Immunol Rev* 259: 40-59.

45. Schorle, H., T. Holtschke, T. Hünig, A. Schimpl, and I. Horak. 1991. Development and function of T cells in mice rendered interleukin-2 deficient by gene targeting. *Nature* 352: 621-624.

46. Willerford, D. M., J. Chen, J. A. Ferry, L. Davidson, A. Ma, and F. W. Alt. 1995. Interleukin-2 receptor alpha chain regulates the size and content of the peripheral lymphoid compartment. *Immunity* 3: 521-530.

47. Morgan, D. A., F. W. Ruscetti, and R. Gallo. 1976. Selective in vitro growth of T lymphocytes from normal human bone marrows. *Science* 193: 1007-1008.

48. Sakaguchi, S., N. Sakaguchi, M. Asano, M. Itoh, and M. Toda. 1995. Immunologic self-tolerance maintained by activated T cells expressing IL-2 receptor alpha-chains (CD25). Breakdown of a single mechanism of self-tolerance causes various autoimmune diseases. *J Immunol* 155: 1151-1164.

49. Chen, X., M. Bäumel, D. N. Männel, O. M. Howard, and J. J. Oppenheim. 2007. Interaction of TNF with TNF receptor type 2 promotes expansion and function of mouse CD4+CD25+ T regulatory cells. *J Immunol* 179: 154-161.

50. Kuniyasu, Y., T. Takahashi, M. Itoh, J. Shimizu, G. Toda, and S. Sakaguchi. 2000. Naturally anergic and suppressive CD25(+)CD4(+) T cells as a functionally and phenotypically distinct immunoregulatory T cell subpopulation. *Int Immunol* 12: 1145-1155.

51. Schmidt, A., N. Oberle, and P. H. Krammer. 2012. Molecular mechanisms of treg-mediated T cell suppression. *Front Immunol* 3: 51.

52. Sharabi, A., M. G. Tsokos, Y. Ding, T. R. Malek, D. Klatzmann, and G. C. Tsokos. 2018. Regulatory T cells in the treatment of disease. *Nature Reviews Drug Discovery* 17: 823-844.

53. Wan, Y. Y., and R. A. Flavell. 2007. Regulatory T cells, transforming growth factor-beta, and immune suppression. *Proc Am Thorac Soc* 4: 271-276.

54. O'Keefe, G. M., V. T. Nguyen, and E. N. Benveniste. 1999. Class II transactivator and class II MHC gene expression in microglia: modulation by the cytokines TGF-β, IL-4, IL-13 and IL-10. *European Journal of Immunology* 29: 1275-1285.

55. Zhang, F., H. Wang, X. Wang, G. Jiang, H. Liu, G. Zhang, H. Wang, R. Fang, X. Bu, S. Cai, and J. Du. 2016. TGF-β induces M2-like macrophage polarization via SNAIL-mediated suppression of a pro-inflammatory phenotype. *Oncotarget* 7: 52294-52306.

56. Cazac, B. B., and J. Roes. 2000. TGF-β Receptor Controls B Cell Responsiveness and Induction of IgA In Vivo. *Immunity* 13: 443-451.

57. Lee, Y. J., Y. Han, H. T. Lu, V. Nguyen, H. Qin, P. H. Howe, B. A. Hocevar, J. M. Boss, R. M. Ransohoff, and E. N. Benveniste. 1997. TGF-beta suppresses IFN-gamma induction of class II MHC gene expression by inhibiting class II transactivator messenger RNA expression. *The Journal of Immunology* 158: 2065.

58. Omenetti, S., and T. T. Pizarro. 2015. The Treg/Th17 Axis: A Dynamic Balance Regulated by the Gut Microbiome. *Frontiers in immunology* 6: 639-639.

59. Omenetti, S., and T. T. Pizarro. 2015. The Treg/Th17 Axis: A Dynamic Balance Regulated by the Gut Microbiome. *Front Immunol* 6: 639.

60. Sawant, D. V., K. Hamilton, and D. A. Vignali. 2015. Interleukin-35: Expanding Its Job Profile. *J Interferon Cytokine Res* 35: 499-512.

61. Collison, L. W., C. J. Workman, T. T. Kuo, K. Boyd, Y. Wang, K. M. Vignali, R. Cross, D. Sehy, R. S. Blumberg, and D. A. Vignali. 2007. The inhibitory cytokine IL-35 contributes to regulatory T-cell function. *Nature* 450: 566-569.

62. Collison, L. W., M. R. Pillai, V. Chaturvedi, and D. A. Vignali. 2009. Regulatory T cell suppression is potentiated by target T cells in a cell contact, IL-35- and IL-10-dependent manner. *J Immunol* 182: 6121-6128.

63. Moore, K. W., R. de Waal Malefyt, R. L. Coffman, and A. O'Garra. 2001. Interleukin-10 and the Interleukin-10 Receptor. *Annual Review of Immunology* 19: 683-765.

64. Uhlig, H. H., J. Coombes, C. Mottet, A. Izcue, C. Thompson, A. Fanger, A. Tannapfel, J. D. Fontenot, F. Ramsdell, and F. Powrie. 2006. Characterization of Foxp3+CD4+CD25+ and IL-10-secreting CD4+CD25+ T cells during cure of colitis. *J Immunol* 177: 5852-5860.

65. Tarique, M., H. Naz, S. V. Kurra, C. Saini, R. A. Naqvi, R. Rai, M. Suhail, N. Khanna, D. N. Rao, and A. Sharma. 2018. Interleukin-10 Producing Regulatory B Cells Transformed CD4. *Front Immunol* 9: 1636.

66. Anderson, C. A., G. Boucher, C. W. Lees, A. Franke, M. D'Amato, K. D. Taylor, J. C. Lee, P. Goyette, M. Imielinski, A. Latiano, C. Lagacé, R. Scott, L. Amininejad, S. Bumpstead, L. Baidoo, R. N. Baldassano, M. Barclay, T. M. Bayless, S. Brand, C. Büning, J.-F. Colombel, L. A. Denson, M. De Vos, M. Dubinsky, C. Edwards, D. Ellinghaus, R. S. N. Fehrmann, J. A. B. Floyd, T. Florin, D. Franchimont, L. Franke, M. Georges, J. Glas, N. L. Glazer, S. L. Guthery, T. Haritunians, N. K. Hayward, J.-P. Hugot, G. Jobin, D. Laukens, I. Lawrance, M. Lémann, A. Levine, C. Libioulle, E. Louis, D. P. McGovern, M. Milla, G. W. Montgomery, K. I. Morley, C. Mowat, A. Ng, W. Newman, R. A. Ophoff, L. Papi, O. Palmieri, L. Peyrin-Biroulet, J. Panés, A. Phillips, N. J. Prescott, D. D. Proctor, R. Roberts, R. Russell, P. Rutgeerts, J. Sanderson, M. Sans, P. Schumm, F. Seibold, Y. Sharma, L. A. Simms, M. Seielstad, A. H. Steinhart, S. R. Targan, L. H. van den Berg, M. Vatn, H. Verspaget, T. Walters, C. Wijmenga, D. C. Wilson, H.-J. Westra, R. J. Xavier, Z. Z. Zhao, C. Y. Ponsioen, V. Andersen, L. Torkvist, M. Gazouli, N. P. Anagnou, T. H. Karlsen, L. Kupcinskas, J. Sventoraityte, J. C. Mansfield, S. Kugathasan, M. S. Silverberg, J. Halfvarson, J. I. Rotter, C. G. Mathew, A. M. Griffiths, R. Gearry, T. Ahmad, S. R. Brant, M. Chamaillard, J. Satsangi, J. H. Cho, S. Schreiber, M. J. Daly, J. C. Barrett, M. Parkes, V. Annese, H. Hakonarson, G. Radford-Smith, R. H. Duerr, S. Vermeire, R. K. Weersma, and J. D. Rioux. 2011. Meta-analysis identifies 29 additional ulcerative colitis risk loci, increasing the number of confirmed associations to 47. *Nature Genetics* 43: 246-252.

67. Chinen, T., A. K. Kannan, A. G. Levine, X. Fan, U. Klein, Y. Zheng, G. Gasteiger, Y. Feng, J. D. Fontenot, and A. Y. Rudensky. 2016. An essential role for the IL-2 receptor in Treg cell function. *Nat Immunol* 17: 1322-1333.

68. Hayes, E. T., C. E. Hagan, L. Khoryati, M. A. Gavin, and D. J. Campbell. 2020. Regulatory T Cells Maintain Selective Access to IL-2 and Immune Homeostasis despite Substantially Reduced CD25 Function. *J Immunol* 205: 2667-2678.

69. Banchereau, J., F. Briere, C. Caux, J. Davoust, S. Lebecque, Y. J. Liu, B. Pulendran, and K. Palucka. 2000. Immunobiology of dendritic cells. *Annu Rev Immunol* 18: 767-811.

70. Read, S., V. Malmström, and F. Powrie. 2000. Cytotoxic T lymphocyte-associated antigen 4 plays an essential role in the function of CD25(+)CD4(+) regulatory cells that control intestinal inflammation. *J Exp Med* 192: 295-302.

71. Bachmann, M. F., G. Köhler, B. Ecabert, T. W. Mak, and M. Kopf. 1999. Cutting edge: lymphoproliferative disease in the absence of CTLA-4 is not T cell autonomous. *J Immunol* 163: 1128-1131.

72. Qureshi, O. S., Y. Zheng, K. Nakamura, K. Attridge, C. Manzotti, E. M. Schmidt, J. Baker, L. E. Jeffery, S. Kaur, Z. Briggs, T. Z. Hou, C. E. Futter, G. Anderson, L. S. K. Walker, and D. M. Sansom. 2011. Trans-Endocytosis of CD80 and CD86: A Molecular Basis for the Cell-Extrinsic Function of CTLA-4. *Science* 332: 600.

73. Huang, C. T., C. J. Workman, D. Flies, X. Pan, A. L. Marson, G. Zhou, E. L. Hipkiss, S. Ravi, J. Kowalski, H. I. Levitsky, J. D. Powell, D. M. Pardoll, C. G. Drake, and D. A. Vignali. 2004. Role of LAG-3 in regulatory T cells. *Immunity* 21: 503-513.

74. Akkaya, B., Y. Oya, M. Akkaya, J. Al Souz, A. H. Holstein, O. Kamenyeva, J. Kabat, R. Matsumura, D. W. Dorward, D. D. Glass, and E. M. Shevach. 2019. Regulatory T cells mediate specific suppression by depleting peptide–MHC class II from dendritic cells. *Nature Immunology* 20: 218-231.

75. Borsellino, G., M. Kleinewietfeld, D. Di Mitri, A. Sternjak, A. Diamantini, R. Giometto, S. Höpner, D. Centonze, G. Bernardi, M. L. Dell'Acqua, P. M. Rossini, L. Battistini, O. Rötzschke, and K. Falk. 2007. Expression of ectonucleotidase CD39 by Foxp3+ Treg cells: hydrolysis of extracellular ATP and immune suppression. *Blood* 110: 1225-1232.

76. Kobie, J. J., P. R. Shah, L. Yang, J. A. Rebhahn, D. J. Fowell, and T. R. Mosmann. 2006. T regulatory and primed uncommitted CD4 T cells express CD73, which suppresses effector CD4 T cells by converting 5'-adenosine monophosphate to adenosine. *J Immunol* 177: 6780-6786.

77. Deaglio, S., K. M. Dwyer, W. Gao, D. Friedman, A. Usheva, A. Erat, J.-F. Chen, K. Enjyoji, J. Linden, M. Oukka, V. K. Kuchroo, T. B. Strom, and S. C. Robson. 2007. Adenosine generation catalyzed by CD39 and CD73 expressed on regulatory T cells mediates immune suppression. *Journal of Experimental Medicine* 204: 1257-1265.

78. Gregory, S., and M. Kern. 1978. Adenosine and adenine nucleotides are mitogenic for mouse thymocytes. *Biochemical and Biophysical Research Communications* 83: 1111-1116.

79. Baricordi, O. R., D. Ferrari, L. Melchiorri, P. Chiozzi, S. Hanau, E. Chiari, M. Rubini, and F. Di Virgilio. 1996. An ATP-activated channel is involved in mitogenic stimulation of human T lymphocytes. *Blood* 87: 682-690.

80. Gravano, D. M., and D. A. Vignali. 2012. The battle against immunopathology: infectious tolerance mediated by regulatory T cells. *Cell Mol Life Sci* 69: 1997-2008.

81. Tran, D. Q. 2012. TGF-beta: the sword, the wand, and the shield of FOXP3(+) regulatory T cells. *J Mol Cell Biol* 4: 29-37.

82. Rosenblum, M. D., K. A. Remedios, and A. K. Abbas. 2015. Mechanisms of human autoimmunity. *J Clin Invest* 125: 2228-2233.

83. Cusick, M. F., J. E. Libbey, and R. S. Fujinami. 2012. Molecular Mimicry as a Mechanism of Autoimmune Disease. *Clinical Reviews in Allergy & Immunology* 42: 102-111.

84. Guilherme, L. 2006. Molecular mimicry in the autoimmune pathogenesis of rheumatic heart disease. Jorge Kalil ed. Autoimmunity.

85. Moulton, V. R., and G. C. Tsokos. 2015. T cell signaling abnormalities contribute to aberrant immune cell function and autoimmunity. *J Clin Invest* 125: 2220-2227.

86. Shim, C. H., S. Cho, Y. M. Shin, and J. M. Choi. 2022. Emerging role of bystander T cell activation in autoimmune diseases. *BMB Rep* 55: 57-64.

87. Kim, J., D. Y. Chang, H. W. Lee, H. Lee, J. H. Kim, P. S. Sung, K. H. Kim, S. H. Hong, W. Kang, J. Lee, S. Y. Shin, H. T. Yu, S. You, Y. S. Choi, I. Oh, D. H. Lee, M. K. Jung, K. S. Suh, S. Hwang, W. Kim, S. H. Park, H. J. Kim, and E. C. Shin. 2018. Innate-like Cytotoxic Function of Bystander-Activated CD8. *Immunity* 48: 161-173.e165.

88. Bertrams, J. 1984. The HLA association of insulin-dependent (type I) diabetes mellitus. *Behring Inst Mitt*: 89-99.

89. Kochi, Y. 2016. Genetics of autoimmune diseases: perspectives from genome-wide association studies. *International Immunology* 28: 155-161.

90. Flesher, D. L. T., X. Sun, T. W. Behrens, R. R. Graham, and L. A. Criswell. 2010. Recent advances in the genetics of systemic lupus erythematosus. *Expert review of clinical immunology* 6: 461-479.

91. Franke, A., D. P. B. McGovern, J. C. Barrett, K. Wang, G. L. Radford-Smith, T. Ahmad, C. W. Lees, T. Balschun, J. Lee, R. Roberts, C. A. Anderson, J. C. Bis, S. Bumpstead, D. Ellinghaus, E. M. Festen, M. Georges, T. Green, T. Haritunians, L. Jostins, A. Latiano, C. G. Mathew, G. W. Montgomery, N. J. Prescott, S. Raychaudhuri, J. I. Rotter, P. Schumm, Y. Sharma, L. A. Simms, K. D. Taylor, D. Whiteman, C. Wijmenga, R. N. Baldassano, M. Barclay, T. M. Bayless, S. Brand, C. Büning, A. Cohen, J.-F. Colombel, M. Cottone,

L. Stronati, T. Denson, M. De Vos, R. D'Inca, M. Dubinsky, C. Edwards, T. Florin, D. Franchimont, R. Gearry, J. Glas, A. Van Gossum, S. L. Guthery, J. Halfvarson, H. W. Verspaget, J.-P. Hugot, A. Karban, D. Laukens, I. Lawrance, M. Lemann, A. Levine, C. Libioulle, E. Louis, C. Mowat, W. Newman, J. Panés, A. Phillips, D. D. Proctor, M. Regueiro, R. Russell, P. Rutgeerts, J. Sanderson, M. Sans, F. Seibold, A. H. Steinhart, P. C. F. Stokkers, L. Torkvist, G. Kullak-Ublick, D. Wilson, T. Walters, S. R. Targan, S. R. Brant, J. D. Rioux, M. D'Amato, R. K. Weersma, S. Kugathasan, A. M. Griffiths, J. C. Mansfield, S. Vermeire, R. H. Duerr, M. S. Silverberg, J. Satsangi, S. Schreiber, J. H. Cho, V. Annese, H. Hakonarson, M. J. Daly, and M. Parkes. 2010. Genome-wide meta-analysis increases to 71 the number of confirmed Crohn's disease susceptibility loci. *Nature Genetics* 42: 1118-1125.

92. Petukhova, L., M. Duvic, M. Hordinsky, D. Norris, V. Price, Y. Shimomura, H. Kim, P. Singh, A. Lee, W. V. Chen, K. C. Meyer, R. Paus, C. A. B. Jahoda, C. I. Amos, P. K. Gregersen, and A. M. Christiano. 2010. Genome-wide association study in alopecia areata implicates both innate and adaptive immunity. *Nature* 466: 113-117.

93. Cho, J. H., and P. K. Gregersen. 2011. Genomics and the Multifactorial Nature of Human Autoimmune Disease. *New England Journal of Medicine* 365: 1612-1623.

94. Wang, L., F.-S. Wang, and M. E. Gershwin. 2015. Human autoimmune diseases: a comprehensive update. *Journal of Internal Medicine* 278: 369-395.

95. Shamim, E. A., and F. W. Miller. 2000. Familial autoimmunity and the idiopathic inflammatory myopathies. *Curr Rheumatol Rep* 2: 201-211.

96. Quintero-Ronderos, P., and G. Montoya-Ortiz. 2012. Epigenetics and autoimmune diseases. *Autoimmune Dis* 2012: 593720.

97. Dobson, R., and G. Giovannoni. 2019. Multiple sclerosis - a review. *Eur J Neurol* 26: 27-40.

98. Hunter, S. F. 2016. Overview and diagnosis of multiple sclerosis. *Am J Manag Care* 22: s141-150.

99. Lassmann, H., J. van Horssen, and D. Mahad. 2012. Progressive multiple sclerosis: pathology and pathogenesis. *Nat Rev Neurol* 8: 647-656.

100. Chitnis, T. 2007. The role of CD4 T cells in the pathogenesis of multiple sclerosis. *Int Rev Neurobiol* 79: 43-72.

101. Hoglund, R. A., and A. A. Maghazachi. 2014. Multiple sclerosis and the role of immune cells. *World J Exp Med* 4: 27-37.

102. Dendrou, C. A., L. Fugger, and M. A. Friese. 2015. Immunopathology of multiple sclerosis. *Nat Rev Immunol* 15: 545-558.

103. Fletcher, J. M., S. J. Lalor, C. M. Sweeney, N. Tubridy, and K. H. Mills. 2010. T cells in multiple sclerosis and experimental autoimmune encephalomyelitis. *Clin Exp Immunol* 162: 1-11.

104. Fernando, V., S. Omura, F. Sato, E. Kawai, N. E. Martinez, S. F. Elliott, K. Yoh, S. Takahashi, and I. Tsunoda. 2014. Regulation of an autoimmune model for multiple sclerosis in Th2-biased GATA3 transgenic mice. *Int J Mol Sci* 15: 1700-1718.

105. Duda, P. W., M. C. Schmied, S. L. Cook, J. I. Krieger, and D. A. Hafler. 2000. Glatiramer acetate (Copaxone) induces degenerate, Th2-polarized immune responses in patients with multiple sclerosis. *J Clin Invest* 105: 967-976.

106. Disanto, G., J. M. Morahan, M. H. Barnett, G. Giovannoni, and S. V. Ramagopalan. 2012. The evidence for a role of B cells in multiple sclerosis. *Neurology* 78: 823-832.

107. Negron, A., O. Stüve, and T. G. Forsthuber. 2020. Ectopic Lymphoid Follicles in Multiple Sclerosis: Centers for Disease Control? *Front Neurol* 11: 607766.

108. Krumbholz, M., T. Derfuss, R. Hohlfeld, and E. Meinl. 2012. B cells and antibodies in multiple sclerosis pathogenesis and therapy. *Nat Rev Neurol* 8: 613-623.

109. Rosser, E. C., and C. Mauri. 2015. Regulatory B cells: origin, phenotype, and function. *Immunity* 42: 607-612.

110. Wolf, S. D., B. N. Dittel, F. Hardardottir, and C. A. Janeway. 1996. Experimental autoimmune encephalomyelitis induction in genetically B cell-deficient mice. *J Exp Med* 184: 2271-2278.

111. Mishra, M. K., and V. W. Yong. 2016. Myeloid cells - targets of medication in multiple sclerosis. *Nat Rev Neurol* 12: 539-551.

112. Agrawal, S. M., J. Williamson, R. Sharma, H. Kebir, K. Patel, A. Prat, and V. W. Yong. 2013. Extracellular matrix metalloproteinase inducer shows active perivascular cuffs in multiple sclerosis. *Brain* 136: 1760-1777.

113. Sorokin, L. 2010. The impact of the extracellular matrix on inflammation. *Nat Rev Immunol* 10: 712-723.

114. Jiang, Z., J. X. Jiang, and G. X. Zhang. 2014. Macrophages: a double-edged sword in experimental autoimmune encephalomyelitis. *Immunol Lett* 160: 17-22.

115. Danikowski, K. M., S. Jayaraman, and B. S. Prabhakar. 2017. Regulatory T cells in multiple sclerosis and myasthenia gravis. *J Neuroinflammation* 14: 117.

116. Haas, J., A. Hug, A. Viehover, B. Fritzsching, C. S. Falk, A. Filser, T. Vetter, L. Milkova, M. Korporal, B. Fritz, B. Storch-Hagenlocher, P. H. Krammer, E. Suri-Payer, and B. Wildemann. 2005. Reduced suppressive effect of CD4+CD25high regulatory T cells on the T cell immune response against myelin oligodendrocyte glycoprotein in patients with multiple sclerosis. *Eur J Immunol* 35: 3343-3352.

117. Venken, K., N. Hellings, M. Thewissen, V. Somers, K. Hensen, J.-L. Rummens, R. Medaer, R. Hupperts, and P. Stinissen. 2008. Compromised CD4+ CD25(high) regulatory T-cell function in patients with relapsing-remitting multiple sclerosis is correlated with a reduced frequency of FOXP3-positive cells and reduced FOXP3 expression at the single-cell level. *Immunology* 123: 79-89.

118. Vasileiadis, G. K., E. Dardiotis, A. Mavropoulos, Z. Tsouris, V. Tsimourtou, D. P. Bogdanos, L. I. Sakkas, and G. M. Hadjigeorgiou. 2018. Regulatory B and T lymphocytes in multiple sclerosis: friends or foes? *Auto Immun Highlights* 9: 9.

119. Astier, A. L., and D. A. Hafler. 2007. Abnormal Tr1 differentiation in multiple sclerosis. *J Neuroimmunol* 191: 70-78.

120. Kieseier, B. C. 2011. The mechanism of action of interferon-β in relapsing multiple sclerosis. *CNS Drugs* 25: 491-502.

121. Wang, D., D. Ghosh, S. M. Islam, C. D. Moorman, A. E. Thomason, D. S. Wilkinson, and M. D. Mannie. 2016. IFN-β Facilitates Neuroantigen-Dependent Induction of CD25+ FOXP3+ Regulatory T Cells That Suppress Experimental Autoimmune Encephalomyelitis. *J Immunol* 197: 2992-3007.

122. Ingwersen, J., O. Aktas, P. Kuery, B. Kieseier, A. Boyko, and H. P. Hartung. 2012. Fingolimod in multiple sclerosis: mechanisms of action and clinical efficacy. *Clin Immunol* 142: 15-24.

123. 't Hart, B. A., B. Gran, and R. Weissert. 2011. EAE: imperfect but useful models of multiple sclerosis. *Trends Mol Med* 17: 119-125.

124. Bernard, C. C., and P. R. Carnegie. 1975. Experimental autoimmune encephalomyelitis in mice: immunologic response to mouse spinal cord and myelin basic proteins. *J Immunol* 114: 1537-1540.

125. Constantinescu, C. S., N. Farooqi, K. O'Brien, and B. Gran. 2011. Experimental autoimmune encephalomyelitis (EAE) as a model for multiple sclerosis (MS). *Br J Pharmacol* 164: 1079-1106.

126. Cabeza-Cabrerizo, M., A. Cardoso, C. M. Minutti, M. Pereira Da Costa, and C. Reis E Sousa. 2021. Dendritic Cells Revisited. *Annual Review of Immunology* 39: 131-166.

127. Guilliams, M., B. N. Lambrecht, and H. Hammad. 2013. Division of labor between lung dendritic cells and macrophages in the defense against pulmonary infections. *Mucosal Immunol* 6: 464-473.

128. Chieppa, M., M. Rescigno, A. Y. Huang, and R. N. Germain. 2006. Dynamic imaging of dendritic cell extension into the small bowel lumen in response to epithelial cell TLR engagement. *J Exp Med* 203: 2841-2852.

129. Blanco, P., A. Palucka, V. Pascual, and J. Banchereau. 2008. Dendritic cells and cytokines in human inflammatory and autoimmune diseases. *Cytokine & Growth Factor Reviews* 19: 41-52.

130. Thaiss, C. A., V. Semmling, L. Franken, H. Wagner, and C. Kurts. 2011. Chemokines: a new dendritic cell signal for T cell activation. *Front Immunol* 2: 31.

131. Worbs, T., S. I. Hammerschmidt, and R. Förster. 2017. Dendritic cell migration in health and disease. *Nature Reviews Immunology* 17: 30-48.

132. Allan, R. S., J. Waithman, S. Bedoui, C. M. Jones, J. A. Villadangos, Y. Zhan, A. M. Lew, K. Shortman, W. R. Heath, and F. R. Carbone. 2006. Migratory Dendritic Cells Transfer Antigen to a Lymph Node-Resident Dendritic Cell Population for Efficient CTL Priming. *Immunity* 25: 153-162.

133. Helft, J., B. Manicassamy, P. Guermonprez, D. Hashimoto, A. Silvin, J. Agudo, B. D. Brown, M. Schmolke, J. C. Miller, M. Leboeuf, K. M. Murphy, A. García-Sastre, and M. Merad. 2012. Cross-presenting CD103+ dendritic cells are protected from influenza virus infection. *Journal of Clinical Investigation* 122: 4037-4047.

134. Ten Broeke, T., R. Wubbolts, and W. Stoorvogel. 2013. MHC Class II Antigen Presentation by Dendritic Cells Regulated through Endosomal Sorting. *Cold Spring Harbor Perspectives in Biology* 5: a016873-a016873.

135. Cella, M., M. Salio, Y. Sakakibara, H. Langen, I. Julkunen, and A. Lanzavecchia. 1999. Maturation, Activation, and Protection of Dendritic Cells Induced by Double-stranded RNA. *Journal of Experimental Medicine* 189: 821-829.

136. Embgenbroich, M., and S. Burgdorf. 2018. Current Concepts of Antigen Cross-Presentation. *Front Immunol* 9: 1643.

137. Kushwah, R., and J. Hu. 2011. Role of dendritic cells in the induction of regulatory T cells. *Cell & Bioscience* 1: 20.

138. Reis E Sousa, C. 2006. Dendritic cells in a mature age. *Nature Reviews Immunology* 6: 476-483.

139. Sittig, S. P., G. Bakdash, J. Weiden, A. E. Sköld, J. Tel, C. G. Figdor, I. J. de Vries, and G. Schreibelt. 2016. A Comparative Study of the T Cell Stimulatory and Polarizing Capacity of Human Primary Blood Dendritic Cell Subsets. *Mediators Inflamm* 2016: 3605643.

140. Geginat, J., G. Nizzoli, M. Paroni, S. Maglie, P. Larghi, S. Pascolo, and S. Abrignani. 2015. Immunity to Pathogens Taught by Specialized Human Dendritic Cell Subsets. *Front Immunol* 6: 527.

141. Collin, M., and V. Bigley. 2018. Human dendritic cell subsets: an update. *Immunology* 154: 3-20.

142. Eisenbarth, S. C. 2019. Dendritic cell subsets in T cell programming: location dictates function. *Nat Rev Immunol* 19: 89-103.

143. Williams, J. W., M. Y. Tjota, B. S. Clay, B. Vander Lugt, H. S. Bandukwala, C. L. Hrusch, D. C. Decker, K. M. Blaine, B. R. Fixsen, H. Singh, R. Sciammas, and A. I. Sperling. 2013. Transcription factor IRF4 drives dendritic cells to promote Th2 differentiation. *Nat Commun* 4: 2990.

144. Deckers, J., H. Hammad, and E. Hoste. 2018. Langerhans Cells: Sensing the Environment in Health and Disease. *Front Immunol* 9: 93.

145. Bao, M., and Y. J. Liu. 2013. Regulation of TLR7/9 signaling in plasmacytoid dendritic cells. *Protein Cell* 4: 40-52.

146. Schmidt, S. V., A. C. Nino-Castro, and J. L. Schultze. 2012. Regulatory dendritic cells: there is more than just immune activation. *Front Immunol* 3: 274.

147. del Rio, M. L., G. Bernhardt, J. I. Rodriguez-Barbosa, and R. Förster. 2010. Development and functional specialization of CD103+ dendritic cells. *Immunol Rev* 234: 268-281.

148. Scott, C. L., A. M. Aumeunier, and A. M. Mowat. 2011. Intestinal CD103+ dendritic cells: master regulators of tolerance? *Trends Immunol* 32: 412-419.

149. Iliev, I. D., I. Spadoni, E. Mileti, G. Matteoli, A. Sonzogni, G. M. Sampietro, D. Foschi, F. Caprioli, G. Viale, and M. Rescigno. 2009. Human intestinal epithelial cells promote the differentiation of tolerogenic dendritic cells. *Gut* 58: 1481-1489.

150. De Smedt, T., M. Van Mechelen, G. De Becker, J. Urbain, O. Leo, and M. Moser. 1997. Effect of interleukin-10 on dendritic cell maturation and function. *Eur J Immunol* 27: 1229-1235.

151. von Bergwelt-Baildon, M. S., A. Popov, T. Saric, J. Chemnitz, S. Classen, M. S. Stoffel, F. Fiore, U. Roth, M. Beyer, S. Debey, C. Wickenhauser, F. G. Hanisch, and J. L. Schultze. 2006. CD25 and indoleamine 2,3-dioxygenase are up-regulated by prostaglandin E2 and expressed by tumor-associated dendritic cells in vivo: additional mechanisms of T-cell inhibition. *Blood* 108: 228-237.

152. Li, J., E. Lu, T. Yi, and J. G. Cyster. 2016. EBI2 augments Tfh cell fate by promoting interaction with IL-2-quenching dendritic cells. *Nature* 533: 110-114.

153. Driesen, J., A. Popov, and J. L. Schultze. 2008. CD25 as an immune regulatory molecule expressed on myeloid dendritic cells. *Immunobiology* 213: 849-858.

154. Wuest, S. C., J. H. Edwan, J. F. Martin, S. Han, J. S. Perry, C. M. Cartagena, E. Matsuura, D. Maric, T. A. Waldmann, and B. Bielekova. 2011. A role for interleukin-2 trans-presentation in dendritic cell-mediated T cell activation in humans, as revealed by daclizumab therapy. *Nat. Med.* 17: 604-609.

155. Greenhill, C. 2018. New role for indoleamine 2,3-dioxygenase. *Nature Reviews Endocrinology* 14: 504-504.

156. Naranjo-Gómez, M., H. Oliva, N. Climent, M. A. Fernández, M. Ruiz-Riol, M. Bofill, J. M. Gatell, T. Gallart, R. Pujol-Borrell, and F. E. Borràs. 2007. Expression and function of the IL-2 receptor in activated human plasmacytoid dendritic cells. *Eur J Immunol* 37: 1764-1772.

157. Soto, J. A., N. M. S. Gálvez, C. A. Andrade, G. A. Pacheco, K. Bohmwald, R. V. Berrios, S. M. Bueno, and A. M. Kalergis. 2020. The Role of Dendritic Cells During Infections Caused by Highly Prevalent Viruses. *Front Immunol* 11: 1513.

158. Wu, X., and F. Xu. 2014. Dendritic cells during Staphylococcus aureus infection: subsets and roles. *J Transl Med* 12: 358.

159. Xie, Z. X., H. L. Zhang, X. J. Wu, J. Zhu, D. H. Ma, and T. Jin. 2015. Role of the immunogenic and tolerogenic subsets of dendritic cells in multiple sclerosis. *Mediators Inflamm* 2015: 513295.

160. Diebold, S. S. 2008. Determination of T-cell fate by dendritic cells. *Immunol Cell Biol* 86: 389-397.

161. Greter, M., F. L. Heppner, M. P. Lemos, B. M. Odermatt, N. Goebels, T. Laufer, R. J. Noelle, and B. Becher. 2005. Dendritic cells permit immune invasion of the CNS in an animal model of multiple sclerosis. *Nat Med* 11: 328-334.

162. Hirata, S., H. Matsuyoshi, D. Fukuma, A. Kurisaki, Y. Uemura, Y. Nishimura, and S. Senju. 2007. Involvement of regulatory T cells in the experimental autoimmune encephalomyelitis-preventive effect of dendritic cells expressing myelin oligodendrocyte glycoprotein plus TRAIL. *J Immunol* 178: 918-925.

163. Cyster, J. G. 2010. B cell follicles and antigen encounters of the third kind. *Nat Immunol* 11: 989-996.

164. Dustin, M. L. 2014. The Immunological Synapse. *Cancer Immunology Research* 2: 1023-1033.

165. Comrie, W. A., S. Li, S. Boyle, and J. K. Burkhardt. 2015. The dendritic cell cytoskeleton promotes T cell adhesion and activation by constraining ICAM-1 mobility. *J Cell Biol* 208: 457-473.

166. Pasquier, B., L. Yin, M.-C. FondanèChe, F. Relouzat, C. Bloch-Queyrat, N. Lambert, A. Fischer, G. V. De Saint-Basile, and S. Latour. 2005. Defective NKT cell development in mice and humans lacking the adapter SAP, the X-linked lymphoproliferative syndrome gene product. *Journal of Experimental Medicine* 201: 695-701.

167. Inaba, K., M. Witmer-Pack, M. Inaba, K. S. Hathcock, H. Sakuta, M. Azuma, H. Yagita, K. Okumura, P. S. Linsley, S. Ikehara, S. Muramatsu, R. J. Hodes, and R. M. Steinman. 1994. The tissue distribution of the B7-2 costimulator in mice: abundant expression on dendritic cells in situ and during maturation in vitro. *Journal of Experimental Medicine* 180: 1849-1860.

168. Bromley, S. K., A. Iaboni, S. J. Davis, A. Whitty, J. M. Green, A. S. Shaw, A. Weiss, and M. L. Dustin. 2001. The immunological synapse and CD28-CD80 interactions. *Nature Immunology* 2: 1159-1166.

169. Esensten, H., Jonathan, A. Helou, Ynes, G. Chopra, A. Weiss, and A. Bluestone, Jeffrey. 2016. CD28 Costimulation: From Mechanism to Therapy. *Immunity* 44: 973-988.

170. Zhang, R., A. Huynh, G. Whitcher, J. Chang, J. S. Maltzman, and L. A. Turka. 2013. An obligate cell-intrinsic function for CD28 in Tregs. *Journal of Clinical Investigation*.

171. Howland, K. C., L. J. Ausubel, C. A. London, and A. K. Abbas. 2000. The Roles of CD28 and CD40 Ligand in T Cell Activation and Tolerance. *The Journal of Immunology* 164: 4465-4470.

172. Michel, N. A., A. Zirlik, and D. Wolf. 2017. CD40L and Its Receptors in Atherothrombosis-An Update. *Front Cardiovasc Med* 4: 40.

173. Banchereau, J., F. Bazan, D. Blanchard, F. Brière, J. P. Galizzi, C. van Kooten, Y. J. Liu, F. Rousset, and S. Saeland. 1994. The CD40 antigen and its ligand. *Annu Rev Immunol* 12: 881-922.

174. Clark, E. A., and J. A. Ledbetter. 2012. Activation of human B cells mediated through two distinct cell surface differentiation antigens, Bp35 and Bp50. Proc. Natl. Acad. Sci. 1986. 83: 4494-4498. *J Immunol* 188: 4130-4134.

175. Elgueta, R., M. J. Benson, V. C. de Vries, A. Wasiuk, Y. Guo, and R. J. Noelle. 2009. Molecular mechanism and function of CD40/CD40L engagement in the immune system. *Immunol Rev* 229: 152-172.

176. Conley, M. E., M. Larché, V. R. Bonagura, A. R. Lawton, R. H. Buckley, S. M. Fu, E. Coustan-Smith, H. G. Herrod, and D. Campana. 1994. Hyper IgM syndrome associated with defective CD40-mediated B cell activation. *Journal of Clinical Investigation* 94: 1404-1409.

177. Thusberg, J., and M. Vihinen. 2007. The structural basis of hyper IgM deficiency - CD40L mutations. *Protein Eng Des Sel* 20: 133-141.

178. Banchereau, J., and R. M. Steinman. 1998. Dendritic cells and the control of immunity. *Nature* 392: 245-252.

179. Frleta, D., J. T. Lin, S. A. Quezada, T. K. Wade, R. J. Barth, R. J. Noelle, and W. F. Wade. 2003. Distinctive maturation of in vitro versus in vivo anti-CD40 mAb-matured dendritic cells in mice. *J Immunother* 26: 72-84.

180. Elgueta, R., M. J. Benson, V. C. De Vries, A. Wasiuk, Y. Guo, and R. J. Noelle. 2009. Molecular mechanism and function of CD40/CD40L engagement in the immune system. *Immunological Reviews* 229: 152-172.

181. Ouaaz, F., J. Arron, Y. Zheng, Y. Choi, and A. A. Beg. 2002. Dendritic cell development and survival require distinct NF-kappaB subunits. *Immunity* 16: 257-270.

182. O'Sullivan, B. J., and R. Thomas. 2002. CD40 Ligation Conditions Dendritic Cell Antigen-Presenting Function Through Sustained Activation of NF-κB. *The Journal of Immunology* 168: 5491-5498.

183. Mai, G., M.-L. Del Rio, J. Tian, P. Ramirez, L. Buhler, and J.-I. Rodriguez-Barbosa. 2007. Blockade of the PD-1/PD-1L pathway reverses the protective effect of anti-CD40L therapy in a rat to mouse concordant islet xenotransplantation model. *Xenotransplantation* 14: 243-248.

184. Kraj, P., and L. Ignatowicz. 2018. The mechanisms shaping the repertoire of CD4⁺ Foxp3⁺regulatory T cells. *Immunology* 153: 290-296.

185. Benson, M. J., K. Pino-Lagos, M. Rosemblatt, and R. J. Noelle. 2007. All-trans retinoic acid mediates enhanced T reg cell growth, differentiation, and gut homing in the face of high levels of co-stimulation. *Journal of Experimental Medicine* 204: 1765-1774.

186. Wikenheiser, D. J., and J. S. Stumhofer. 2016. ICOS Co-Stimulation: Friend or Foe? *Front Immunol* 7: 304.

187. Dong, C., A. E. Juedes, U.-A. Temann, S. Shresta, J. P. Allison, N. H. Ruddle, and R. A. Flavell. 2001. ICOS co-stimulatory receptor is essential for T-cell activation and function. *Nature* 409: 97-101.

188. Tafuri, A., A. Shahinian, F. Bladt, S. K. Yoshinaga, M. Jordana, A. Wakeham, L. M. Boucher, D. Bouchard, V. S. Chan, G. Duncan, B. Odermatt, A. Ho, A. Itie, T. Horan, J. S. Whoriskey, T. Pawson, J. M. Penninger, P. S. Ohashi, and T. W. Mak. 2001. ICOS is essential for effective T-helper-cell responses. *Nature* 409: 105-109.

189. Gao, X., M. Gigoux, J. Yang, J. Leconte, X. Yang, and W.-K. Suh. 2012. Anti-Chlamydial Th17 Responses Are Controlled by the Inducible Costimulator Partially through Phosphoinositide 3-Kinase Signaling. *PLoS ONE* 7: e52657.

190. Nouailles, G., T. A. Day, S. Kuhlmann, D. Loewe, A. Dorhoi, P. Gamradt, R. Hurwitz, S. Jörg, L. Pradl, A. Hutloff, M. Koch, M. Kursar, and S. H. E. Kaufmann. 2011. Impact of inducible co-stimulatory molecule (ICOS) on T-cell responses and protection against Mycobacterium tuberculosis infection. *European Journal of Immunology* 41: 981-991.

191. This, S., S. F. Valbon, M.-È. Lebel, and H. J. Melichar. 2021. Strength and Numbers: The Role of Affinity and Avidity in the 'Quality' of T Cell Tolerance. *Cells* 10: 1530.

192. Korb, L. C., S. Mirshahidi, K. Ramyar, A. A. Sadighi Akha, and S. Sadegh-Nasseri. 1999. Induction of T cell anergy by low numbers of agonist ligands. *J Immunol* 162: 6401-6409.

193. Skokos, D., G. Shakhar, R. Varma, J. C. Waite, T. O. Cameron, R. L. Lindquist, T. Schwickert, M. C. Nussenzweig, and M. L. Dustin. 2007. Peptide-MHC potency governs dynamic interactions between T cells and dendritic cells in lymph nodes. *Nature Immunology* 8: 835-844.

194. Courtney, A. H., W.-L. Lo, and A. Weiss. 2018. TCR Signaling: Mechanisms of Initiation and Propagation. *Trends in Biochemical Sciences* 43: 108-123.

195. Štefanová, I., B. Hemmer, M. Vergelli, R. Martin, W. E. Biddison, and R. N. Germain. 2003. TCR ligand discrimination is enforced by competing ERK positive and SHP-1 negative feedback pathways. *Nature Immunology* 4: 248-254.

196. King, G., Carolyn, S. Koehli, B. Hausmann, M. Schmaler, D. Zehn, and E. Palmer. 2012. T Cell Affinity Regulates Asymmetric Division, Effector Cell Differentiation, and Tissue Pathology. *Immunity* 37: 709-720.

197. Gomez-Rodriguez, J., E. A. Wohlfert, R. Handon, F. Meylan, J. Z. Wu, S. M. Anderson, M. R. Kirby, Y. Belkaid, and P. L. Schwartzberg. 2014. Itk-mediated integration of T cell receptor and cytokine signaling regulates the balance between Th17 and regulatory T cells. *J Exp Med* 211: 529-543.

198. Sprouse, M. L., I. Shevchenko, M. A. Scavuzzo, F. Joseph, T. Lee, S. Blum, M. Borowiak, M. L. Bettini, and M. Bettini. 2018. Cutting Edge: Low-Affinity TCRs Support Regulatory T Cell Function in Autoimmunity. *The Journal of Immunology* 200: 909-914.

199. Bhattacharyya, N. D., and C. G. Feng. 2020. Regulation of T Helper Cell Fate by TCR Signal Strength. *Front Immunol* 11: 624.

200. Zehn, D., S. Y. Lee, and M. J. Bevan. 2009. Complete but curtailed T-cell response to very low-affinity antigen. *Nature* 458: 211-214.

201. Constant, S., C. Pfeiffer, A. Woodard, T. Pasqualini, and K. Bottomly. 1995. Extent of T cell receptor ligation can determine the functional differentiation of naive CD4+ T cells. *Journal of Experimental Medicine* 182: 1591-1596.

202. Ise, W., M. Totsuka, Y. Sogawa, A. Ametani, S. Hachimura, T. Sato, Y. Kumagai, S. Habu, and S. Kaminogawa. 2002. Naive CD4⁺T Cells Exhibit Distinct Expression Patterns of Cytokines and Cell Surface Molecules on Their Primary Responses to Varying Doses of Antigen. *The Journal of Immunology* 168: 3242-3250.

203. Pollard, A. J., and E. M. Bijker. 2021. A guide to vaccinology: from basic principles to new developments. *Nature Reviews Immunology* 21: 83-100.

204. Minor, P. D. 2015. Live attenuated vaccines: Historical successes and current challenges. *Virology* 479-480: 379-392.

205. Elliman, D., and H. Bedford. 2001. MMR vaccine: the continuing saga. *BMJ* 322: 183-184.

206. Nypaver, C., C. Dehlinger, and C. Carter. 2021. Influenza and Influenza Vaccine: A Review. *Journal of Midwifery & Women's Health* 66: 45-53.

207. Berger, A. 1998. Science commentary: why conjugate vaccines protect longer. *BMJ* 316: 1571.

208. Mascellino, M. T., F. Di Timoteo, M. De Angelis, and A. Oliva. 2021. Overview of the Main Anti-SARS-CoV-2 Vaccines: Mechanism of Action, Efficacy and Safety. *Infection and Drug Resistance* Volume 14: 3459-3476.

209. Musher, D. M., R. Sampath, and M. C. Rodriguez-Barradas. 2011. The potential role for protein-conjugate pneumococcal vaccine in adults: what is the supporting evidence? *Clin Infect Dis* 52: 633-640.

210. Avery, O. T., and W. F. Goebel. 1929. CHEMO-IMMUNOLOGICAL STUDIES ON CONJUGATED CARBOHYDRATE-PROTEINS. *Journal of Experimental Medicine* 50: 533-550.

211. Rappuoli, R., E. De Gregorio, and P. Costantino. 2019. On the mechanisms of conjugate vaccines. *Proceedings of the National Academy of Sciences* 116: 14-16.

212. Moorman, C. D., S. J. Sohn, and H. Phee. 2021. Emerging Therapeutics for Immune Tolerance: Tolerogenic Vaccines, T cell Therapy, and IL-2 Therapy. *Front Immunol* 12: 657768.

213. Serra, P., and P. Santamaria. 2019. Antigen-specific therapeutic approaches for autoimmunity. *Nat Biotechnol* 37: 238-251.

214. Szczepanik, M. 2014. Skin-induced tolerance as a new needle free therapeutic strategy. *Pharmacol Rep* 66: 192-197.

215. Yu, W., D. M. H. Freeland, and K. C. Nadeau. 2016. Food allergy: immune mechanisms, diagnosis and immunotherapy. *Nat Rev Immunol* 16: 751-765.

216. Chinthrajah, R. S., J. D. Hernandez, S. D. Boyd, S. J. Galli, and K. C. Nadeau. 2016. Molecular and cellular mechanisms of food allergy and food tolerance. *J Allergy Clin Immunol* 137: 984-997.

217. Wang, X., A. Sherman, G. Liao, K. W. Leong, H. Daniell, C. Terhorst, and R. W. Herzog. 2013. Mechanism of oral tolerance induction to therapeutic proteins. *Adv Drug Deliv Rev* 65: 759-773.

218. Castenmiller, C., B. C. Keumatio-Doungtsop, R. van Ree, E. C. de Jong, and Y. van Kooyk. 2021. Tolerogenic Immunotherapy: Targeting DC Surface Receptors to Induce Antigen-Specific Tolerance. *Front Immunol* 12: 643240.

219. Mirshafiey, A., and M. Kianiaslani. 2013. Autoantigens and autoantibodies in multiple sclerosis. *Iran J Allergy Asthma Immunol* 12: 292-303.

220. Riedhammer, C., and R. Weissert. 2015. Antigen Presentation, Autoantigens, and Immune Regulation in Multiple Sclerosis and Other Autoimmune Diseases. *Front Immunol* 6: 322.

221. Steinman, L. 2015. The re-emergence of antigen-specific tolerance as a potential therapy for MS. *Mult Scler* 21: 1223-1238.

222. Hohlfeld, R., K. Dornmair, E. Meinl, and H. Wekerle. 2016. The search for the target antigens of multiple sclerosis, part 1: autoreactive CD4+ T lymphocytes as pathogenic effectors and therapeutic targets. *Lancet Neurol* 15: 198-209.

223. Mekala, D. J., R. S. Alli, and T. L. Geiger. 2005. IL-10-dependent infectious tolerance after the treatment of experimental allergic encephalomyelitis with redirected CD4+CD25+ T lymphocytes. *Proc Natl Acad Sci U S A* 102: 11817-11822.

224. Sullivan, J. A., D. P. AlAdra, B. M. Olson, D. G. McNeel, and W. J. Burlingham. 2020. Infectious Tolerance as Seen With 2020 Vision: The Role of IL-35 and Extracellular Vesicles. *Front Immunol* 11: 1867.

225. Abbott, D. J., J. L. Blanchfield, D. A. Martinson, S. C. Russell, N. Taslim, A. D. Curtis, and M. D. Mannie. 2011. Neuroantigen-specific, tolerogenic vaccines: GM-CSF is a fusion partner that facilitates tolerance rather than immunity to dominant self-epitopes of myelin in murine models of experimental autoimmune encephalomyelitis (EAE). *BMC Immunol* 12: 72.

226. Blanchfield, J. L., and M. D. Mannie. 2010. A GMCSF-neuroantigen fusion protein is a potent tolerogen in experimental autoimmune encephalomyelitis (EAE) that is associated with efficient targeting of neuroantigen to APC. *J Leukoc Biol* 87: 509-521.

227. Islam, S. M., A. D. Curtis, N. Taslim, D. S. Wilkinson, and M. D. Mannie. 2014. GM-CSF-neuroantigen fusion proteins reverse experimental autoimmune encephalomyelitis

and mediate tolerogenic activity in adjuvant-primed environments: association with inflammation-dependent, inhibitory antigen presentation. *J Immunol* 193: 2317-2329.

228. Mannie, M. D., J. L. Blanchfield, S. M. Islam, and D. J. Abbott. 2012. Cytokine-neuroantigen fusion proteins as a new class of tolerogenic, therapeutic vaccines for treatment of inflammatory demyelinating disease in rodent models of multiple sclerosis. *Front Immunol* 3: 255.

229. Moorman, C. D., A. D. Curtis, A. G. Bastian, S. E. Elliott, and M. D. Mannie. 2018. A GMCSF-Neuroantigen Tolerogenic Vaccine Elicits Systemic Lymphocytosis of CD4. *Front Immunol* 9: 3119.

230. Moorman, C. D., A. G. Bastian, K. B. DeOca, and M. D. Mannie. 2020. A GM-CSF-neuroantigen tolerogenic vaccine elicits inefficient antigen recognition events below the CD40L triggering threshold to expand CD4. *J Neuroinflammation* 17: 180.

231. Kool, M., K. Fierens, and B. N. Lambrecht. 2012. Alum adjuvant: some of the tricks of the oldest adjuvant. *Journal of Medical Microbiology* 61: 927-934.

232. Ghimire, T. R. 2015. The mechanisms of action of vaccines containing aluminum adjuvants: an in vitro vs in vivo paradigm. *SpringerPlus* 4.

233. Kool, M., T. Soullié, M. Van Nimwegen, M. A. M. Willart, F. Muskens, S. Jung, H. C. Hoogsteden, H. Hammad, and B. N. Lambrecht. 2008. Alum adjuvant boosts adaptive immunity by inducing uric acid and activating inflammatory dendritic cells. *Journal of Experimental Medicine* 205: 869-882.

234. Mannie, M. D., D. J. Abbott, and J. L. Blanchfield. 2009. Experimental autoimmune encephalomyelitis in Lewis rats: IFN-beta acts as a tolerogenic adjuvant for induction of neuroantigen-dependent tolerance. *J Immunol* 182: 5331-5341.

235. Wigren, M., D. Bengtsson, P. DunéR, K. Olofsson, H. BjöRkbacka, E. Bengtsson, G. N. Fredrikson, and J. Nilsson. 2009. Atheroprotective Effects of Alum Are Associated With Capture of Oxidized LDL Antigens and Activation of Regulatory T Cells. *Circulation Research* 104: e62-e70.

236. Keijzer, C., R. van der Zee, W. van Eden, and F. Broere. 2013. Treg inducing adjuvants for therapeutic vaccination against chronic inflammatory diseases. *Front Immunol* 4: 245.

237. Pulendran, B., P. S. Arunachalam, and D. T. O'Hagan. 2021. Emerging concepts in the science of vaccine adjuvants. *Nature Reviews Drug Discovery* 20: 454-475.

238. Bertani, B., and N. Ruiz. 2018. Function and Biogenesis of Lipopolysaccharides. *EcoSal Plus* 8.

239. Opal, S. M. 2010. Endotoxins and other sepsis triggers. *Contrib Nephrol* 167: 14-24.

240. Casella, C. R., and T. C. Mitchell. 2008. Putting endotoxin to work for us: monophosphoryl lipid A as a safe and effective vaccine adjuvant. *Cell Mol Life Sci* 65: 3231-3240.

241. Mata-Haro, V., C. Cekic, M. Martin, P. M. Chilton, C. R. Casella, and T. C. Mitchell. 2007. The vaccine adjuvant monophosphoryl lipid A as a TRIF-biased agonist of TLR4. *Science* 316: 1628-1632.

242. DeOca, K. B., C. D. Moorman, B. L. Garcia, and M. D. Mannie. 2020. Low-Zone IL-2 Signaling: Fusion Proteins Containing Linked CD25 and IL-2 Domains Sustain Tolerogenic Vaccination. *Front Immunol* 11: 541619.

243. Dalod, M., R. Chelbi, B. Malissen, and T. Lawrence. 2014. Dendritic cell maturation: functional specialization through signaling specificity and transcriptional programming. *The EMBO Journal* 33: 1104-1116.

244. Hashimoto, S. I., T. Suzuki, S. Nagai, T. Yamashita, N. Toyoda, and K. Matsushima. 2000. Identification of genes specifically expressed in human activated and mature dendritic cells through serial analysis of gene expression. *Blood* 96: 2206-2214.

245. Le Naour, F., L. Hohenkirk, A. Grolleau, D. E. Misek, P. Lescure, J. D. Geiger, S. Hanash, and L. Beretta. 2001. Profiling changes in gene expression during differentiation and maturation of monocyte-derived dendritic cells using both oligonucleotide microarrays and proteomics. *J Biol Chem* 276: 17920-17931.

246. Xu, H., L. N. Liew, I. C. Kuo, C. H. Huang, D. L.-M. Goh, and K. Y. Chua. 2008. The modulatory effects of lipopolysaccharide-stimulated B cells on differential T-cell polarization. *Immunology* 125: 218-228.

247. Bailey, J. D., A. Shaw, E. McNeill, T. Nicol, M. Diotallevi, S. Chuaiphichai, J. Patel, A. Hale, K. M. Channon, and M. J. Crabtree. 2020. Isolation and culture of murine bone marrow-derived macrophages for nitric oxide and redox biology. *Nitric Oxide* 100-101: 17-29.

248. Brasel, K., T. De Smedt, J. L. Smith, and C. R. Maliszewski. 2000. Generation of murine dendritic cells from flt3-ligand-supplemented bone marrow cultures. *Blood* 96: 3029-3039.

249. Karsunky, H., M. Merad, A. Cozzio, I. L. Weissman, and M. G. Manz. 2003. Flt3 Ligand Regulates Dendritic Cell Development from Flt3+ Lymphoid and Myeloid-committed Progenitors to Flt3+ Dendritic Cells In Vivo. *Journal of Experimental Medicine* 198: 305-313.

250. Cavanagh, L. L., R. J. Saal, K. L. Grimmett, and R. Thomas. 1998. Proliferation in monocyte-derived dendritic cell cultures is caused by progenitor cells capable of myeloid differentiation. *Blood* 92: 1598-1607.

251. Fontenot, J. D., J. P. Rasmussen, M. A. Gavin, and A. Y. Rudensky. 2005. A function for interleukin 2 in Foxp3-expressing regulatory T cells. *Nat Immunol* 6: 1142-1151.

252. Scheffold, A., K. M. Murphy, and T. Höfer. 2007. Competition for cytokines: T(reg) cells take all. *Nat Immunol* 8: 1285-1287.

253. Segel, G. B., G. R. Cokelet, and M. A. Lichtman. 1981. The measurement of lymphocyte volume: importance of reference particle deformability and counting solution tonicity. *Blood* 57: 894-899.

254. Gergely, P., I. Ernberg, G. Klein, and M. Steinitz. 1977. Blastogenic response of purified human T-lymphocyte populations to Epstein-Barr virus (EBV). *Clin Exp Immunol* 30: 347-353.

255. Mirshahidi, S., C.-T. Huang, and S. Sadegh-Nasseri. 2001. Anergy in Peripheral Memory Cd4+ T Cells Induced by Low Avidity Engagement of T Cell Receptor. *Journal of Experimental Medicine* 194: 719-732.

256. Baaten, B. J., R. Tinoco, A. T. Chen, and L. M. Bradley. 2012. Regulation of Antigen-Experienced T Cells: Lessons from the Quintessential Memory Marker CD44. *Front Immunol* 3: 23.

257. Lesley, J., N. Howes, A. Perschl, and R. Hyman. 1994. Hyaluronan binding function of CD44 is transiently activated on T cells during an in vivo immune response. *Journal of Experimental Medicine* 180: 383-387.

258. Liu, T., L. Soong, G. Liu, R. König, and A. K. Chopra. 2009. CD44 expression positively correlates with Foxp3 expression and suppressive function of CD4+ Treg cells. *Biology Direct* 4: 40.

259. Iriki, H., H. Takahashi, N. Wada, H. Nomura, M. Mukai, A. Kamata, H. Ito, J. Yamagami, T. Matsui, Y. Kurebayashi, S. Mise-Omata, H. Nishimasu, O. Nureki, A. Yoshimura, S. Hori, and M. Amagai. 2021. Peripheral tolerance by Treg via constraining

OX40 signal in autoreactive T cells against desmoglein 3, a target antigen in pemphigus. *Proceedings of the National Academy of Sciences* 118: e2026763118.

260. Leignadier, J., M.-P. Hardy, M. Cloutier, J. Rooney, and N. Labrecque. 2008. Memory T-lymphocyte survival does not require T-cell receptor expression. *Proceedings of the National Academy of Sciences* 105: 20440-20445.

261. Rosenthal, K. M., L. J. Edwards, J. J. Sabatino, J. D. Hood, H. A. Wasserman, C. Zhu, and B. D. Evavold. 2012. Low 2-dimensional CD4 T cell receptor affinity for myelin sets in motion delayed response kinetics. *PLoS One* 7: e32562.

262. Freeman, G. J., A. J. Long, Y. Iwai, K. Bourque, T. Chernova, H. Nishimura, L. J. Fitz, N. Malenkovich, T. Okazaki, M. C. Byrne, H. F. Horton, L. Fouser, L. Carter, V. Ling, M. R. Bowman, B. M. Carreno, M. Collins, C. R. Wood, and T. Honjo. 2000. Engagement of the PD-1 immunoinhibitory receptor by a novel B7 family member leads to negative regulation of lymphocyte activation. *J Exp Med* 192: 1027-1034.

263. Gianchecchi, E., and A. Fierabracci. 2018. Inhibitory Receptors and Pathways of Lymphocytes: The Role of PD-1 in Treg Development and Their Involvement in Autoimmunity Onset and Cancer Progression. *Front Immunol* 9: 2374.

264. Moorman, C. D., A. G. Bastian, K. B. DeOca, and M. D. Mannie. 2020. A GM-CSF-neuroantigen tolerogenic vaccine elicits inefficient antigen recognition events below the CD40L triggering threshold to expand CD4(+) CD25(+) FOXP3(+) Tregs that inhibit experimental autoimmune encephalomyelitis (EAE). *J Neuroinflammation* 17: 180.

265. Krummey, S. M., T. L. Floyd, D. Liu, M. E. Wagener, M. Song, and M. L. Ford. 2014. Candida-elicited murine Th17 cells express high Ctla-4 compared with Th1 cells and are resistant to costimulation blockade. *J Immunol* 192: 2495-2504.

266. Matsunaga, T., T. Ishida, M. Takekawa, S. Nishimura, M. Adachi, and K. Imai. 2002. Analysis of Gene Expression During Maturation of Immature Dendritic Cells Derived from Peripheral Blood Monocytes. *Scandinavian Journal of Immunology* 56: 593-601.

267. Leslie, M. 2016. Why endosomes recycle GPCRs. *Journal of Cell Biology* 214: 785-785.

268. Macary, P. A., M. Lindsay, M. A. Scott, J. I. O. Craig, J. P. Luzio, and P. J. Lehner. 2001. Mobilization of MHC class I molecules from late endosomes to the cell surface following activation of CD34-derived human Langerhans cells. *Proceedings of the National Academy of Sciences* 98: 3982-3987.

269. Schinnerling, K., P. García-González, and J. C. Aguillón. 2015. Gene Expression Profiling of Human Monocyte-derived Dendritic Cells - Searching for Molecular Regulators of Tolerogenicity. *Front Immunol* 6: 528.

270. DiToro, D., C. J. Winstead, D. Pham, S. Witte, R. Andargachew, J. R. Singer, C. G. Wilson, C. L. Zindl, R. J. Luther, D. J. Silberger, B. T. Weaver, E. M. Kolawole, R. J. Martinez, H. Turner, R. D. Hatton, J. J. Moon, S. S. Way, B. D. Evavold, and C. T. Weaver. 2018. Differential IL-2 expression defines developmental fates of follicular versus nonfollicular helper T cells. *Science* 361.

271. Pyle, C. J., L. Labeur-Iurman, H. T. Groves, F. Puttur, C. M. Lloyd, J. S. Tregoning, and J. A. Harker. 2021. Enhanced IL-2 in early life limits the development of TFH and protective antiviral immunity. *J Exp Med* 218.

272. Graßhoff, H., S. Comdühr, L. R. Monne, A. Müller, P. Lamprecht, G. Riemekasten, and J. Y. Humrich. 2021. Low-Dose IL-2 Therapy in Autoimmune and Rheumatic Diseases. *Front Immunol* 12: 648408.

273. Wilkinson, D. S., D. Ghosh, R. A. Nickle, C. D. Moorman, and M. D. Mannie. 2017. Partial CD25 Antagonism Enables Dominance of Antigen-Inducible CD25. *Front Immunol* 8: 1782.

274. Ritchie, M., L. Tchistiakova, and N. Scott. 2013. Implications of receptor-mediated endocytosis and intracellular trafficking dynamics in the development of antibody drug conjugates. *mAbs* 5: 13-21.

275. Pekalski, M. L., R. C. Ferreira, R. M. Coulson, A. J. Cutler, H. Guo, D. J. Smyth, K. Downes, C. A. Dendrou, X. Castro Dopico, L. Esposito, G. Coleman, H. E. Stevens, S. Nutland, N. M. Walker, C. Guy, D. B. Dunger, C. Wallace, T. I. Tree, J. A. Todd, and L. S. Wicker. 2013. Postthymic expansion in human CD4 naive T cells defined by expression of functional high-affinity IL-2 receptors. *J Immunol* 190: 2554-2566.

276. Akkaya, B., Y. Oya, M. Akkaya, J. Al Souz, A. H. Holstein, O. Kamenyeva, J. Kabat, R. Matsumura, D. W. Dorward, D. D. Glass, and E. M. Shevach. 2019. Regulatory T cells mediate specific suppression by depleting peptide-MHC class II from dendritic cells. *Nat Immunol* 20: 218-231.

277. Sakaguchi, S., T. Yamaguchi, T. Nomura, and M. Ono. 2008. Regulatory T cells and immune tolerance. *Cell* 133: 775-787.

278. Shevyrev, D., and V. Tereshchenko. 2019. Treg Heterogeneity, Function, and Homeostasis. *Front Immunol* 10: 3100.

279. Hilligan, K. L., and F. Ronchese. 2020. Antigen presentation by dendritic cells and their instruction of CD4+ T helper cell responses. *Cellular & Molecular Immunology* 17: 587-599.

280. Goenka, R., L. G. Barnett, J. S. Silver, P. J. O'Neill, C. A. Hunter, M. P. Cancro, and T. M. Laufer. 2011. Cutting Edge: Dendritic Cell-Restricted Antigen Presentation Initiates the Follicular Helper T Cell Program but Cannot Complete Ultimate Effector Differentiation. *The Journal of Immunology* 187: 1091-1095.

281. Nakano, H., K. L. Lin, M. Yanagita, C. Charbonneau, D. N. Cook, T. Kakiuchi, and M. D. Gunn. 2009. Blood-derived inflammatory dendritic cells in lymph nodes stimulate acute T helper type 1 immune responses. *Nature Immunology* 10: 394-402.

282. Kim, B., and T. H. Kim. 2018. Fundamental role of dendritic cells in inducing Th2 responses. *The Korean Journal of Internal Medicine* 33: 483-489.

283. Satpathy, A. T., C. G. Briseño, J. S. Lee, D. Ng, N. A. Manieri, W. Kc, X. Wu, S. R. Thomas, W.-L. Lee, M. Turkoz, K. G. Mcdonald, M. M. Meredith, C. Song, C. J. Guidos, R. D. Newberry, W. Ouyang, T. L. Murphy, T. S. Stappenbeck, J. L. Gommerman, M. C. Nussenzweig, M. Colonna, R. Kopan, and K. M. Murphy. 2013. Notch2-dependent classical dendritic cells orchestrate intestinal immunity to attaching-and-effacing bacterial pathogens. *Nature Immunology* 14: 937-948.

284. Maldonado, R. A., and U. H. Von Andrian. 2010. How Tolerogenic Dendritic Cells Induce Regulatory T Cells. In *Advances in Immunology*. Elsevier. 111-165.

285. Van Montfoort, N., M. G. Camps, S. Khan, D. V. Filippov, J. J. Weterings, J. M. Griffith, H. J. Geuze, T. Van Hall, J. S. Verbeek, C. J. Melief, and F. Ossendorp. 2009. Antigen storage compartments in mature dendritic cells facilitate prolonged cytotoxic T lymphocyte cross-priming capacity. *Proceedings of the National Academy of Sciences* 106: 6730-6735.

286. Wilson, N. S., D. El-Sukkari, and J. A. Villadangos. 2004. Dendritic cells constitutively present self antigens in their immature state in vivo and regulate antigen presentation by controlling the rates of MHC class II synthesis and endocytosis. *Blood* 103: 2187-2195.

287. Li, C., M. R. Buckwalter, S. Basu, M. Garg, J. Chang, and P. K. Srivastava. 2012. Dendritic cells sequester antigenic epitopes for prolonged periods in the absence of antigen-encoding genetic information. *Proceedings of the National Academy of Sciences* 109: 17543-17548.

288. Su, L. F., D. Del Alcazar, E. Stelekati, E. J. Wherry, and M. M. Davis. 2016. Antigen exposure shapes the ratio between antigen-specific Tregs and conventional T cells in human peripheral blood. *Proc Natl Acad Sci U S A* 113: E6192-E6198.

289. Mannie, M. D., K. B. DeOca, A. G. Bastian, and C. D. Moorman. 2020. Tolerogenic vaccines: Targeting the antigenic and cytokine niches of FOXP3. *Cell Immunol* 355: 104173.

290. Kedl, R. M., B. C. Schaefer, J. W. Kappler, and P. Marrack. 2002. T cells down-modulate peptide-MHC complexes on APCs in vivo. *Nat Immunol* 3: 27-32.

291. Bahcheli, D., V. Hay, J. L. Nadeau, and C. A. Piccirillo. 2011. Transfer of cell membrane components via trogocytosis occurs in CD4+ Foxp3+ CD25+ regulatory T-cell contact-dependent suppression. *Autoimmunity* 44: 607-615.

292. Wetzel, S. A., T. W. Mckeithan, and D. C. Parker. 2005. Peptide-Specific Intercellular Transfer of MHC Class II to CD4⁺ T Cells Directly from the Immunological Synapse upon Cellular Dissociation. *The Journal of Immunology* 174: 80-89.

293. Muthuswamy, R., J. Urban, J. J. Lee, T. A. Reinhart, D. Bartlett, and P. Kalinski. 2008. Ability of mature dendritic cells to interact with regulatory T cells is imprinted during maturation. *Cancer Res* 68: 5972-5978.

294. Chen, C., C. Zhang, R. Li, Z. Wang, Y. Yuan, H. Li, Z. Fu, M. Zhou, and L. Zhao. 2019. Monophosphoryl-Lipid A (MPLA) is an Efficacious Adjuvant for Inactivated Rabies Vaccines. *Viruses* 11.

295. Van Maren, W. W. C., J. F. M. Jacobs, I. J. M. De Vries, S. Nierkens, and G. J. Adema. 2008. Toll-like receptor signalling on Tregs: to suppress or not to suppress? *Immunology* 124: 445-452.

296. Reynolds, J. M., G. J. Martinez, Y. Chung, and C. Dong. 2012. Toll-like receptor 4 signaling in T cells promotes autoimmune inflammation. *Proceedings of the National Academy of Sciences* 109: 13064-13069.

297. Borrello, I., and D. Pardoll. 2002. GM-CSF-based cellular vaccines: a review of the clinical experience. *Cytokine Growth Factor Rev* 13: 185-193.

298. Somasundraam, r. 2015. Recent Advances and Current Status of GM-CSF as an Adjuvant in DNA Vaccines for Viral Diseases. *Journal of Investigative Genomics* 2: 54-56.

299. Chang, D. Z., W. Lomazow, C. Joy Somberg, R. Stan, and M. A. Perales. 2004. Granulocyte-macrophage colony stimulating factor: an adjuvant for cancer vaccines. *Hematology* 9: 207-215.

300. Jones, T., A. Stern, and R. Lin. 1994. Potential role of granulocyte-macrophage colony-stimulating factor as vaccine adjuvant. *Eur. J. Clin. Microbiol. Infect. Dis.* 13 Suppl 2: S47-53.

301. Boyton, R. J., and D. M. Altmann. 2002. Is selection for TCR affinity a factor in cytokine polarization? *Trends Immunol* 23: 526-529.

302. Purvis, H. A., J. N. Stoop, J. Mann, S. Woods, A. E. Kozijn, S. Hambleton, J. H. Robinson, J. D. Isaacs, A. E. Anderson, and C. M. Hilkens. 2010. Low-strength T-cell activation promotes Th17 responses. *Blood* 116: 4829-4837.

303. Kapsenberg, M. L. 2003. Dendritic-cell control of pathogen-driven T-cell polarization. *Nat Rev Immunol* 3: 984-993.

304. Clark, M., C. J. Kroger, Q. Ke, and R. M. Tisch. 2020. The Role of T Cell Receptor Signaling in the Development of Type 1 Diabetes. *Front Immunol* 11: 615371.

305. Bosselut, R. 2019. T cell antigen recognition: Evolution-driven affinities. *Proceedings of the National Academy of Sciences* 116: 21969-21971.

306. Huppa, J. B., and M. M. Davis. 2003. T-cell-antigen recognition and the immunological synapse. *Nature Reviews Immunology* 3: 973-983.

307. Vogel, I., B. Verbinnen, S. Van Gool, and J. L. Ceuppens. 2016. Regulatory T Cell–Dependent and –Independent Mechanisms of Immune Suppression by CD28/B7 and CD40/CD40L Costimulation Blockade. *The Journal of Immunology* 197: 533-540.

308. Roser-Page, S., T. Vikulina, K. Yu, M. E. McGee-Lawrence, and M. N. Weitzmann. 2018. Neutralization of CD40 ligand costimulation promotes bone formation and accretion of vertebral bone mass in mice. *Rheumatology (Oxford)* 57: 1105-1114.

309. Mannie, M. D., and A. D. Curtis. 2013. Tolerogenic vaccines for Multiple sclerosis. *Hum Vaccin Immunother* 9: 1032-1038.

APPENDIX

East Carolina University
Tomorrow starts here.

Animal Care and
Use Committee
212 Ed Warren Life
Sciences Building
East Carolina University
Greenville, NC 27834-4354

252-744-2436 office
252-744-2355 fax

September 24, 2018

Mark Mannie, Ph.D.
Department of Micro/Immuno
Brody 5E
East Carolina University

Dear Dr. Mannie:

Your Animal Use Protocol entitled, "Antigen-Specific Tolerogenic Vaccines for Murine EAE" (AUP #K147d) was reviewed by this institution's Animal Care and Use Committee on September 24, 2018. The following action was taken by the Committee:

"Approved as submitted"

Please contact Aaron Hinkle at 744-2997 prior to hazard use

A copy is enclosed for your laboratory files. Please be reminded that all animal procedures must be conducted as described in the approved Animal Use Protocol. Modifications of these procedures cannot be performed without prior approval of the ACUC. The Animal Welfare Act and Public Health Service Guidelines require the ACUC to suspend activities not in accordance with approved procedures and report such activities to the responsible University Official (Vice Chancellor for Health Sciences or Vice Chancellor for Academic Affairs) and appropriate federal Agencies. **Please ensure that all personnel associated with this protocol have access to this approved copy of the AUP and are familiar with its contents.**

Sincerely yours,

Susan McRae, Ph.D.
Chair, Animal Care and Use Committee

SM/jd

Enclosure

Amendment #1
AUP K147d

Administrative Approval by Dr. McRae 7/1/19

East Carolina University Animal Use Protocol (AUP) Amendment Form
Latest Revision, March 2016

FOR IACUC USE ONLY	
AUP # K147d	
Date received: 6/25/19	
Full Review and date:	Designated Reviewer and date:
Approval date: 7/1/19	IBC: 6/25/19 - transgenics
Pain Category: D	
Amendments approved: 1	
Minor Amendment: 1 admin	
Significant Amendment:	If so, number?

Please fill out completely and email to davenportp@ecu.edu or iacuc@ecu.edu

PROJECT INFORMATION: Please list AUP Number and Title

AUP K147d Antigen-Specific Tolerogenic Vaccines for Murine EAE

+30D

Principal Investigator:

Mark Mannie, PhD

1. Please explain in simple, non-technical language, the purpose or rationale for the protocol amendment.

We are currently developing a tolerogenic vaccine for use as a therapeutic treatment of the inflammatory demyelinating disease Multiple Sclerosis (MS). We are currently testing this tolerogenic vaccine in a preclinical model of MS known as experimental autoimmune encephalomyelitis (EAE) in C57BL/6 mice. A major goal of our funded research (National Institutes of Health 1 R01 AI126398-01) is to understand mechanisms by which our tolerogenic vaccine inhibits pathogenic T cells responses in EAE. An improved understanding of the mechanism will enable derivation of more effective second-generation vaccines with improved tolerogenic efficacy. Our current tolerogenic vaccine contains a mixture of Interferon-beta (IFN-β), a neuroantigen (synthetic peptide representing the Myelin Oligodendrocyte Glycoprotein MOG35-55 sequence), and Alhydrogel (common adjuvant used in human vaccination). This vaccine signals via the heterodimeric Type I Interferon IFNAR receptor, which is comprised of IFNAR1 and IFNAR2 proteins. By use of several global and conditional *Ifnar1* knockout models, we have spent several years studying how this vaccine signals through IFNAR1. Due to emerging research outcomes, we now need to understand how this vaccine signals through the IFNAR2 component of the receptor, and therefore now need to acquire a new mouse strain bearing a global *Ifnar2* gene deficiency. In this amendment, we request permission to import the C57BL/6N-*Ifnar2tm1.1(KOMP)Vlcg*/MbpMmucd strain, which would be obtained from the Mutant Mouse Resource & Research Center (UC Davis). This amendment would cover import, breeding, and husbandry of this new mouse strain at ECU DCM. We will address experimentation in a subsequent amendment or AUP once we successfully establish the strain in our facility.

Amendment #2

ECU

Animal Care and Use Committee
003 Ed Warren Life Sciences Building | East Carolina University | Greenville NC 27354 - 4354
252-744-2436 office | 252-744-2355 fax

May 13, 2020

Mark Mannie, Ph.D.
Department of Microbiology and Immunology, ECU

Subject: Protocol K147d, original approval date 09/24/2018

Dear Dr. Mannie:

The amendment to your Animal Use Protocol entitled, "Antigen-Specific Tolerogenic Vaccines for Murine EAE " (AUP#K147d) was reviewed by this institution's Animal Care and Use Committee on 05/11/2020. The following action was taken by the Committee:

"Approved as submitted"

****Please contact Aaron Hinkle prior to any hazard use****

A copy of the protocols is enclosed for your laboratory files. Please be reminded that all animal procedures must be conducted as described in the approved Animal Use Protocol. Modifications of these procedures cannot be performed without prior approval of the ACUC. The Animal Welfare Act and Public Health Service Guidelines require the ACUC to suspend activities not in accordance with approved procedures and report such activities to the responsible University Official (Vice Chancellor for Health Sciences or Vice Chancellor for Academic Affairs) and appropriate federal Agencies. **Please ensure that all personnel associated with this protocol have access to this approved copy of the AUP/Amendment and are familiar with its contents.**

Sincerely yours,

Sue McRae, Ph.D.
Chair, Animal Care and Use Committee

SM/GD

enclosure

www.ecu.edu

Amendment #3

ECU

Animal Care and Use Committee
003 Ed Warren Life Sciences Building | East Carolina University | Greenville NC 27354 - 4354
252-744-2436 office | 252-744-2355 fax

August 10, 2020

Mark Mannie, Ph.D.
Department of Microbiology, ECU

Subject: Protocol K147d, original approval date: 9/24/2018

Dear Dr. Mannie:

The amendment#3 to your Animal Use Protocols entitled, "Antigen-specific tolerogenic vaccines for murine EAE" (AUP#K147d) was reviewed by this institution's Animal Care and Use Committee on 08/07/2020. The following action was taken by the Committee:

"Approved as submitted"

****Please contact Aaron Hinkle prior to any hazard use****

A copy of the protocols is enclosed for your laboratory files. Please be reminded that all animal procedures must be conducted as described in the approved Animal Use Protocol. Modifications of these procedures cannot be performed without prior approval of the ACUC. The Animal Welfare Act and Public Health Service Guidelines require the ACUC to suspend activities not in accordance with approved procedures and report such activities to the responsible University Official (Vice Chancellor for Health Sciences or Vice Chancellor for Academic Affairs) and appropriate federal Agencies. **Please ensure that all personnel associated with this protocol have access to this approved copy of the AUP/Amendment and are familiar with its contents.**

Sincerely yours,

SB McRae

Sue McRae, Ph.D.
Chair, Animal Care and Use Committee

SM/GD

enclosure

www.ecu.edu

ECU

Animal Care and Use Committee
003 Ed Warren Life Sciences Building | East Carolina University | Greenville NC 27354 - 4354
252-744-2436 office | 252-744-2355 fax

August 11, 2020

Mannie Mark, Ph.D.
Department of Microbiology, ECU

Dear Dr. Mannie:

Your Animal Use Protocol entitled, "Antigen-specific tolerogenic vaccines for murine EAE" (AUP #K158c) was reviewed by this institution's Animal Care and Use Committee on 08/10/2020. The following action was taken by the Committee:

"Approved as submitted"

****Please contact Aaron Hinkle prior to any hazard use****

A copy of the protocols is enclosed for your laboratory files. Please be reminded that all animal procedures must be conducted as described in the approved Animal Use Protocol. Modifications of these procedures cannot be performed without prior approval of the ACUC. The Animal Welfare Act and Public Health Service Guidelines require the ACUC to suspend activities not in accordance with approved procedures and report such activities to the responsible University Official (Vice Chancellor for Health Sciences or Vice Chancellor for Academic Affairs) and appropriate federal Agencies. **Please ensure that all personnel associated with this protocol have access to this approved copy of the AUP/Amendment and are familiar with its contents.**

Sincerely yours,

Susan McRae, Ph.D.
Chair, Animal Care and Use Committee

SM/GD

enclosure

Animal Care and Use Committee
003 Ed Warren Life Sciences Building | East Carolina University | Greenville NC 27834 - 4354
252-744-2436 office | 252-744-2355 fax

July 27, 2021

Mark Mannie, Ph.D.
Department of Microbiology and Immunology, ECU

Subject: Protocol K158c, original approval date 08/10/2020

Dear Dr. Mannie:

The amendment#1 to your Animal Use Protocol entitled, "Antigen-specific tolerogenic vaccines for murine EAE" (AUP#K158c) was reviewed by this institution's Animal Care and Use Committee on 07/26/2021. The following action was taken by the Committee:

"Approved as submitted"

Please contact Aaron Hinkle prior to any hazard use

A copy of the protocols is enclosed for your laboratory files. Please be reminded that all animal procedures must be conducted as described in the approved Animal Use Protocol. Modifications of these procedures cannot be performed without prior approval of the ACUC. The Animal Welfare Act and Public Health Service Guidelines require the ACUC to suspend activities not in accordance with approved procedures and report such activities to the responsible University Official (Vice Chancellor for Health Sciences or Vice Chancellor for Academic Affairs) and appropriate federal Agencies. Please ensure that all personnel associated with this protocol have access to this approved copy of the AUP/Amendment and are familiar with its contents.

Sincerely yours,

Sue McRae, Ph.D.
Chair, Animal Care and Use Committee

SM/GD

enclosure

The Brody School of Medicine
Office of Prospective Health
East Carolina University
188 Warren Life Sciences Building • Greenville, NC 27834
252-744-2070 office • 252-744-2417 fax

Occupational Medicine
Employee Health
Radiation Safety
Infection Control
Biological Safety

TO: Dr. Mark Mannie
Department of Microbiology & Immunology

FROM: John Baumgartner
Biological Safety Officers

RE: Registration Final Approval

Date: January 7, 2020

Your Biological Safety Protocol, **Transgenic mouse models** has received **final approval** to be conducted at Biosafety Level 2 and Animal Biosafety Level 2 in Brody 5W-41, 43, 60, 62, 5N-51, GW-67, 69, and GE-22 based on your registration/revisions submitted,

using: A. Biohazards

- ☐ Infectious Agent(s)
- ☒ Biotoxin(s)
- ☐ Allergen(s)
- ☐ Prion(s)
- ☒ Human blood, fluid, cells, tissue or cell cultures
- ☐ Transformed cells
- ☐ Other

and/or B. ☒ NIH Use of Recombinant DNA (or RNA) molecules, microorganisms use or breeding transgenic or techniques (plasmids, viral vectors, transfection); of transgenic animals or plants at NIH Category III-E.

This approval is effective for a period of 3 years and may be renewed with an updated registration if needed at that time. Your laboratory will be inspected periodically (every 1-3 years) depending upon the materials/techniques used.

Please notify the Animal Care staff before beginning work with Biohazard agents in animals. Also, please keep in mind all individuals who will be exposed to or handle human-derived biohazardous agents will be due for Blood Borne Pathogens refresher training annually.

Please do not hesitate to contact Biological Safety at 744-2070 if you have any questions, concerns, or need any additional information. Best wishes on your research.

cc: Dr. Daniel Martin, Chair, Biosafety Committee
Dr. Everett Pesci, Department Chair
Jeffrey McKithen, IACUC
Dr. Susan McRae, IACUC
Aaron Hinkle, Comparative Medicine